

ISTANBUL TECHNICAL UNIVERSITY ★ GRADUATE SCHOOL OF SCIENCE
ENGINEERING AND TECHNOLOGY

**DEVELOPMENT OF EXTRUDED HIGH IMPACT POLYSTYRENE
FOAMS**



M.Sc. THESIS

Emre DEMİRTAŞ

Department of Materials&Metallurgical Engineering

Materials Engineering Programme

JUNE 2018

ISTANBUL TECHNICAL UNIVERSITY ★ GRADUATE SCHOOL OF SCIENCE
ENGINEERING AND TECHNOLOGY

**DEVELOPMENT OF EXTRUDED HIGH IMPACT POLYSTYRENE
FOAMS**



M.Sc. THESIS

Emre DEMİRTAŞ
506161414

Department of Materials&Metallurgical Engineering

Materials Engineering Programme

Thesis Advisor: Assist. Prof. Dr. Mohammadreza NOFAR

JUNE 2018

İSTANBUL TEKNİK ÜNİVERSİTESİ ★ FEN BİLİMLERİ ENSTİTÜSÜ

**EKSTRÜZYON YÖNTEMİYLE YÜKSEK DARBE DAYANIMLI POLİSTİREN
KÖPÜK MALZEMESİNİN GELİŞTİRİLMESİ**

YÜKSEK LİSANS TEZİ

**Emre DEMİRTAŞ
506161414**

Malzeme&Metalurji Mühendisliği Anabilim Dalı

Malzeme Mühendisliği Programı

Tez Danışmanı: Yrd. Doç. Dr. Mohammadreza NOFAR

HAZİRAN 2018

Emre Demirtaş, a M.Sc. student of ITU Graduate School of Science Engineering and Technology student ID 506161414, successfully defended the thesis/dissertation entitled “DEVELOPMENT OF EXTRUDED HIGH IMPACT POLYSTYRENE FOAMS”, which he prepared after fulfilling the requirements specified in the associated legislations, before the jury whose signatures are below.

Thesis Advisor : **Assistant Professor Mohammadreza NOFAR**
İstanbul Technical University

Jury Members : **Associate Professor Sevim İşci**
İstanbul Technical University

Associate Professor Ali DURMUŞ
İstanbul University

Date of Submission : 04.05.2018

Date of Defense : 04.06.2018





To my dearest family and lovely friends,



FOREWORD

First of all, I would like to express my deep and sincere gratitude to my thesis supervisor Assist. Prof. Dr. Mohammadreza NOFAR. His valued supervision, guidance and support have made me go this far. The knowledge I have learned from him will have a great impact on my future career.

I would like to thank to ARÇELİK A.Ş. Central R&D Department Director Nihat BAYIZ, Materials Technologies R&D Department Manager Dr. Mustafa SEZER, and Polymer&Chemistry Team Leader Dr. Yusuf YUSUFOĞLU, for supporting my research activities.

I would also thank to Hakan ÖZKAN who always took the time to listen and give priceless comments for this study. I have learned a lot of precious information through my M.Sc project period from him to improve my personality. Also, I would thank to Umut KILIÇ for help and support during experimental works.

I would like to thank my colleagues in the ARÇELİK A.Ş. Central R&D Materials Technologies Department for their help and friendship over the past years.

I would also like to specially thank to the most thoughtful person in the world, my awesome lasagna Dicle ÇEVİK for her full support, motivation and love. Also, I would thank to my troublesome sister in law Bilge ÇEVİK for her encouragements and supports. Many thanks to GZ on the beach team.

Finally, I owe a big thanks to my wonderful parents Selçuk&Sema DEMİRTAŞ and my sister Ayşe DEMİRTAŞ for their never-ending unconditional support, encouragement and patience throughout the years.

June 2018

Emre DEMİRTAŞ
(Metallurgy&Materials Engineer)



TABLE OF CONTENTS

	<u>Page</u>
FOREWORD	ix
TABLE OF CONTENTS	xi
ABBREVIATIONS	xiii
SYMBOLS	xv
LIST OF TABLES	xvii
LIST OF FIGURES	xix
SUMMARY	xxi
ÖZET	xxiii
1. INTRODUCTION	1
2. LITERATURE REVIEW	5
2.1 Polystyrene	5
2.1.1 History	5
2.1.2 Structure	5
2.1.3 Types of PS	8
2.1.4 Properties	9
2.1.4.1 Mechanical	9
2.1.4.2 Chemical	9
2.1.4.3 Processing	9
2.1.5 Applications	10
2.2 Overview of Plastic Foaming	10
2.2.1 Background of foaming	10
2.2.2 Foaming concepts and classifications	11
2.2.2.1 Cell dimension and structure.....	11
2.2.3 Blowing agents for foaming.....	14
2.2.3.1 Physical blowing agent	14
2.2.3.2 Chemical blowing agent.....	15
2.2.4 Plastic foaming mechanism	16
2.2.4.1 Formation of polymer/gas solution	16
2.2.4.2 Fundamentals of cell nucleation.....	22
2.2.4.3 Cell growth and stabilization	26
2.2.5 Foam manufacturing technologies	27
2.2.5.1 Batch foaming process	28
2.2.5.2 Continuous foaming process	29
2.2.5.3 Design of foam extrusion processing.....	32
2.2.5.4 Die design in foam extrusion	33
2.2.5.5 Rheological behaviors of polymers in foam extrusion	34
2.2.5.6 Common foam extrusion systems	35
2.3 HIPS Foaming	36
2.3.1 Effect of gases	36
2.3.2 Effect of the processing pressure	37
2.3.3 Effect of injected gas amount.....	38
2.3.4 Effect of pressure drop rate	39

2.3.5 Effect of die temperature.....	39
2.3.6 Effect of nucleating agent	40
3. EXPERIMENTAL PROCEDURE.....	41
3.1 Materials.....	41
3.1.1 Polymer resin.....	41
3.1.2 Chemical blowing agents	42
3.1.3 Nucleating agents	43
3.2 Experimental Setup and Procedure	43
3.2.1 Twin screw extrusion system	44
3.2.2 Filamentary die.....	44
3.2.3 Experimental setup and procedure	44
3.2.3.1 Processing temperatures of the extrusion system.....	45
3.2.3.2 Die temperature profile	46
3.2.3.3 CBA type and content	46
3.2.3.4 Screw Speed (RPM).....	47
3.2.3.5 HIPS-GPPS blending ratios	47
3.2.3.6 Nucleating agent type and content	48
3.2.4 Rheological measurements.....	48
3.2.5 Characterization techniques	48
3.2.5.1 Density measurement & void fraction	48
3.2.5.2 Morphological analysis and foam cell density characterization	49
4. RESULTS AND DISCUSSION.....	51
4.1 Polybutylene (PB) Size Determination in PS Matrix	51
4.2 Melt Behavior of the HIPS, GPPS and Their Blends.....	51
4.3 Temperature Profile.....	53
4.3.1 Effect of processing temperature on cell nucleation for two different chemical blowing agents.....	53
4.3.2 Effect of die temperature on cell nucleation for two different chemical blowing agents	55
4.4 Chemical Blowing Agent	58
4.4.1 Effect of chemical blowing agent content on cell nucleation for two different chemical blowing agents.....	58
4.5 Screw RPM.....	59
4.5.1 Effect of screw rpm on cell nucleation for two different chemical blowing agents	59
4.6 Foaming Behavior of PS Blends	61
4.6.1 Effect of GPPS on cell nucleation for two different chemical blowing agents	61
4.7 Foaming Behavior of PS Composites.....	62
4.7.1 Effect of Inorganic filler on cell nucleation for two different chemical blowing agents	62
5. CONCLUSION.....	65
REFERENCES.....	67
CURRICULUM VITAE	75

ABBREVIATIONS

CBA	: Chemical Blowing Agent
CNT	: Classical Nucleation Theory
GPPS	: General Purpose Polystyrene
HIPS	: High Impact Polystyrene
PBA	: Physical Blowing Agent
PS	: Polystyrene
RPM	: Revolution Per Minute
SEM	: Scanning Electron Microscope
TEM	: Transmission Electron Microscope



SYMBOLS

D	: Diffusivity
t_D	: Time of absorption
h/2	: Diffusion distance
D₀	: Diffusivity coefficient constant
E_d	: Activation energy for diffusion.
M_t	: Mass uptake at time
h	: Sheet thickness
M_∞	: Equilibrium mass uptake after an infinite time
S	: Solubility
H	: Henry's law constant
P	: Gas pressure
R	: Gas constant
T	: Temperature
H₀	: Solubility coefficient constant
ΔH_s	: Molar heat of sorption
A_{lg}	: Surface area at the liquid-gas interface.
T_{sys}	: The systems absolute temperature
k_B	: The Boltzmann constant
C_r	: The gas concentration
C_{sat}	: The saturated gas concentration
ΔP	: The pressure drop
L	: The length of piece
M	: The firmness
R_h	: The dimension of hydraulic radius
W	: The rate of throughput
a, b	: The shape aspects
n	: The power law exponent
ρ	: The specific gravity of the melt
A	: The area of flow
P_{bub}	: The pressure inside the bubble;
P_{sys}	: The surrounding system pressure
V_g	: The bubble volume
Y_{lg}	: The interfacial energy at the liquid-gas interface.



LIST OF TABLES

	<u>Page</u>
Table 2.1 : Properties of HIPS and GPPS	8
Table 2.2 : Advantages and disadvantage of typical foam extrusion system	35
Table 3.1 : Various temperature profiles for CBA-1.	45
Table 3.2 : Various temperature profiles for CBA-2.	46
Table 3.3 : Different temperature profiles for die section.	46
Table 3.4 : Different CBA contents for CBA-1.	47
Table 3.5 : Different CBA contents for CBA-2.	47
Table 3.6 : Different CBA contents for CBA-1.	47
Table 3.7 : Different CBA contents for CBA-2.	48



LIST OF FIGURES

	<u>Page</u>
Figure 2.1 : Styrene part production	6
Figure 2.2 : Polymerization of styrene	6
Figure 2.3 : Polystyrene manufacturing diagram	7
Figure 2.4 : TEM Images of HIPS	9
Figure 2.5 : SEM image of (a) open-cell foam; and (b) closed-cell foam.	12
Figure 2.6 : Polymer foaming process by using a physical blowing agent	16
Figure 2.7 : CO ₂ and N ₂ solubility in PS	18
Figure 2.8 : CO ₂ and N ₂ solubility in PLA at: (a) 180 °C and (b) 200 °C	19
Figure 2.9 : Temperature effect on solubility of PLA8051D	19
Figure 2.10 : Solubility of CO ₂ in PLA8051D at 180 °C and 200 °C with different pressures	20
Figure 2.11 : The system of general gas/polymer sorption isotherm	20
Figure 2.12 : CO ₂ diffusivity in PS with varying temperature	21
Figure 2.13 : N ₂ and CO ₂ diffusivity in PLA at 180 and 200 °C	22
Figure 2.14 : The schematic of homogeneous and heterogeneous nucleation	23
Figure 2.15 : Homogenous bubble nucleation free energy change	24
Figure 2.16 : The schematic of cell coalescence phenomena	27
Figure 2.17 : Laboratory-scale batch foaming system	28
Figure 2.18 : EPS production steps	29
Figure 2.19 : Process flow chart of EPS production	30
Figure 2.20 : Low pressure foam reciprocating injection molding machine	30
Figure 2.21 : Gas counter pressure foam injection molding machine	31
Figure 2.22 : Simultaneously handling gas and melt modified injection molding machine	31
Figure 2.23 : Microcellular injection molding system directing the melt-gas through its shutoff nozzle into the mold cavity	32
Figure 2.24 : Schematic design of annular foam die	34
Figure 2.25 : Plot of pressure drop in a die of constant cross section	35
Figure 2.26 : Tandem extrusion foaming system	36
Figure 2.27 : Morphology of extruded HIPS at different processing pressures	37
Figure 2.28 : The processing pressure effect on the cell density of extruded HIPS.	38
Figure 2.29 : The injected gas content effect on the cell density of extruded HIPS.	38
Figure 2.30 : The pressure drop rate effect on the cell density of extruded HIPS.	39
Figure 2.31 : The die temperature effect on the cell density of PLA	40
Figure 2.32 : PS foaming micrographs with CO ₂ at 180°C: (a) neat PS and (b) PS + 5 wt% talc	40
Figure 3.1 : HIPS as a granule form.	41
Figure 3.2 : Chemical structure of HIPS.	41
Figure 3.3 : Granule form of GPPS.	42
Figure 3.4 : Chemical structure of GPPS.	42

Figure 3.5 : DSC Heating thermograms (a) and TGA curves (b) of the CBAs used during the foaming.	43
Figure 3.6 : Twin screw extruder and its barrel zones.	44
Figure 3.7 : The filamentary die that was used in thesis studies.	44
Figure 3.8 : Barrel sections of the twin screw extruder.	45
Figure 3.9 : The samples for rheological studies.	48
Figure 3.10 : Mettler density measurement device.	49
Figure 3.11 : Scanning electron microscope (SEM).	50
Figure 4.1 : Optical microscope images of neat HIPS reflecting the PB droplet sizes before and after process. The scale bars are 20 μm respectively.	51
Figure 4.2 : MFI results of HIPS, GPPS and their blends.	52
Figure 4.3 : Complex shear viscosity of HIPS and their blends with GPPS at 200°C.	52
Figure 4.4 : Effect of (a) processing temperature on void fraction and (b) cell density of HIPS foams using moderate content of CBA 1 (moderate RPM). ...	53
Figure 4.5 : Effect of (a) processing temperature on void fraction and (b) cell density of HIPS foams using moderate content of CBA 2 (moderate RPM). ...	54
Figure 4.6 : Die pressure variations with varying temperature profiles for both CBAs.	54
Figure 4.7 : SEM images of the HIPS foamed samples at various processing temperatures with CBA 1 and CBA 2.	55
Figure 4.8 : Effect of (a) die temperature on void fraction and (b) cell density of HIPS foams using moderate content of CBA 1 (moderate RPM), and on (c) die pressure variations.	56
Figure 4.9 : SEM images of the HIPS foamed samples at various die temperatures with CBA 1 and CBA 2.	57
Figure 4.10 : Effect of CBA content on (a) void fraction and (b) cell density of HIPS foams at optimized at low die temperature and high die temperature, for CBA 1 and CBA 2, respectively (moderate RPM) and, on (c) die pressure variations.	58
Figure 4.11 : SEM images of the HIPS foamed samples with various CBA contents for CBA 1 and CBA 2.	59
Figure 4.12 : Effect of RPM on (a) void fraction and (b) cell density of HIPS foams at low die temperature and high die temperature, for CBA 1 and CBA 2, respectively (moderate RPM) and on (c) die pressure variations.	60
Figure 4.13 : SEM images of the HIPS foams at different screw RPMs for samples foamed with two CBAs.	61
Figure 4.14 : Effect of GPPS content on (a) void fraction and (b) cell density using high content of CBA 1 at low die temperature (low RPM).	62
Figure 4.15 : SEM images of the HIPS blend foams using high content CBA 1 at low die temperature (low RPM).	62
Figure 4.16 : Effect of various inorganic fillers on (a) void fraction and (b) cell density of the HIPS composite foams using high content of CBA 1 at low die temperature (low RPM).	63
Figure 4.17 : SEM images of the HIPS composite foams using high content CBA 1 at low die temperature (low RPM).	63

DEVELOPMENT OF EXTRUDED HIGH IMPACT POLYSTYRENE FOAMS

SUMMARY

The use of polymers has been increased significantly since the second world war. Currently, hundreds of millions of polymeric products are being manufactured. This is due to the advantages that polymers could provide compared to other metallic or ceramic counterparts. Firstly, polymers possess low density and their manufacturing is cheaper and easier. In addition, polymers are corrosion resistant materials.

Polystyrene (PS) is an amorphous polymer that has glass transition temperature of around 105 °C. It is cheap and one of the mostly used polymers in commodity applications. There are many areas for the use of PS such as plastic cutlery, pots, toys, automotive industry, whitegoods industry, electronics etc. General purpose PS (GPPS) and High impact PS (HIPS) are the types of PS that are widely being used in various areas. GPPS is a transparent and brittle material and it is known as crystal in plastic industry. HIPS is also a blend of PS which contains around 5-15 wt % polybutadiene (PB) rubber. These two polymers form an immiscible blend of PS and PB.

Foamed polymers can be defined as polymers include bubbles and pores. Foamed polymers are very light weight and cost-effective materials. In addition, they have comparable mechanical properties and very high strength to weight ratios as it is compared to conventional neat polymers. Because of such advantages, the polymeric foams are used in many applications such as automobile parts, packaging industry, sandwich caps, insulators in construction industry, sport industry etc.

The use of blowing agents are required in order to obtain foamed structure in foaming process. Blowing agents are classified into two groups as physical blowing agents (PBAs) and chemical blowing agents (CBAs). PBAs are directly injected into the polymer matrix melt during processing and they are in the form of gas, liquid or supercritical phase. On the other hand, CBAs decompose and generate gases during processing and they are in the form of solid granules or powder.

Polymeric foams can be classified as open or closed cell foams based on the morphology; microcellular, fine celled and conventional foams as the cell density; high density, medium density and low density based on void fraction or expansion ratio. Many of traditional polymer processing methods can be performed in order to produce polymeric foams. Batch process and continuous process are the two techniques for foam production. Continuous process also classified into two groups as foam extrusion and foam injection molding (semi-continuous).

In foam extrusion process, polymer/gas mixture starts to be generated by the directly injection of PBA or decomposition of CBA under higher pressure during processing. The gas dissolve in to polymer matrix when the pressure is under the solubility limit of polymer. When the polymer/gas mixture flew through the extruder die, the sudden

pressure drop at the die nozzle creates thermodynamic instability and causes cell nucleation and growth during the foaming step.

This thesis studies the extrusion foaming behavior of HIPS through a twin-screw extruder using two various types of CBAs. The filamentary die having 4 mm length and 2 mm diameter was used in order to obtain foamed filament samples for each experiment. The CBAs differences is about their decomposition temperatures. These CBAs were named as CBA-1 and CBA-2 and they were thermally analyzed in order to observe the thermal properties and decomposition temperatures by using differential scanning calorimetry (DSC) and thermal gravimetric analysis (TGA).

Three and five different extruder barrel temperature profiles were determined in order to observe the effect of processing temperature for CBA-1 and CBA-2, respectively. After the determination of optimum processing temperature profile for both CBAs, the five different die temperature profiles (from the highest to the lowest temperature) were tailored during the foaming of HIPS for two different CBAs. The effect of the die temperature on the foaming behavior of HIPS was observed, and the optimum die temperature profile was determined.

The next step is to verify the CBA content effect on the foamed HIPS for both CBAs. Three different contents (i.e., low, moderate and high content) of chemical blowing agents were used for each CBAs and content of CBA on foamig was investigated. After the determination of optimum CBA content for both CBAs, effect of screw RPM (revolution per minute) on the foaming behavior of HIPS was, subsequently, illustrated for both CBAs. Four different screw RPM (low, moderate, high, very high RPM) were tailored during the foaming of HIPS for two different CBAs and the most proper RPM conditions were selected for CBA-1 and CBA-2.

The HIPS extrusion foaming behavior was further investigated via blending it with GPPS at the various blending cotents (neat HIPS, HIPS with low content GPPS, HIPS with high content GPPS). The effect of GPPS and its blending content was investigated for both CBAs. After that, foaming behavior was also examined via compounding HIPS with three different inorganic fillers (i.e., microlamellar talc, talc, and calcium carbonate) at three different contents (i.e., low, moderate and high content). The effect of the inorganic fillers as a nucleating agent and the effect of inorganic filler type and content were investigated with this study.

The foamed HIPS samples were characterized in two aspects. Firstly, the density of foamed samples were measured in pure water and calculated by using archimedes equation. After the determination of the density of foamed HIPS samples, the void fractions of each sample was calculated. On the other hand, the morphology of cellular structure in foamed samples were observed by using scanning electron microscope (SEM). Firstly the foamed HIPS filaments were broken under liquid nitrogen and the samples were coated with gold. After the observation of cellular morphology; cell distributions and cell dimensions were examined and the cell density of each of filamentary samples were calculated.

EKSTRÜZYON PROSESİNDE YÜKSEK DARBE DAYANIMLI POLİSTİREN KÖPÜK MALZEMESİNİN GELİŞTİRİLMESİ

ÖZET

İkinci dünya savaşından günümüze kadar, polimer endüstrisi yıldan yıla gelişerek büyümüştür. Günümüzde, kullanılan polimer malzeme miktarları oldukça fazla olup, yılda yüzlerce milyon polimer ürün üretilmektedir. Polimer sektörünün bu denli büyümesinin ana nedeni, polimer malzemelerin özelliklerinin diğer metalik ve seramik malzemeler ile kıyaslandığında avantajlarının oldukça fazla olmasıdır. Öncelikle, polimerler pek çok malzemeye oranla daha hafif materyeller olup, üretimleri oldukça kolaydır. Ayrıca polimerler metaller gibi korozyona uğrayarak aşınmazlar.

Polistiren (PS) amorf kimyasal yapıdaki polimerlerden olup, 105 °C camı geçiş sıcaklığına sahiptir. Fiyat olarak pahalı değildir ve en çok kullanım alanına sahip olan polimer malzemelerden biridir. Kullanım alanlarına örnek olarak ise: plastik çatal, bıçak ve tabak parçaları, oyuncaklar, otomotiv endüstrisi, beyaz eşya endüstrisi ve elektronik olarak gösterilebilir. Genel amaçlı polistiren (GPPS) ve yüksek darbe dayanımlı polistiren (HIPS) polistiren malzeme türlerindedir. GPPS, şeffaf ve kırılğan yapıda bir malzeme olup, polimer sektöründe daha çok kristal adıyla bilinmektedir. HIPS ise, içeriğinde % 5-15 aralığında polibütadien (PB) kauçuğu bulundurmaktadır. Darbeyi daha iyi sönmleme özelliği, yapısındaki kauçuktan gelmektedir. HIPS, PS ve PB malzemelerinin birbiri içerisinde karışmayan harman yapısından oluşmaktadır.

Köpürtülmüş polimerler, polimer matriksin içerisinde gaz boşlukları (hücre) ve porlar içeren polimerler olarak tanımlanabilir. Köpürtülmüş polimerler oldukça hafif ve düşük maliyetli ürünlerdir. Ayrıca, geleneksel köpürtülmemiş polimerlerle kıyaslandığında, karşılaştırılabilir mekanik özelliklere ve ağırlıklarına oranla oldukça yüksek mukavemet değerlerine sahiptirler. Bu gibi avantajlarından dolayı, polimer köpük malzemeler otomobil parçaları, paketleme sektörü, sandviç kapları, inşaat yalıtım sektörü, spor ekipmanları endüstrisi gibi bir çok uygulama alanında kullanılmaktadır.

Köpürtülmüş ürünler elde edebilmek için, polimer malzemenin yanı sıra köpürtücü ajanların da kullanılması gerekmektedir. Köpürtücü ajanlar, fiziksel köpürtücü ajanlar (PBAs) ve kimyasal köpürtücü ajanlar (CBAs) olmak üzere iki sınıfa ayrılmaktadırlar. Fiziksel köpürtücü ajanlar; gaz, sıvı veya süper-kritik faz formunda olup, proses esnasında polimer matriksin içerisine direkt olarak enjekte edilmektedir. Kimyasal köpürtücü ajanlar ise katı granül veya toz formunda malzemeler olup, proses esnasında sıcaklıkla beraber dekompoze olarak gaz açığa çıkarmakta, bu sayede polimer malzemedeki köpürtme sağlanmaktadır.

Polimer köpük malzemeler hücre morfolojisine göre açık veya kapalı hücreli; şişme oranına göre yüksek yoğunluklu, orta yoğunluklu ve düşük yoğunluklu, hücre yoğunluğu ve hücre boyutuna göre mikro hücreli, ince hücreli ve geleneksel

köpükler olmak üzere sınıflandırılırlar. Polimer köpük malzemeler üretebilmek için pek çok geleneksel polimer proses etme yöntemi kullanılabilir. Sürekli prosesler ve batch prosesi, iki farklı polimer köpük üretim yöntemine örnektir. Sürekli prosesler de kendi içerisinde ekstrüzyon köpürtme ve emjeksiyon köpürtme (yarı-sürekli) prosesleri olarak iki farklı grupta incelenebilir.

Ekstrüzyon köpürtme prosesinde, proses esnasında direkt olarak fiziksel köpürtücü ajan enjeksiyonu veya kimyasal köpürtücü ajanın dekompozisyonu ile polimer/gaz karışımı yüksek basınç altında oluşturulur. Proses içerisindeki basınç, polimerin gaz çözünürlük limitinin altındayken gaz, polimer içerisinde çözünür. Polimer/gaz karışımı ekstrüderin kalıp bölgesine geldiğinde ise, burada oluşan ani basınç düşüşü termodinamik bir kararsızlık yaratır. Bu sayede, bu bölgede hücre çekirdeklenmesi ve büyümesi başlar.

Bu tez çalışmasında, çift vidalı ekstrüderde, iki farklı kimyasal köpürtücü ajan kullanılarak, HIPS polimerinin köpürtme davranışı incelenmiştir. Köpürtülmüş numuneleri elde etmek için, 4 mm uzunluğunda ve 2 mm çapında filament kalıbı kullanılmıştır. Kimyasal köpürtücü ajanların birbirinden farklı tarafı ajanların dekompozisyon sıcaklıklarıdır. CBA-1 ve CBA-2 olarak adlandırılan bu iki kimyasal köpürtücü ajanın, diferansiyel taramalı kalorimetri (DSC) ve termal gravimetrik analiz (TGA) cihazları kullanılarak termal özellikleri ve dekompozisyon sıcaklıkları belirlenmiştir.

Proses sıcaklıklarının köpürtme davranışı üzerindeki etkisinin görülmesi amacıyla, CBA-1 için üç, CBA-2 için ise beş farklı ekstrüder kovan sıcaklık profili belirlenmiştir. Her iki köpürtücü ajan için de optimum proses sıcaklık profili belirlendikten sonra, beş farklı kalıp sıcaklığı kullanılarak (en düşük sıcaklıktan en yüksek sıcaklığa kadar), her iki köpürtücü ajan için de denemeler yapılmıştır. Bu deneyler ile, kalıp sıcaklığının HIPS polimerinin köpürtme davranışı üzerindeki etkisi incelenmiş, her iki köpürtücü ajan için de en uygun kalıp sıcaklıkları belirlenmiştir.

Bir sonraki adımda, köpürtücü ajan oranının köpürtme üzerindeki etkisi incelenmiştir. Her iki köpürtücü ajandan da üç farklı oranda (düşük, ortalama ve yüksek oran) kullanılarak deneyler gerçekleştirilmiştir. En uygun köpürtücü ajan oranları belirlendikten sonra, ekstrüder vida dönüş hızının (RPM) HIPS polimerinin köpürtme davranışına etkisi incelenmiştir. Dört farklı vida dönüş hızı (düşük, ortalama, yüksek ve çok yüksek RPM) uygulanmış, ve her iki köpürtücü ajan için de en uygun RPM belirlenmiştir.

Bu tez çalışmasında, HIPS polimerinin köpürtme davranışının incelenmesine, GPPS ve HIPS polimerlerinin farklı oranlarda harmanlanmasıyla devam edilmiştir. Ağırlıkça farklı oranlarında (sadece HIPS, HIPS ve düşük oranda GPPS harmanı, HIPS ve yüksek oranda GPPS harmanı) harmanlar hazırlanarak, GPPS'in köpürtme üzerindeki etkisi, her iki köpürtücü ajan için de incelenmiştir. Sonrasında, çekirdeklendirici ajan olarak farklı oranlarda, üç farklı inorganik katkı kullanılmış ve farklı oranlardaki farklı çekirdeklendirici ajanların, HIPS polimerinin köpürtme davranışı üzerindeki etkisi incelenmiştir. Çekirdeklendirici ajan olarak; düşük, ortalama ve yüksek oranlarda talk, kalsiyum karbonat ve mikro lamel yapıları kullanılmıştır.

Köpürtülmüş HIPS filament numuneleri iki farklı açıdan karakterize edilmiştir. Öncelikle, köpürtülmüş numunelerin yoğunlukları saf su içerisinde ölçülüp, Arşimed eşitliği kullanılarak hesaplanmıştır. Sonrasında, her bir numunenin içerisindeki

boşluk oranları hesaplanmıştır. Ayrıca, taramalı elektron mikroskobu (SEM) kullanılarak, köpürtülmüş numunelerin hücresel yapıları incelenmiştir. İlk olarak, köpürtülmüş HIPS filamentleri sıvı azot altında kırılmış ve her bir numune altın ile kaplanmıştır. Elektron mikroskobunda hücresel yapı tayini yapıldıktan sonra ise, tüm numunelerin hücre boyutları, hücrelerin polimer matriks içerisindeki dağılımları incelenmiş, hücre yoğunlukları hesaplanmıştır.





1. INTRODUCTION

Polystyrene (PS) is an amorphous thermoplastic with a glass transition temperature around 105°C and is widely being used in commodity applications due to its low-cost and reasonable physical and mechanical properties. Among the PS products, the use of PS foams is also of a great interest in variety of commodity applications, such as packaging, cushioning, construction, and food application. This is due to the reduced weight and cost benefit of the foamed samples while not a high mechanical properties are expected in most of the noted applications. PS foams are currently being manufactured in various structures such as extruded PS sheets (XPS), expanded bead foams (EPS), and three-dimensional complex geometries via such manufacturing technologies as extrusion foaming, bead foaming, and foam injection molding, respectively [1].

Extrusion foaming is widely being used in manufacturing continuous simple two-dimensional profiles through which various foam densities could be obtained. The foam morphology in extrusion foaming could be controlled via controlling several parameters such as die temperature profile, die geometry (i.e., L/D ratio), die pressure and pressure drop rate, melt rheological properties, crystallization kinetics of the polymer/gas mixture, and the type and content of blowing agents. Among the blowing agents, despite their high solubility in polymer melts, the use of hydrofluorocarbons (HFCs), hydrochlorofluorocarbon (HCFCs) and hydrocarbons is banned due to their toxic and flammable features. Therefore, the attempts are being made to use green blowing agents such as gas and supercritical CO₂ and N₂ in manufacturing of plastic foams. Among these, however, CO₂ reveals high solubility than N₂ which causes the achievement of lower density foams when using CO₂ [2]. On the other hand, N₂ possesses higher cell nucleation power due to its high diffusivity . During the extrusion foaming, the decrease in barrel temperature increases the solubility of the CO₂ inside the polymer melts whereas the solubility of N₂ increase with barrel temperature increase [3]. In this context, to manufacture continuous foam products, the use of CO₂ or N₂ as PBAs are highly preferred than

CBAAs due to the achievements of foams with more uniform structure and the lower cost of the blowing agents. On the other hand, CBAAs do not require much of side accessories and equipment such as a continuous syringe pump and extruder modifications required when using PBAs. Therefore, a lot of industries might be interested in using CBAAs in order to avoid the modification of their production line.

When the polymer melts along the extruder, with the addition of CBA or injecting the PBA into the melt, polymer/gas mixture starts to be generated under higher pressure and the mixture will be flowing along the extruder. However, the generated pressure must stay beyond the solubility limit of polymer/gas in order to avoid having undissolved gas within the melt along the extruder. The die pressure and the pressure drop rate could be controlled by the die temperature, die geometry, and melt viscosity of the polymer/gas mixture. The sudden pressure drop at the die nozzle creates thermodynamic instability and causes cell nucleation and growth during the foaming step [4]. When the die temperature is too high, the die pressure drops and the gas loss through the hot skin layer of the polymer foam is more likely. Due to the increased gas loss and the low melt strength of the polymer, the cell coalescence would also be more probable. On the other hand, if the die temperature is too low, the polymer melt becomes too stiff to be expanded although the cell nucleation could be promoted with the increased die pressure and pressure drop rate.

Moreover, in order to improve the cell nucleation and to control the growth, and hence the final foams properties, inorganic fillers could be used as cell nucleating agents during foaming. The stress variations around the rigid fillers will generate pressure variation which causes heterogeneous cell nucleation around these solid particles. In the case of low melt strength polymers, the existence of these fillers could also improve the melt strength during the foaming and thereby the cell coalescence could be hindered while more expansion could be obtained.

In 1993, it is [5] illustrated the microcellular foaming of HIPS through extrusion foaming using CO₂ as PBA. They showed that the cell size reduction is highly dependent on the pressure drop rate and the L/D ratio of the filamentary die. They also observed that increasing the die pressure and the melt strength by lowering the die temperature profile profoundly increases the cell nucleation. Park et al. also showed that the increase in CO₂ content increases the cell density of HIPS foams.

This was also shown by Shimbo et al. during the extrusion foaming of PS when using CO₂ as the PBA [6].

In this thesis study, we investigated how the processing parameters and materials modification influence the extrusion foaming behavior of HIPS when using CBA. Moreover, the variations of foam morphology were explored when using HIPS blends with GPPS and composites by adding inorganic fillers.





2. LITERATURE REVIEW

2.1 Polystyrene

2.1.1 History

Polystyrene was discovered in 1839 by Eduard Simon who is an apothecary in Germany but he did not have any idea about what he had discovered [7]. Soon after that, in 1845, John Blyth and August Wilhelm von Hofman discovered that styrene and meta-styrene's empirical formulas were the same [8]. In 1866, French chemist Marcelin Berthelot determined the formation of metastyrol from styrol as a polymerization method. In 1922, one more step was taken when Moureu and Dufraisse discovered that the monomer could be stabilised with the addition of small amounts of aromatic amines and phenols. After that, the reaction had been used to study the mechanism of polymerisation during the 1920s [7].

Finally, all works done by Herman Staudinger and Carl Wolff gave an opportunity to the I.G Farben company in Germany to start the production of PS in 1931. A reactor vessel created by them enabled the PS to be extruded through a heated tube and cutter so this led to the polymer being molded into a pellet form which was easier to use.

2.1.2 Structure

PS is produced by the polymerization technique which is free radical vinyl polymerization [9]. There is a long hydrocarbon chain in its chemical structure which has the phenyl group attached to every other carbon.

Polymerization

Addition polymerization from the styrene monomer units is the production method of PS. The direct catalytic dehydrogenation of ethyl benzene is the principal route of styrene production:

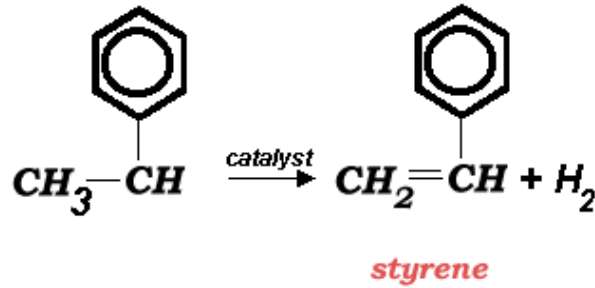


Figure 2.1 : Styrene part production [12].

The heat of reaction in Figure 2.1 is -121 kJ/mol (endothermic) and almost 65% of styrene is reacted to produce polystyrene. The overall reaction of styrene polymerization is shown in Figure 2.2.

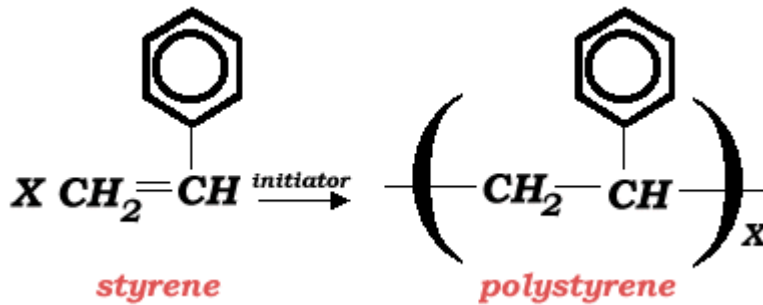


Figure 2.2 : Polymerization of styrene [13].

That reaction is obtained in an inert organic solvent and it supplies the reaction medium for the cationic polymerization reaction. The mostly known solvent for that reaction is 1,2 -dichloroethane (EDC). In addition to this, there are various solvents which are suitable for this reaction e.g: Carbon tetrachloride, ethyl chloride, methylene dichloride, benzene, toluene, ethylbenzene, or chlorobenzene and a mixture of boron trifluoride and water is preferred as initiator [10].

There are three methods for styrene polymerization:

1. Solution (bulk) polymerization
2. Emulsion polymerization
3. Suspension polymerization

Solution polymerization

The most of PS is produced by solution polymerization which is also known as mass polymerization in the industry. There are two different types of solution polymerization which are batch and continuous. Generally, styrene monomer or ethyl

benzene are used as solvents in this process. Continuous mass polymerization is more preferred to produce of PS nowadays. The holding vessel is used for preparation of the solution and then it is injected to the reactor system.

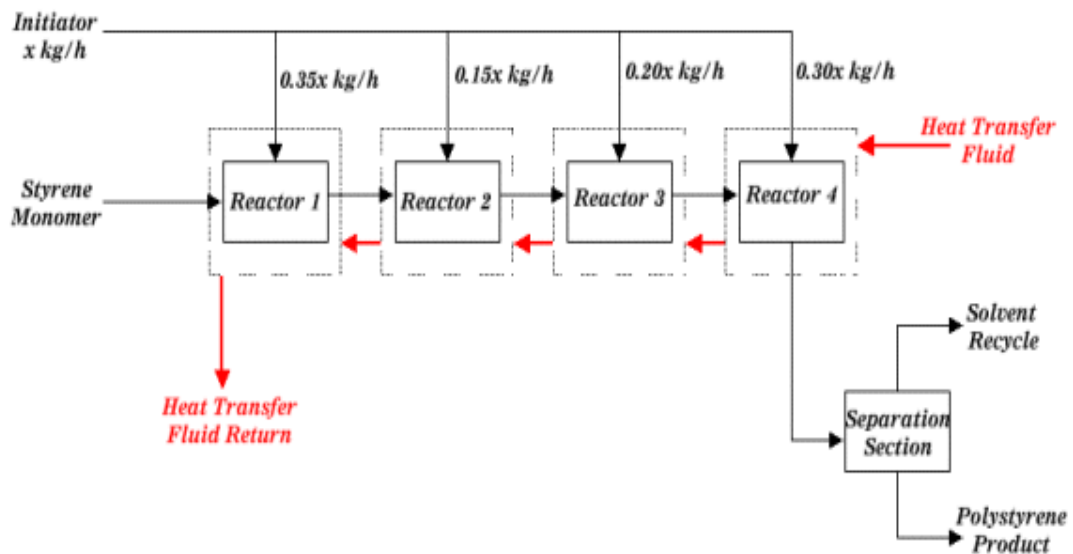


Figure 2.3 : Polystyrene manufacturing diagram [14].

As it is shown in Figure 2.3, Reactor 1 contains 50% weight of styrene monomer, 2000 ppm boron trifluoride and 100 ppm water based on styrene weight and also the balance being organic solvent. Then, the reaction of polymerization occurs and releases heat to the system. The temperature of the reaction change between 40°C and 70°C which can also be arranged by tube heat exchangers and intermediate shell [10].

Emulsion polymerization

With the help of emulsion polymerization, styrene polymerization with other monomers or polymers can be achieved. The most popular usages of emulsion polymerization is production of GPPS or HIPS. Unless the monomer droplets of emulsion polymerization are microscopic in size, emulsion and suspension polymerization are similar in many aspects [10].

Suspension polymerization

Suspension polymerization has an advantage to manufacture large scale polymers of high average molecular weight. Many kinds of properties and processing characteristics are obtained with different polymerization circumstances. All stages are provided by the manufacturers to meet the various requirements of the conversion process and the final product. There are various ways of suspension

process to manufacture PS. The most popular of them is batch process. On the other hand, continuous process is not work but there is no reason to explain why this is not suitable. When the styrene drops' diameter are small as 0.15-0.50 mm, the reaction occurs and they are suspended in water. In order to assist that the styrene drops have appropriate size, the suspending agent is used and to keep these drops at the same size, the stabilizing agent is added. Also the catalyst is added to keep under control the reaction rate. When it is compared with single phase techniques, suspension polymerization is more advantageous but the requirement of dispersing agent could be a problem [10].

2.1.3 Types of PS

HIPS and GPPS are the main types of PS. GPPS has the clear resin appearance and it is named as crystal in plastic sector. It is transparent, and has perfect electrical properties, high stiffness, low cost and low specific gravity, thus this resin is preferred commercially. Easy flow GPPS, medium flow GPPS and high heat GPPS are the types of GPPS. They are classified according to the production method and melt flow properties. For instance, the injection molded GPPS products are produced by using easy and medium flow grades [12]. HIPS is the immiscible blend of PS and PB rubber including 5-15 % wt. PB. The former is also known as graft-high impact strength polystyrene and it is assigned by Ontological-suspension polymerization and bulk polymerization system. For this reason, HIPS is one of the lowest cost plastic and moreover it's process is very simple. Therefore, it is used when the cheapness, impact resistance and machinability are needed [11]. Figure 2.4 shows the transmission electron microscope (TEM) images of HIPS and the butadiene rubber is seen in polymer matrix clearly [15]. It is also food contact material and can be used in applications containing foods. Table 2.1 shows the comparison of PS, HIPS and GPPS materials.

Table 2.1 : Properties of HIPS and GPPS [18-20].

Properties	Units	PS	HIPS	GPPS
Density	g/cm ³	1,06	1.04	1.05
Melt Flow Index	g/10 min	2	3	5
Tg (DSC)	°C	100	110	97
Tensile Strength	kg/cm ²	345-483	240	480

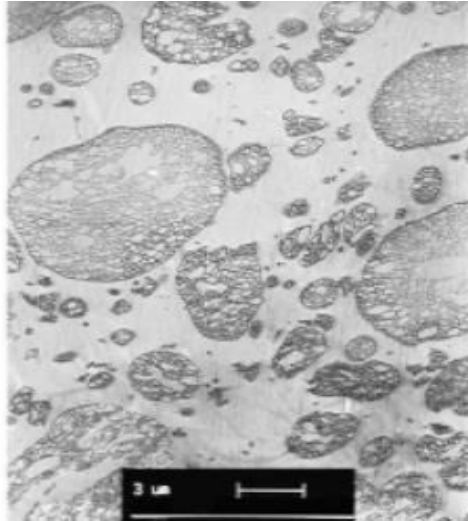


Figure 2.4 : TEM Images of HIPS [15].

2.1.4 Properties

2.1.4.1 Mechanical

While the impact strengths of GPPS material is very low which are less than 0.5 ft-lb, commercial grades of PS has between 1.0 ft-lb and 4.0 ft-lb. The polymerization process have restraints and because of that, polystyrenes are not produced more than 15% of total rubber. Increasing the rubber content, impact resistance of PS also increases, while the strength decreases. In addition, there are some different techniques to increase the impact properties without adding the rubber such as gel percentage control, grafting percentage control, cross-linking etc. While some of GPPS grades show the as low as 1% elongation, some of HIPS grades have so much higher elongation property [13].

2.1.4.2 Chemical

One of the most important situation for PS is the solvent crazing. Especially, this crazing phenomena can be shown between the PS matrix and the rubber particles in HIPS. This is also called as ESCR (environmental stress crack resistance) behaviour of rubber contained PSs. Content and dimension of rubbers, gel and grafting percentages are affected the amount of stress cracking resistance [16].

2.1.4.3 Processing

When the PS production is considered, the most critical flow properties are the flow properties. Solution viscosity and MFI (Melt flow index) are the most important

displays of industrial techniques to measure the flow properties. Viscosity of solution is measured as an 8% solution in toluene. When the molecular weight increases, solution viscosity also increases. On the other hand, MFI of PS is measured by using melt flow indexer and it can be kept under the control with some additives during processing. The MFI of PS varies between 1 to 50 g. per 10 minute and mostly between 2 to 20 g. per 10 minute [17].

2.1.5 Applications

The mostly used area of PS is packaging applications especially in the form of EPS (expanded polystyrene) in order to protect the products such as egg and poultry boxes, against unexpected damages. It is used nearly whole production groups of home appliances and white goods industry such as coolers, ovens, microwaves etc. Its usage area in electronics are very significant because it is expanding day by day with developing technology. It is used for all equipment in IT sector and also for TV's. It is also used for media enclosures, CD's, DVD's etc. When the building and construction activities are considered, most preferred material is PS for many reasons such as its perfect feasibility, good processability. For instance, insulation foam, siding, roofing, panels, bath units, shower units etc. In medical aspect, the PS resins are preferred widely, because of its property of disposable. Tissue culture trays, test tubes, diagnostic components, petri dishes are some example of disposable materials in medicine. PS is used for many consumer goods applications because it has optimum cost per performance ratio and so, it can be preferred instead of more costly polymers. There are various traditional uses of PS and some of them are toys, kitchen and bath accessories, electric lawn and garden equipments [14].

2.2 Overview of Plastic Foaming

2.2.1 Background of foaming

Polymer foaming is a technique of processing which is used the chemical and physical blowing agents in various processes: bead foaming, foam extrusion, foam injection molding etc. The cellular structure is formed in a polymer matrix. The growth trend of polymer foaming is increasing day by day because of the benefits of foaming technology. There are many advantages of foamed products such as lightweight materials, cost advantage, good dielectric properties, good thermal

resistance etc. [19]. The price of polymeric resins increase day by day and the manufacturers use the this technology to reduce the raw material costs. Foaming technology is used in many application areas and sectors thanks to these advantages. Automotive, construction, packaging, furniture, electrical, household, boimedical and pharmaceutical are some of those sectors [20-27]. The properties of final foam product depends on many factor thr polymer matrix, type of blowing agent and the cell structure control.

In foaming process, the gas bubbles are entrapped in polymer melt as the material getting harder. There are two main foaming process which are chemical and physical foaming processes. The cehmical blowing agent decomposes by the reaction of endothermic or exothermic and the gas is produced in polymer matrix and the cellular structure occurs. Moreover, in physical foaming, the gas is directly injected to the system and dissolves into the polymer matrix. Cell nucleation, cell growth and cell stablization follows it, respectively.

Conventional polymer foams having the maximum number of cell density of 10^6 cells/cm³ and the cell size s around 100 μ m. Besides, microcellular foams having the minimum number of cell density is 10^9 cells/cm³ and the cell sizes less than 10 μ m. There are four factors that affect the microcellular foam characteristics which are expansion ratio, cell density, cell integrity and cell sizes, also the final foam morphology is directed by three factors: cell nucleation, cell growth and cell coarsening [28].

There are various types of classifications of foamed polymers. They are classified as low and high density foams by density, fine celled, microcellular or nanocellular foams by cell density and size, closed or open celled foams by structure.

2.2.2 Foaming concepts and classifications

2.2.2.1 Cell dimension and structure

Cell density and cell size classification

Cell density is a definition meaning the counting of cells per unit volume regarding to neat polymer. The number of cells are counted from the micrographs taken with an optical microscope or scanning electron microscope. It can be calculated with following equation:

$$\text{Cell Density} = \left(\frac{n}{A}\right)^{3/2} \cdot \frac{\rho_{\text{polymer}}}{\rho_{\text{foam}}} \quad (2.1)$$

According to this equation; A is the area that is measured, M is the magnification of image and the n is the number of cells that is counted from the image [29].

Polymeric foams are classified according to their cell sizes to four main groups:

- Macrocellular (>100 μm),
- Microcellular (1–100 μm),
- Ultramicrocellular (0.1–1 μm)
- Nanocellular (0.1–100 nm).

When the microcellular and macrocellular foams are compared, the cell sizes are smaller, the cell density is much as higher and the cell distribution is more homogenous for microcellular foam structures. It has superior properties than macrocellular structure because the decreasing the cell size the increasing the cell density is important issue for foaming [30].

Open or closed cell foams

When the open and close cell foams are compared, the main difference is the cell wall structure of each foams. The cell walls are closed and surrounded by each others in close cell foam as it is seen in Figure 2.5. In contrast, the cell walls are open and the air can pass freely between the cells in open cell foam structures [31].

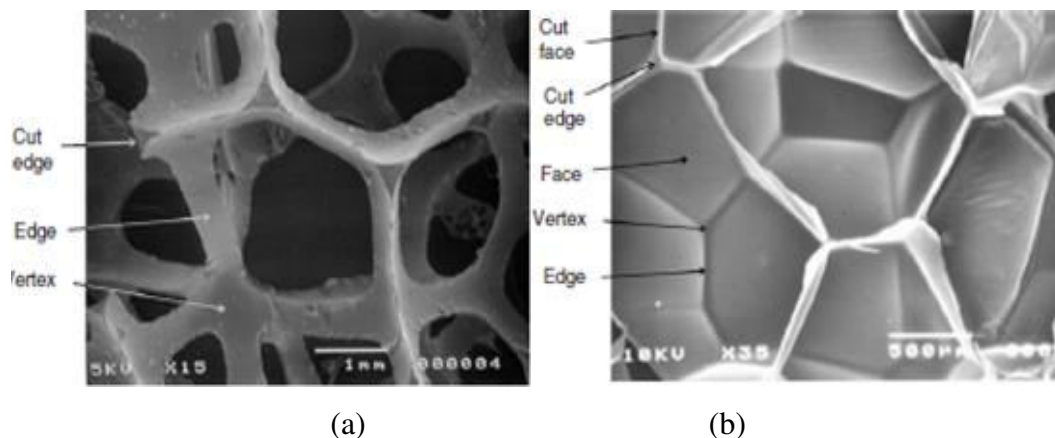


Figure 2.5 : SEM image of (a) open-cell foam; and (b) closed-cell foam [32].

For open cell foams, the foam's stiffness is concluded according to various models which are depend on the cell structure. These models are important to investigate the

foam behavior. One of this theorem is the simple beam theorem and the individuals are cubic and it can be applied:

$$\frac{E^*}{E_S} = C_1 R^2 \quad (2.2)$$

in which C_1 is a constant and $C_1 \approx 1$ [33].

Open cell foams have spongier appearance and strong sound barrier properties. They can be used for applications required silent atmosphere and also they are soft structures [34, 35].

On the other hand, close cell foams have lower permeability and insulation properties and stronger than open cell foams, because of the closed cell walls. The below equation can be used in order to conclude the Young's model for closed cell structures:

$$\frac{E^*}{E_S} = \varphi^2 R^2 + (1 - \varphi) + \frac{\rho_0}{E_s(1 - R)} \quad (2.3)$$

indicates the fraction of solid in the cell faces $(1 - \varphi)$.

Foam Density

The density is one of the most important parameter for foamed structures. This is because the volume expansion ratio and the void fraction of foams are calculated by using the foam density. All of these terms show the amount of material saving and the volume of voids in a material and also directly related with cost reduction. The foam density is calculated from equation 2.4. According to this formula, M is the mass of foam sample and V is the volume of foam sample, (cm^3).

$$df = \frac{(M)}{(V)} \quad (2.4)$$

High density foams, medium density foams and low density foams are three types of polymer foams respect to density. The density of high density foams is between 500 kg/m^3 - 1000 kg/m^3 , medium density foams is between 100 kg/m^3 - 500 kg/m^3 , and the low density foams is below the 100 kg/m^3 . Each of them has own application areas according to densities [36-38].

The void fraction (V_f) is defined the amount of voids in a foamed structure and it can be calculated by using following formula:

$$V_f = 100. \left(1 - \frac{\rho_{foam}}{\rho_{polymer}}\right) \quad (2.5)$$

In addition of void fraction, the volume expansion ratio also shows the how many times polymer density has decreased and it can be calculated by using following formula. It is the ratio of neat polymer bulk density to foamed polymer bulk density [39].

$$VER(\varphi) = \frac{\rho_{polymer}}{\rho_{foam}} \quad (2.6)$$

2.2.3 Blowing agents for foaming

The use of blowing agents are necessary in order to obtain foamed structure in foaming process. They dissolve in polymeric matrix and expands according to thermodynamical conditions. According to formation of gas, the blowing agnets can be clasified in two types which are CBAs and physical blowing agents. CBAs are in the form of solid granules or powder and they decompose and generate gases at the temperatures higher than CBA decomposition temperature during processing. On the other hand, PBAs are in the form of gas, liquid or super-critical and they are directly injected into the polymer matrix during processing [40].

2.2.3.1 Physical blowing agent

In 1935, the first admission is published about foamed PS [41]. In the past, the liquids having low boiling points (butylene, methyl chloride etc.) are used as PBAs. In huge vessels, these PBAs dissolve in PS and this solvent heated and pressurized. After that, the solvent is volatilized and the PS is expanded. Years after, this process turns in to extrusion process and the PS is foamed in extrusion with various PBAs and different type of foamed products are manufactured [42].

In direct gassing technique, the gas is directly injected into the polymer matrix and dissolved, after the polymeric melt reaches the atmospheric conditions, the foamed product is formed [43,44].

Among the blowing agents, despite their high solubility in polymer melts, the use of HFCs, HCFCs and hydrocarbons is banned due to their toxic and flammable features [45-48]. Therefore, the attempts are being made to use green blowing agents such as gas and supercritical CO₂ and N₂ in manufacturing of plastic foams [49]. Among

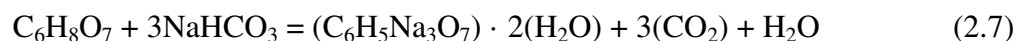
these, however, CO₂ reveals high solubility than N₂ which causes the achievement of lower density foams when using CO₂ [50-51]. On the other hand, N₂ possesses higher cell nucleation power due to its high diffusivity [52]. During the extrusion foaming, the decrease in barrel temperature increases the solubility of the CO₂ inside the polymer melts whereas the solubility of N₂ increase with barrel temperature increase [53-56]. In this context, to manufacture continuous foam products, the use of CO₂ or N₂ as PBAs are highly preferred than CBAs due to the achievements of foams with more uniform structure and the lower cost of the blowing agents.

2.2.3.2 Chemical blowing agent

CBAs decompose within a certain temperature during processing. They can be used alone as blowing agent and also as a nucleating agent in the process of direct gas foaming. The processing temperature must be arranged considering to decomposition temperature of CBA. The temperature of polymer matrix melt should be higher than decomposition temperature of CBA.

There are two types of CBAs in terms of endothermic and exothermic CBAs according to generated gas. While the endothermic CBAs generate CO₂, exothermic CBAs generate nitrogen (N₂) after decomposition. The endothermic CBAs consist of sodium bicarbonate and citric acid in their chemical structures. The changing ratio of sodium bicarbonate to citric acid in blend affects the decomposition temperature of CBA. The following equation shows the endothermic decomposition reaction for these types of CBAs. As it is seen clearly, CO₂ gas generates after decomposition.

Citric acid + Sodium bicarbonate = Sodium citrate dihydrate + Carbon dioxide + Water



As it is mentioned in PBAs part, CO₂ has higher solubility than N₂ in polymers. Therefore, to work with endothermic CBA is easier and also process controlling is more simple than exothermic CBAs. In addition, endothermic CBAs generate better surface quality, finer cells and higher void fractions comparing to exothermic CBAs.

Moreover, as a nucleating agent, the performance of endothermic CBAs for nucleation is better than inactive nucleators as talc. In general, endothermic CBAs are three to five times more effective than talc in nucleating direct gassed foams, but can be up to eight times more efficient [57]. Endothermic CBAs are the most

commonly utilized types for nucleation and are used over less expensive nucleators, such as talc, when finer-celled foam products are required.

The exothermic CBAs with a known name azodicarbonamides includes 65% N₂, 24% CO, 5% CO₂, 5% NH₃ in their chemical structure. The response of azodicarbonamide can take off residual materials as plateout, on kick the tooling of die and mold. Suitable utilize of added substances can minimize or reduce this problem. [58]. On the other hand, CBAs do not require much of side accessories and equipment such as a continuous syringe pump and extruder modifications required when using PBAs. Therefore, a lot of industries might be interested in using CBAs in order to avoid the modification of their production line.

2.2.4 Plastic foaming mechanism

2.2.4.1 Formation of polymer/gas solution

The formation of polymer gas solution is the first step of the foaming mechanism. After the direct gas injection or decomposition of CBAs in polymer matrix, the generated gas dissolves under high pressure and temperature during processing. One of the most important thing is, the polymer gas solubility limit changes according to changing process temperatures and pressures and also extra gas does not dissolve in polymer matrix. The extra undissolved gas is undesirable situation for foaming processing because the large gas voids can be formed and the result is poor foam structure. Figure 2.6 shows the formation of one phase polymer gas solution [4].

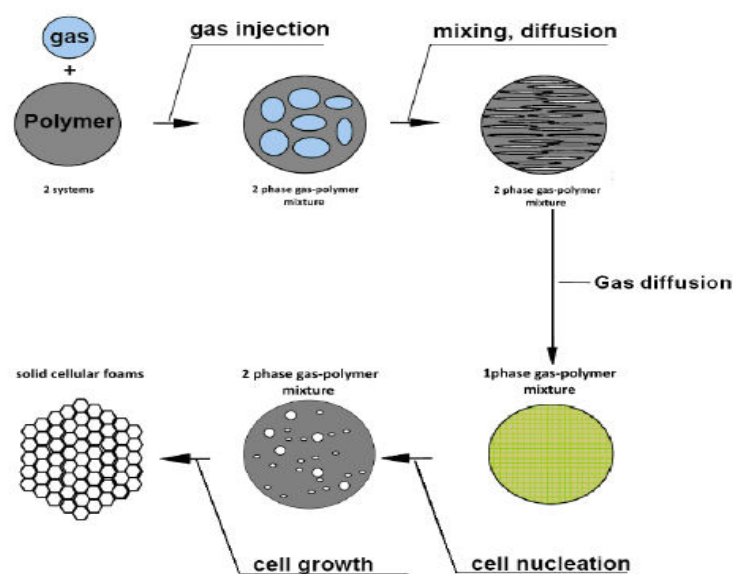


Figure 2.6 : Polymer foaming process by using a physical blowing agent [59].

Solubility

Solubility limit can be defined as the maximum amount of gas that can be dissolved into the polymer matrix. During process, because of the high pressure, the blowing agent starts to diffuse into the polymer matrix, and then diffusion continues until a certain limit of blowing agent concentration is reached. The limit of solubility only could be obtained at time infinity, theoretically. The following equation shows the calculation of instantaneous concentration of the blowing agent in the polymer [60]:

$$\frac{M_t}{M_\infty} = 1 - \frac{8}{\pi^2} \sum_{m=0}^{\infty} \frac{1}{(2m+1)^2} \exp\left[-\frac{D(2m+1)^2\pi^2 t}{h^2}\right] \quad (2.8)$$

In this formula;

D = diffusivity, cm^2/s ,

M_t = mass uptake at time t , g,

h = sheet thickness, cm,

M_∞ = equilibrium mass uptake after an infinite time, g,

t = elapsed time, s.

The absorption time is sufficiently adequate, the mass uptake amount inevitably tends to Maximum achievable amount level, M , which is identified with the limit of the gas solubility in the plastic. The solubility limit can be calculated the mass uptake (M) over the mass of the plastic specimen.

The gas solubility in a molten polymer is explained by the following equation [61]:

$$S = H \cdot P,$$

According to this equation; S is solubility, H is Henry's law constant, and P is gas pressure.

For each polymers, Henry's law constant shows different values for each gas. For instance, CO_2 has 1.5 to 4 times Henry's law constant relative to N_2 . Therefore, the solubility of CO_2 has 2.5 times than N_2 in polyethylene as it is indicated in blowing agents part. This results as the required pressure in order to keep the N_2 in polymer melt is much higher than CO_2 [62].

According to Hnery's rule; H is a constant and function of temperature and can be defined by following equation.

$$H = H_0 \exp\left(-\frac{\Delta H_s}{RT}\right) \quad (2.9)$$

R = gas constant, J/K,

T = temperature, K,

H_0 = solubility coefficient constant, cm³ [STP]/g-Pa,

ΔH_s = molar heat of sorption, J.

According to this equation for most plastics, ΔH_s is negative with the CO₂ is penetrant [57]. The solubility of blowing agents under certain pressure and temperature can be calculated by using the combination of these equations. For instance, the solubility of CO₂ is nearly 11 wt. % in PS under the temperature of 200 °C and pressure of 27,6 MPa [4].

The proportion of flow rate of gas to polymer is critical for extrusion system. According to flow rate of polymer, the gas flow rate also detected and the gas to polymer weight proportion should be kept under the solubility limit. As it is seen in Figure 2.7, the CO₂ solubility decreases when the temperature also increases in PS. In contrast, the solubility of N₂ increases with an increase in temperature [63].

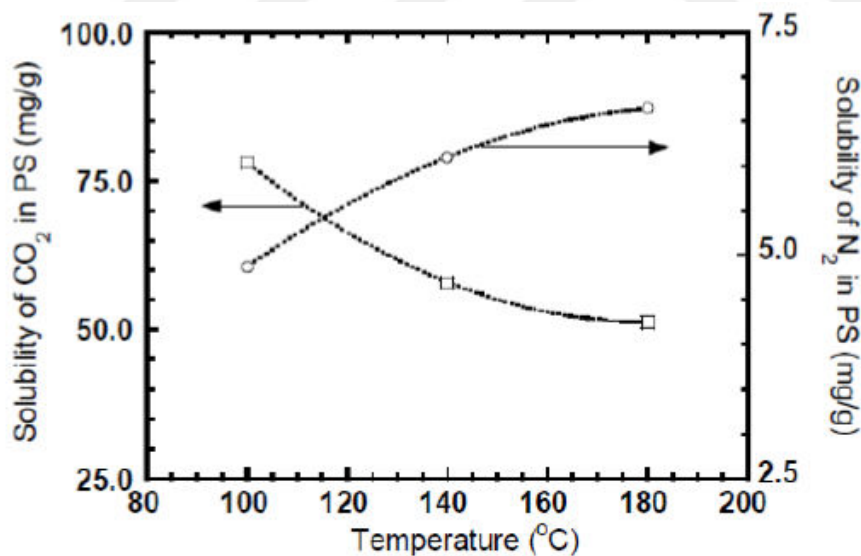


Figure 2.7 : CO₂ and N₂ solubility in PS [63].

As shown in Figure 2.8, the solubility of CO₂ and N₂ in PLA at 180 and 200 °C. The solubility of N₂ in PLA increases as the pressure increases. When it is compared with CO₂, the solubility of N₂ in PLA was much less. The maximum solubility of N₂ in PLA can reach up to 0.0174 g gas/g polymer within the pressure range of interest. When the temperature increased, the solubility of CO₂ in PLA decreased

significantly no matter what EOS was applied. The maximum solubility of CO₂ in PLA at 27.89 MPa was 0.2131 g gas/g polymer at 180 °C and 0.1752 g gas/g polymer at 200 °C when the SL-EOS was employed [54].

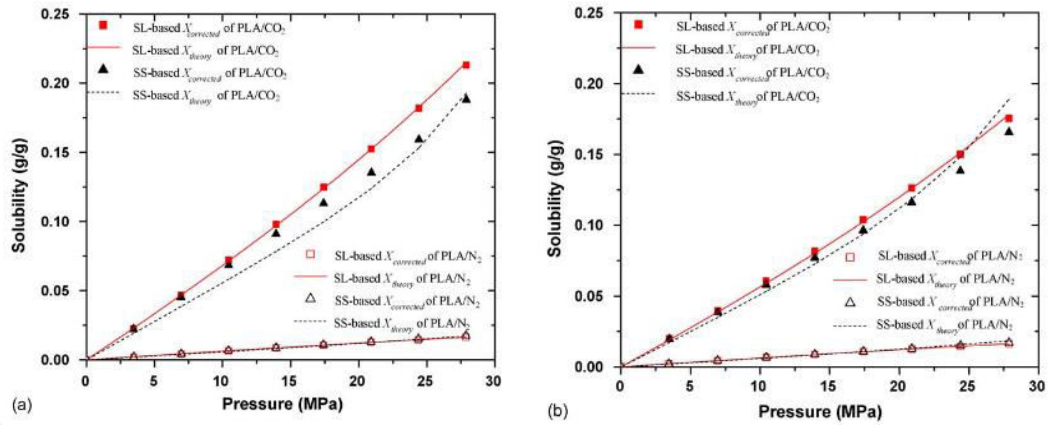


Figure 2.8 : CO₂ and N₂ solubility in PLA at: (a) 180 °C and (b) 200 °C [54].

The solubility of CO₂ increases with an increase in pressure and decreases with increasing temperature. There are two phenomena when a polymer exposed to high pressure gas: Firstly, decreasing the specific volume of polymer gas mixture and the secondly swelling. Normally, when the high pressure gas faces with the polymer, swelling is the more asserting factor. Dissolved CO₂ causes a plasticization effect that reduces the viscosity of the polymer/gas mixture. Because of the rising in free volume due to the swelling of the polymer/gas mixture and reduction in surface tension, the chain mobility is increased [56]. Figure 2.9 and 2.10 also shows the solubility behaviour of CO₂ in PLA 8051D at different temperature and pressures [55].

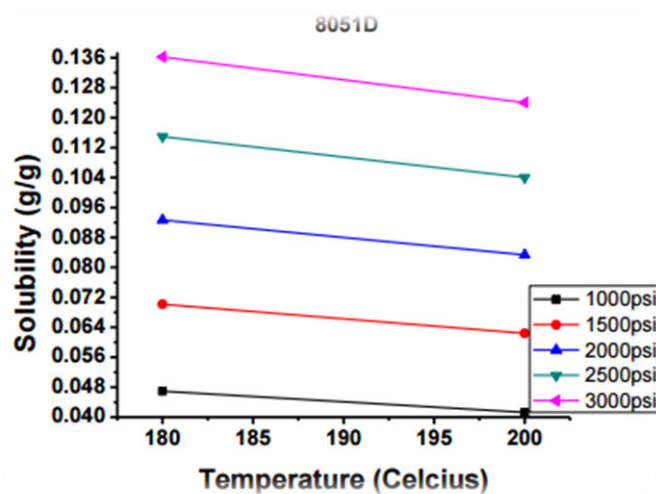


Figure 2.9 : Temperature effect on solubility of PLA8051D [55].

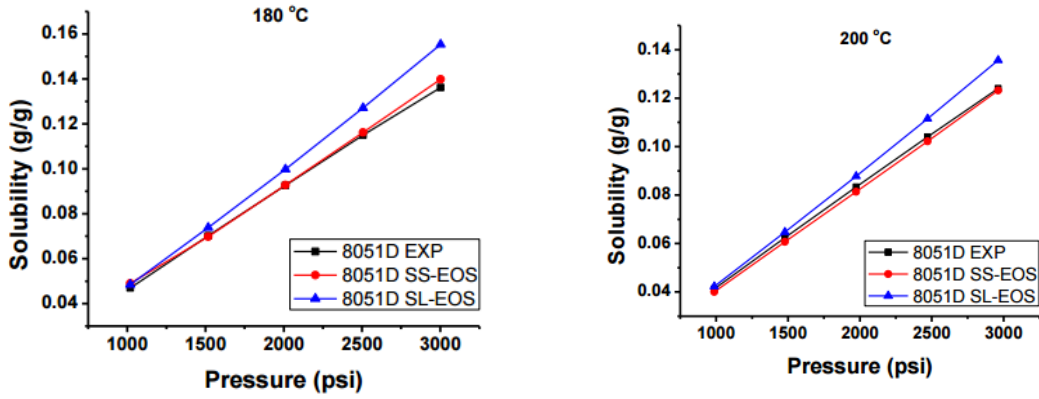


Figure 2.10 : Solubility of CO₂ in PLA8051D at 180 °C and 200 °C with different pressures [55].

Diffusivity

In Figure 2.11, the diffusivity of the blowing agent into polymer matrix is shown as slope of the curve. By using this slope, the diffusivity is calculated according to following equation [54]:

$$D \cong \frac{0.04919}{\left(\frac{t}{h^2}\right)^{\frac{1}{2}}} \quad (2.10)$$

In this formula, $(t/h^2)^{1/2}$ is the value of (t/h^2) at $Mt/M_\infty = 1/2$.

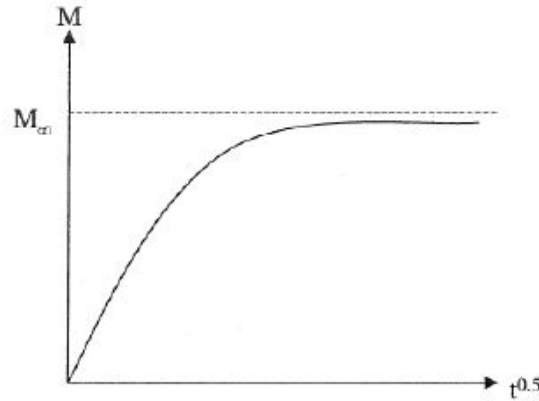


Figure 2.11 : The system of general gas/polymer sorption isotherm [54].

The next formula also explains the time required for ending up the absorption.

$$t_D \cong \frac{\pi h^2}{16D} \quad (2.11)$$

t_D = time of absorption

D = diffusivity

$h/2$ = diffusion distance

In this formula, diffusivity (D) is the temperature function, and the following equation shows the relationship between and the temperature [54,63]:

$$D = D_0 \exp\left(-\frac{E_d}{RT}\right) \quad (2.12)$$

D_0 = diffusivity coefficient constant, cm^2/s ,

E_d = activation energy for diffusion, J.

The graph of temperature versus diffusivity for PS matrix with CO_2 system is seen in Figure 2.12. It is clearly shown that, the diffusivity value at 25 °C ($6 \times 10^{-8} \text{ cm}^2/\text{s}$) is lower than the diffusivity value at 200 °C ($1 \times 10^{-5} \text{ cm}^2/\text{s}$). It is known that 25 °C is batch foaming temperature and 200 °C is the extrusion temperature. This means, in extrusion process the diffusion rate is faster than in batch foaming process. [60].

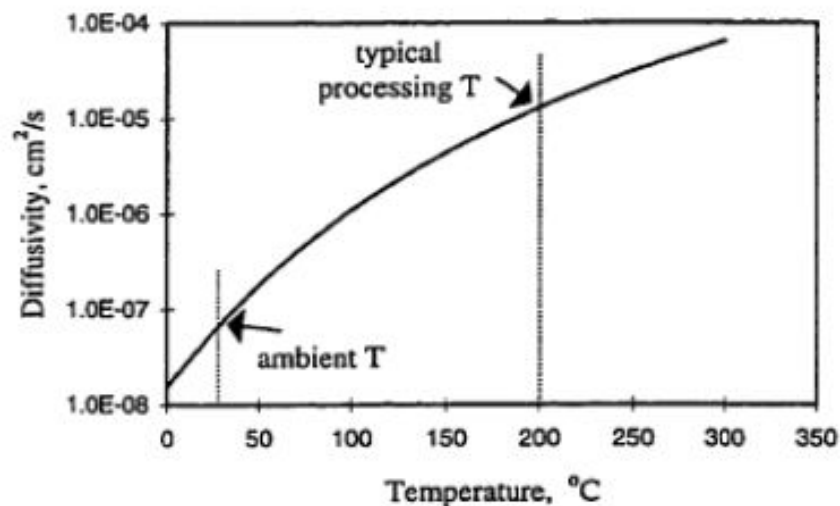


Figure 2.12 : CO_2 diffusivity in PS with varying temperature [60].

As it is noticed earlier, when the temperature is increased, the diffusion coefficient also increases. In addition, N_2 has higher diffusion coefficient than CO_2 . The Figure 2.13 clearly shows that, with an increase in gas pressure the diffusivity decreases for both N_2 and CO_2 . This may be because of the hydrostatic pressure due to free volume loss in the system. According to solubility experimental results performed for PLA melts with CO_2 and N_2 , the apparent differences are observed. While the solubility of N_2 up to 2 %, the CO_2 solubility up to 20 %, and also N_2 illustrated higher diffusivity than CO_2 at the same temperature [54].

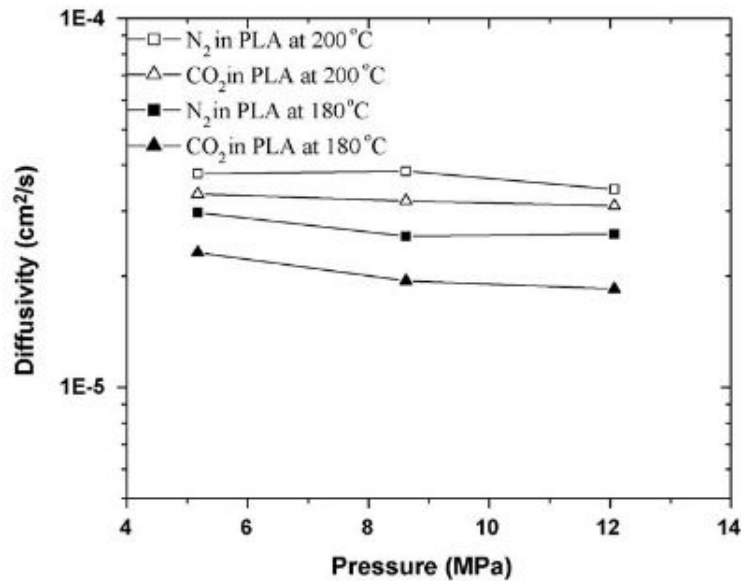


Figure 2.13 : N₂ and CO₂ diffusivity in PLA at 180 and 200 °C [54].

Dissolution

The fully dissolution of gas in polymer matrix is so important in order to obtain perfect foam structure. If higher amount of gas than solubility limit is injected to polymer matrix, the excess gas could not dissolve and the large gas voids form in continuous process. The most critical point is to inject gas below the solubility limit. On the other hand, the gas injection below the solubility limit does not mean the single phase polymer-gas formation is certain. The another important point for fully dissolving is the required time for gas diffusion. The time must be less than the melt residence time. The mixing screw and other equipments (static mixer etc.) are also critical for this situation. The diffusion process is affected from the type of mixing screw [4,64]. All in all, the blowing agent injection below the solubility limit of polymer and improving dissolution and diffusion are the key parameters in order to obtain single phase polymer gas solution.

2.2.4.2 Fundamentals of cell nucleation

In order to obtain foamed structure, polymeric materials generally should be processed in various methods such as foam extrusion foam injection molding and batch foaming. While in physically foaming direct gas injection leads to cell formation, in chemically foaming by the decomposition of CBAs, gas is generated and cells form. In both situations, the cellular structure occurs due to the thermodynamic instability. A minimum required energy to system should be given in order to form cells in

polymer matrix. This energy is obtained by pressure drop or heat. Generally, foaming process is based on some steps: (i) dissolution of gas in a polymer matrix; (ii) cell nucleation; (iii) cell growth; and (iv) stabilization of foam structures [65]. The classical nucleation theory (CNT) is based on homogeneous nucleation and heterogeneous nucleation. In addition, there is another nucleation theory which is pseudo-classical nucleation. Figure 2.14 shows the both homogenous and heterogenous nucleation mechanisms.

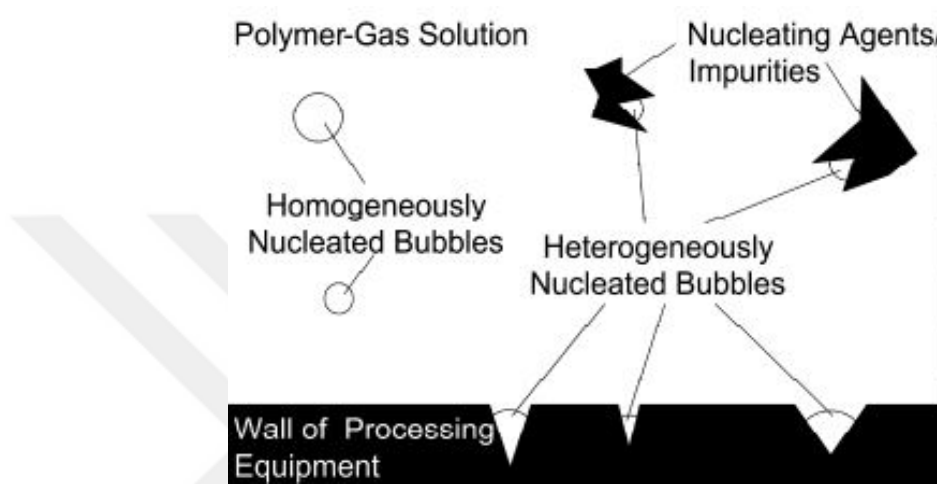


Figure 2.14 : The schematic of homogeneous and heterogeneous nucleation [67].

Homogeneous nucleation

In microcellular foaming, Colton and Suh [67-68] explained a nucleation behavior according to classical nucleation theory. The thermodynamic systems include two objects which are polymer melt and the dissolved gas in foaming process. When the polymer melt or polymer matrix is on the side of cell nucleation, the homogeneous formation of a cells (ΔF_{hom}) can be expressed as

$$\Delta F_{hom} = -(P_{bub} - P_{sys})\Delta V_g + \gamma_{lg}A_{lg} \quad (2.13)$$

P_{bub} = the pressure inside the bubble;

P_{sys} = the surrounding system pressure

V_g = the bubble volume

γ_{lg} = the interfacial energy at the liquid-gas interface.

A_{lg} = surface area at the liquid-gas interface.

According to the equation, Figure 2.15 shows general relationship between ΔF_{hom} and the bubble radius. r_{cr} means critical radius in this figure.

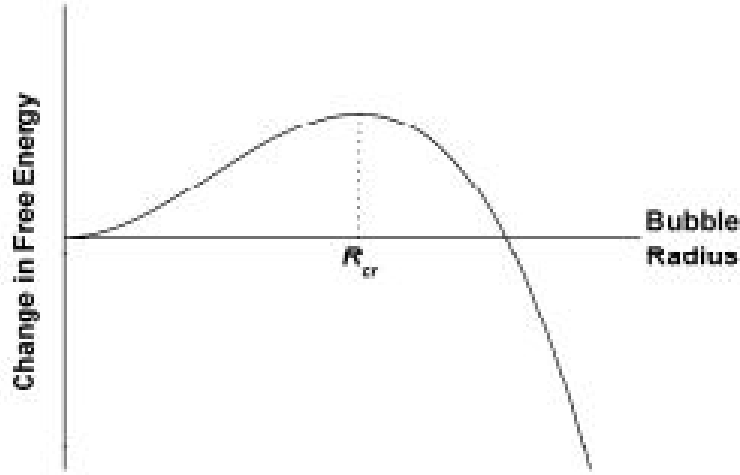


Figure 2.15 : Homogenous bubble nucleation free energy change [69].

The free energy value is related to critical radius of cell or bubble. If the maximum free energy change is required for homogenous forming, it shows unstable equilibrium in the system. If the nuclei or core is smaller than critical radius of cell, it is collapsed. However, the nuclei is larger than critical radius of cell, it will be expanded. The derivative of ΔF_{hom} with respect to the R_{bub} taken and setting it to zero, R_{cr} is defined as [63-64]:

$$R_{\text{crt}} = \frac{2\gamma_g}{P_{\text{bub},\text{cr}} - P_{\text{sys}}} \quad (2.14)$$

In this formula, $P_{\text{bub},\text{cr}}$ is the pressure inside a critical bubble. Free energy barrier for homogeneous nucleation (W_{hom}) is expressed by combining equations in above as [64]:

$$W_{\text{hom}} = \frac{16\pi\gamma_{lg}^3}{3(P_{\text{bub},\text{cr}} - P_{\text{sys}})^2} \quad (2.15)$$

The critical bubble is at an unstable equilibrium state which is surrounded by polymer-gas mixture. It is a fact that R_{cr} and W_{hom} are functions of γ_{lg} and the degree of supersaturation according to above equations. μ_g , and $\mu_{g,\text{sol}}$ are the chemical potential of gas in bubble and in polymer gas solution, respectively. $P_{\text{bub},\text{cr}}$ can be determined as equating μ_g , and $\mu_{g,\text{sol}}$ as it is expressed in following equations.

$$\mu_g(T_{\text{sys}}, P_{\text{bub},\text{cr}}) = \mu_g(T_{\text{sys}}, P_{\text{sys}}) + k_B T_{\text{sys}} \ln\left(\frac{P_{\text{bub},\text{cr}}}{P_{\text{sys}}}\right) \quad (2.16)$$

$$\mu_{g,\text{sol}}(T_{\text{sys}}, P_{\text{bub},\text{cr}}, C_R) = \mu_g(T_{\text{sys}}, P_{\text{sys}}) + k_B T_{\text{sys}} \ln\left(\frac{C_R}{C_{\text{sat}}}\right) \quad (2.17)$$

T_{sys} = the systems absolute temperature

k_B = the Boltzmann constant

C_r = the gas concentration

c_{sat} = the saturated gas concentration

$$P_{bub,cr} = \frac{C_R P_{sys}}{C_{sat}} \quad (2.18)$$

This could also be rewritten as:

$$R_{cr} = \frac{2\gamma_{lg}}{\frac{C_R P_{sys}}{C_{sat}} - P_{sys}} \quad (2.19)$$

Heterogeneous nucleation

Heterogeneous nucleation is the cell nucleation around the nucleating sites or cavity in the bulk. A smooth planar surface does not lead to heterogeneous nucleation. This type of nucleation promotes the foaming with the addition of nucleating agents such as calcium carbonate, talc etc. during process [65]. These nucleating agents create the new sites for nucleation and improve the cell nucleation and to control the growth, and hence the final foams properties. The stress variations around the rigid fillers will generate pressure variation which causes heterogeneous cell nucleation around these solid particles. In the case of low melt strength polymers, the existence of these fillers could also improve the melt strength during the foaming and thereby the cell coalescence could be hindered while more expansion could be obtained [66].

When the system is sited in the border of cell nucleation in the system, change in the free energy is required by heterogeneous cell nucleation. (ΔF_{het}) can be figured as [67-73]:

$$\Delta F_{het} = -(P_{bub} - P_{sys})V_{bub} + (\gamma_{sg} - \gamma_{sl})A_{sg} + \gamma_{lg}A_{lg} \quad (2.20)$$

According to this formula, A_{ij} shows the surface area and γ_{ij} shows the interfacial energy, also s means the solid phase and l means the liquid phase.

Critical Radius (R_{cr}) is also similar in the homogeneous nucleation with R_{cr} for heterogeneous nucleation. W_{het} is expressed by the combination of equations as shown in below. F means the energy reduction factor.

$$W_{het} = \frac{16\pi\gamma_{lg}^3 F}{3(P_{bub,cr} - P_{sys})^2} = W_{hom} \times F \quad (2.21)$$

When the R_{bub} is equal to R_{cr} , the metastable solution or the unstable phase equilibrium in polymer-gas mixture is observed according to thermodynamics. The molecular movement increases the critical bubble radius. There is a strong relationship between the entropy decrement and critical bubble size. The second law of thermodynamics contravenes with this process. In order to anticipate gas bubble formation, the classical thermodynamic is not preferable. To sum up, homogenous nucleation energy barrier (W_{hom}) and heterogenous nucleation energy barrier (W_{het}) can be expressed below:

$$W_{hom} = \frac{16\pi\gamma_{lg}^3}{3(P_{bub,cr} - P_{sys})^2} = \frac{16\pi\gamma_{lg}^3}{3(HC - P_{sys})^2} \quad (2.22)$$

$$\begin{aligned} W_{het} &= W_{hom} F(\theta_c, \beta) \\ &= \frac{W_{hom}}{4} \left[2 - 2 \sin(\theta_c - \beta) + \frac{\cos \theta_c \cos^2(\theta_c - \beta)}{\sin \beta} \right] \end{aligned} \quad (2.23)$$

$F(\theta_c, \beta)$ = the ratio of the volume of the nucleated bubble

θ_c = the contact angle between the bubble surface and the solid surface in the liquid phase.

Pseudo-Classical Nucleation

In this nucleation system, there are both homogenous and heterogenous nucleation from the pre-existing gas cavities at the surface part of the particles and also the equipment surface. In addition, the microvoids also exist in the solution quantity. Pre-existing gas cavity expansion is activated, because of the finite free energy barrier. Increasing the supersaturation rate during stable pressure drop will exceed the energy barrier lastly. All in all, the pre-existing cavities will expand unconsciously.

2.2.4.3 Cell growth and stabilization

When the cells grow because of the thermodynamic instability, it can be faced with the undesirable phenomena. Cell collapse, cell coalescence and the cell coarsening are the mechanisms which result the cellular structure degradation. According to cell coarsening phenomena, because of the the gas volition to move from small bubble to

larger one, the smaller bubbles tend to getting small or disappear and bigger bubbles getting larger.

According to cell coalescence mechanism, when two cells getting grow, their cell walls rupture and they are combined as it is seen in Figure 2.16.

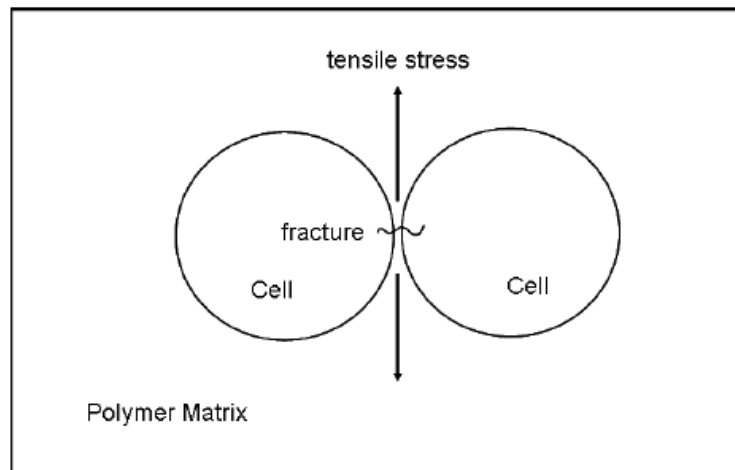


Figure 2.16 : The schematic of cell coalescence phenomena [17].

This cell walls are thin and they have no capability to preserve the tension advanced when the cells are getting grow [75]. There are various studies about these undesired phenomena and the ways to control and stop them. These studies explain the cell coarsening with numerical simulation and the investigation the relationship between rheological behavior and the cell coalescence [76-78] According to results, when the very small cells like nano sized cells face with larger cells, the small cells tend to collapse.

In various interface deformation situations and different rheological natures, the cell coalescence is observed by using foaming visual system. Results show that, during the foaming of newtonian polymers, cell coalescence is observed by cell walls thinning. On the other hand, the bubbles penetrate inside each other during non newtonian polymeric foams. The coalescing time and the cell wall deformation amount are also expressed in these studies.

2.2.5 Foam manufacturing technologies

Many of traditional polymer processing methods can be performed in order to produce polymeric foams. Batch process and continuous process are the two techniques for foam production.

2.2.5.1 Batch foaming process

In this technique, polymer and inert blowing agent are immersed in a pressurized vessel and saturation occurs in a time period as it is figured in Figure 2.17 [79]. This time period can change depend on the temperature which effects the diffusivity of gas and also sample size of polymer.

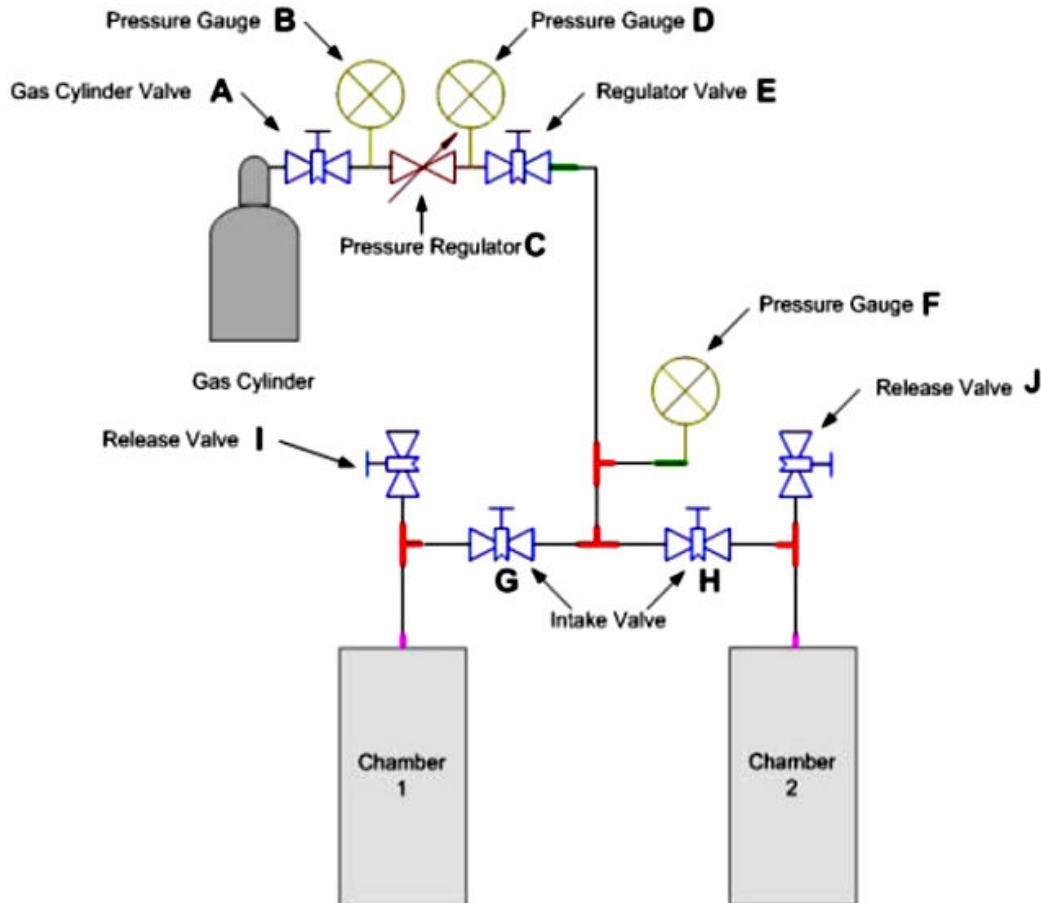


Figure 2.17 : Laboratory-scale batch foaming system [79].

In this process, if the saturation is carried out at low temperatures, the foam morphology tend to be nonuniform from core to skin. As it is noticed earlier, the diffusion is low at the low temperatures. Therefore, saturation also takes very long time. If the temperature is around the melting point of material when the saturation carried out, the morphology of foamed structure would be more homogenous [80-81]. In the batch foaming process, the foaming takes so much time due to the long diffusion times. Thus, this process is not preferable for serial productions and also not a cost effective process. The continuous processes are more suitable for both high capacity productions and cost advantages [79].

2.2.5.2 Continuous foaming process

There are three types of continuous foaming processing techniques in terms of bead foaming, foam extrusion and foam injection molding.

Bead foaming

The foaming beads are produced and molded in this technique. PS is the most used polymer for bead foam production and the bead foamed PS has many applications in packaging, construction, sandwich cups etc. As it is seen in Figure 2.18. 4 to 7 wt% content of N-pentane is used as a blowing agent in EPS production.

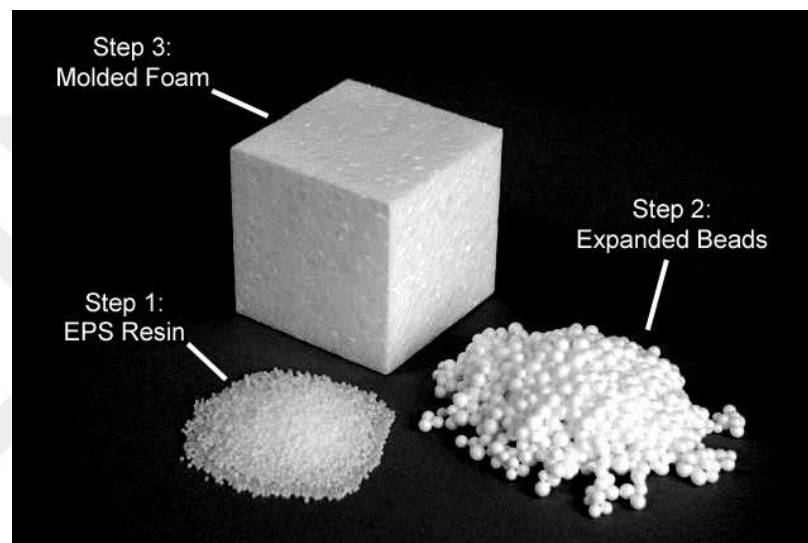


Figure 2.18 : EPS production steps [76].

EPP (expanded polypropylene) is also another bead foam product which is widely used. As it is compared with EPS, EPP has better elasticity and dimensional stability. It has also many application areas such as packaging, automotive bumpers, home appliances etc. In addition, there are another bead foam products manufactured from PLA and PE. Especially, expanded poly lactic acid product has gained importance due to its biodegradability in recent years. Bead foam production starts with the pre-expansion stage by using the pre-expander system. After pre-expansion, the balancing of the beads meaning are carried out in a silo. In this step, the atmosphere pressure and the internal cell pressure elucidated [86-88]. Finally, the beads are molded according to usage area [82,83]. As an example, the eps production process is figured in Figure 2.19.

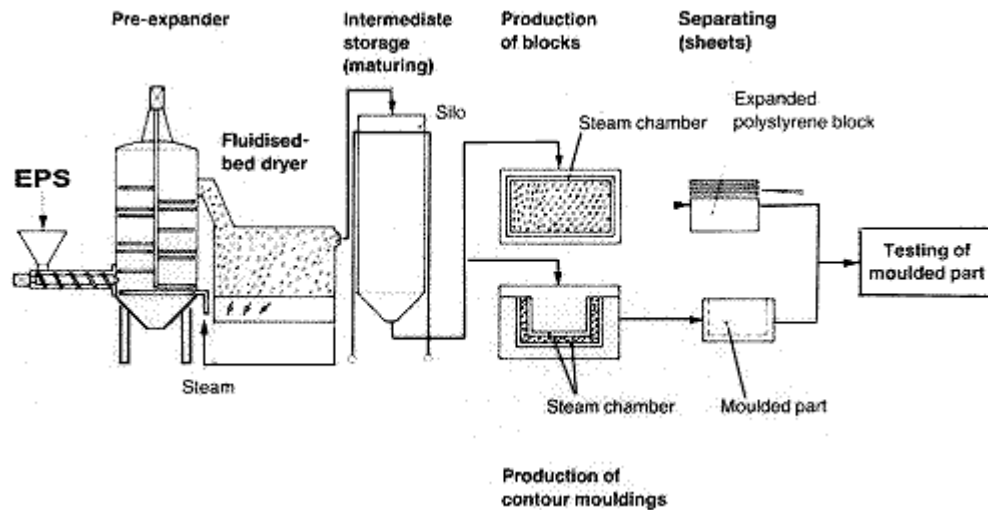


Figure 2.19 : Process flow chart of EPS production [84].

Foam Injection Molding

Foam injection molding is a continuous process which is manufactured large, complex and 3-D foam products. There are various foam injection molding processing methods. In the low pressure technique, the blowing agent is injected and dissolved in barrel section and the mixture of blowing agent and polymer is injected to a mold cavity with a very low cavity pressure. As it is seen in Figure 2.20, the solution of polymer melt and the blowing agent is firstly injected in an accumulator. Then, it is injected in the mold cavity [85].

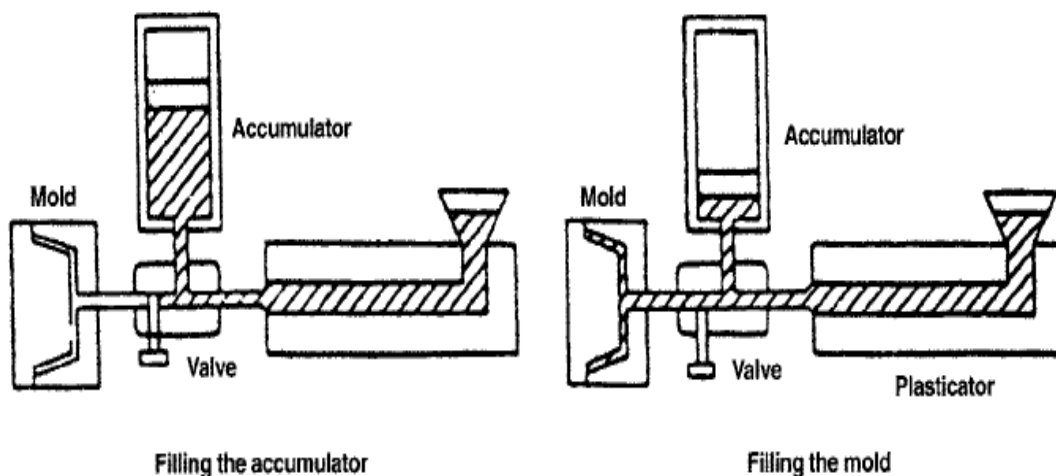


Figure 2.20 : Low pressure foam reciprocating injection molding machine [85].

In foam injection molding process, the processing parameters are critical in order to obtain good foam structure. The first parameter is the shot size. Shot size is measured nearly 10 % below from the current shot size. The injection rate also should arrange

as high as possible in this process. The temperature of melt and mold parts and the blowing agent type, content also another important parameters. As it is schematized in Figure 2.21, the calibrated mold is pressurized with gas, when the arranged shot size is injected, the core part is filled with foam due to the solid skins also formed [85].

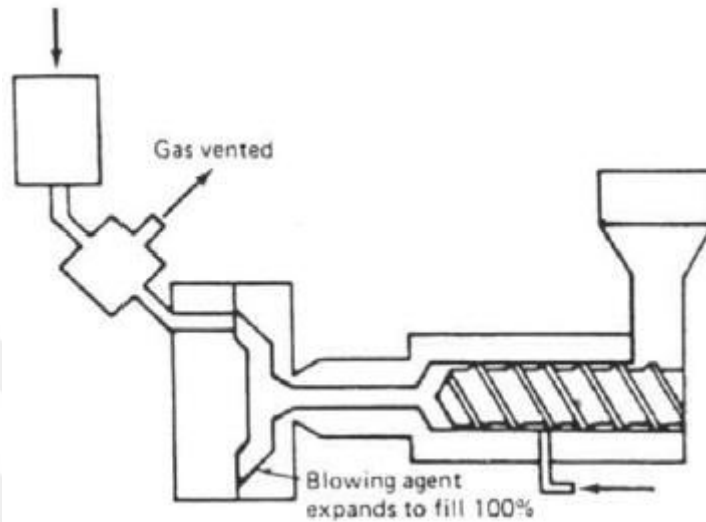


Figure 2.21 : Gas counter pressure foam injection molding machine [85].

Gas injection foam molding is another method to manufacture foamed products. In this method, firstly the polymer is solidified at the surface of the mold and the remaining polymer melt is foamed and the core of structure is formed. There are various designs for this process systems as it is shown in Figure 2.22 and Figure 2.23 [85].

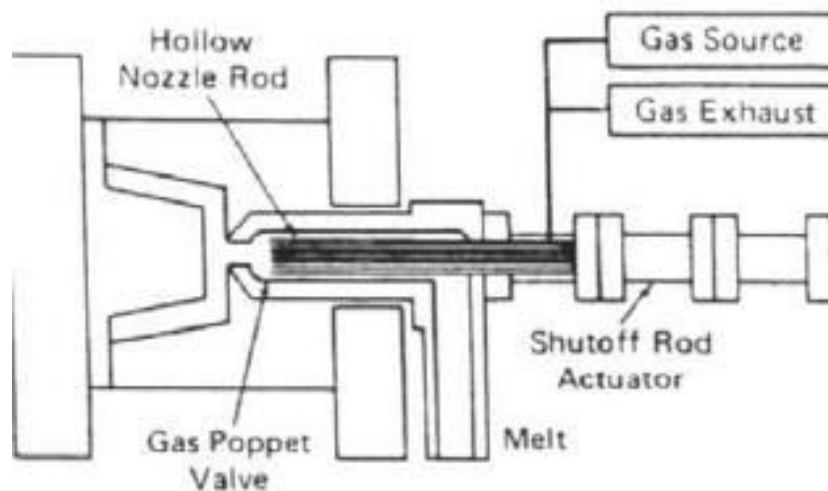


Figure 2.22 : Simultaneously handling gas and melt modified injection molding machine [85].

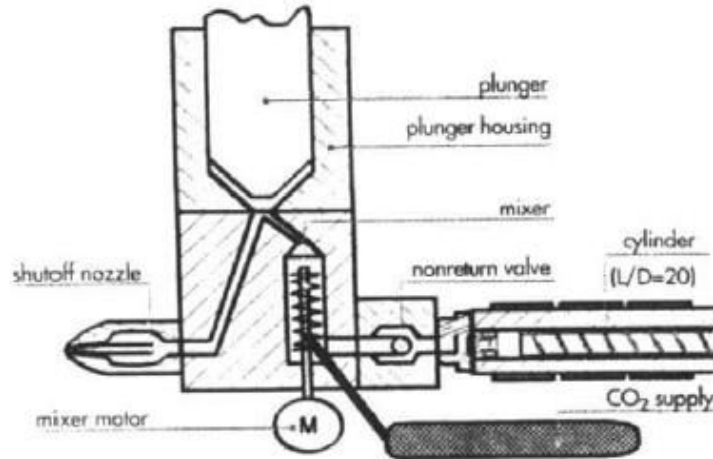


Figure 2.23 : Microcellular injection molding system directing the melt-gas through its shutoff nozzle into the mold cavity [85].

Foam Extrusion

Foam extrusion is used to manufacture polymeric foam products since 1970s. The process of foam extrusion consist of several steps: dissolution of the blowing agent, the melting (plasticization) of the polymer, the nucleation of the bubbles upon pressure release, their growth, and cell stabilization [89]. When the polymer melts along the extruder, with the addition of CBA or injecting the PBA into the melt, polymer/gas mixture starts to be generated under high pressure and the mixture will be flowing along the extruder. However, the generated pressure must stay beyond the solubility limit of polymer/gas in order to avoid having undissolved gas within the melt along the extruder [90-91]. The die pressure and the pressure drop rate could be controlled by the die temperature, die geometry, and melt viscosity of the polymer/gas mixture. The sudden pressure drop at the die nozzle creates thermodynamic instability and causes cell nucleation and growth during the foaming step [28,92]. There are three types of foam extrusion setups in terms of single screw extruder, twin screw extruder and tandem extruder. Three of them have their own strong and weak properties about technical conditions.

2.2.5.3 Design of foam extrusion processing

In polymeric foam process, there are generally two foam structures varying of application area. The first one includes addition of CBAs defined as high density foams. In the second one, the PBA is injected to polymer melt and it is called as low density foams. Poly(vinyl chloride) PVC, polyethylene (PE), acrylonitrile butadiene

styrene (ABS), PS and polypropylene (PP) form high density foam products. CBA decomposes in extruder with the help of temperature and generates gas. There are some critical points in this process and should be well designed. In order to avoid premature gassing in the feeding zone, the temperature here should be as low as possible within the processing range of the polymer. In addition, decomposition temperature of CBA should not be too high because if the temperature will not be reached, the gas could not be generated. In low density foams, PBA is directly injected in to the polymer melt. The PBAs also should act like a strong plasticisers and reduce the viscosity of melt [93, 94]. In addition, the die temperature in extruder should be kept at lower temperatures due to create thermodynamic instability and high cell density products.

2.2.5.4 Die design in foam extrusion

The design of the die is one of the most critical point of foam extrusion. The polymer-gas solution mixes in extruder barrels and comes through to die section, uniformly. The die section provides the optimum pressure in order to exit of material without problems. It should be designed to provide maximum pressure drop in order to improve the thermodynamic instability and perfect cell nucleation. In addition, this pressure drop should be equally distributed to each part of the die in order to control the cell nucleation and shape of the final product. Pressure drop rate is calculated according to Kozicki equation [95]:

$$\Delta P = \frac{mL}{R_h} \left[\frac{W(a + bn)}{1800\rho R_h A n} \right]^n \quad (2.24)$$

ΔP = the pressure drop (psi)

L = the length of piece

M = the firmness (lbf sn/in²)

R_h = the dimension of hydraulic radius (in)

W = the rate of throughput (lb/h)

a, b = the shape aspects,

n = the power law exponent,

ρ = the specific gravity of the melt (lb/in³)

A = the area of flow (in²).

The most commonly, the extruder die design divided in two groups in terms of flat die and annular die. The lips of the flat die is thinner as it is compared with annular die, therefore it is hard to obtain good quality and homogenous foam structure. The schematic of annular die design is shown in Figure 2.24.

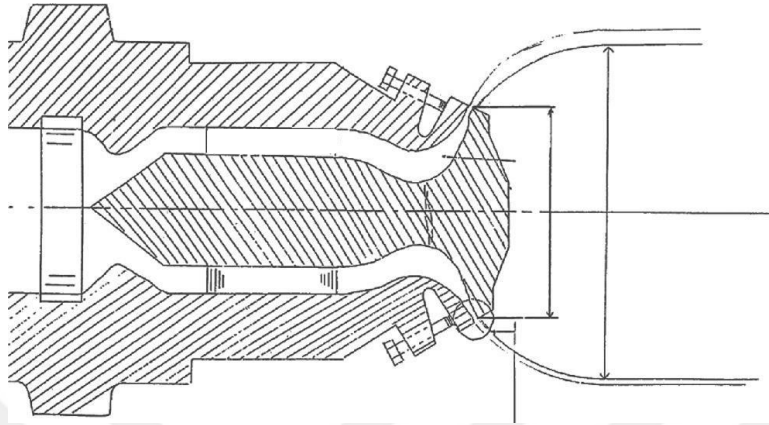


Figure 2.24 : Schematic design of annular foam die [96].

2.2.5.5 Rheological behaviors of polymers in foam extrusion

The rheology information is so critical to understand the behavior of foaming process, conditions and blowing agent attitudes. Blowing agents do not act the same behavior with all polymers due to the plasticization effect. In addition, the rheological behavior of polymer-gas solution varies about processing temperature and pressure, type and content of CBAs. In order to produce new type of blowing agents rheological measurement plays a key role. In order to measure to the rheology of molten polymer and blowing agent solution, closed pressurized rheometer such as slit die and capillary viscometer is required because gas must be kept in the system. The exit of the extruder an apparatus is attached and the rheological behavior is measured in-line, on-line or off-line.

As it is noticed before, the cell nucleation starts at the die section because of the pressure drop rate [97,98]. The shear stress and the pressure profile is affected from the cell nucleation through the axis of the die. The pressure drop in a cross section of die is seen in Figure 2.25. In this figure, until the cells are nucleated, the pressure is linearly dropped. When the nucleation starts, the linearity of graph is deviated. Various solutions can be applied such as gear pumps, valves, pressure transducers etc. against this problem in order to keep the pressure above the critical point which is required for cell nucleation [99-104].

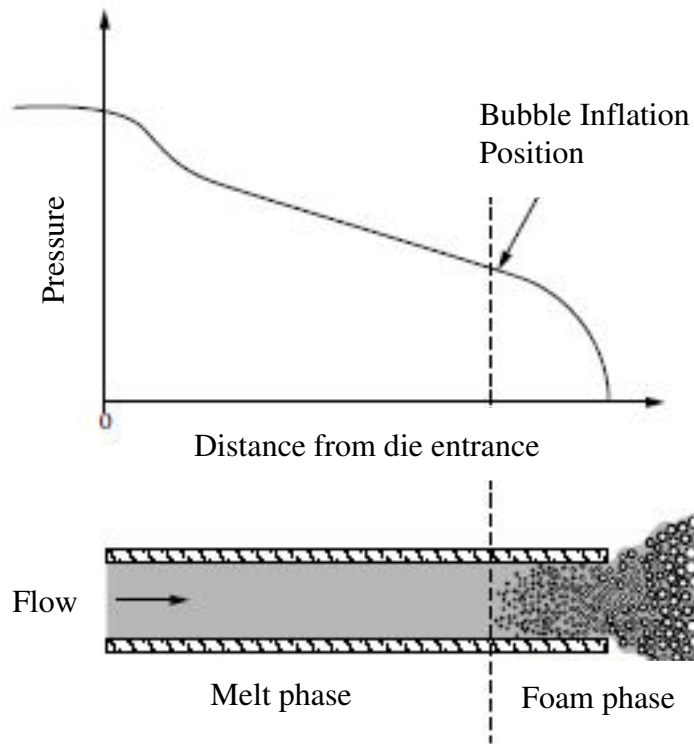


Figure 2.25 : Plot of pressure drop in a die of constant cross section [96].

2.2.5.6 Common foam extrusion systems

There are three common foam extrusion systems which are single screw extruder, twin screw extruder and tandem extruders. The advantages and disadvantages of the system types were explained in table 2.

Table 2.2 : Advantages and disadvantage of typical foam extrusion system [120].

System Type	Advantages	Disadvantages
Single Extruders	<ul style="list-style-type: none"> • Less leaking points • Less investment 	<ul style="list-style-type: none"> • Narrow melting/cooling control • Precise screw design
Tandem Extruders	<ul style="list-style-type: none"> • Independent melting/cooling control • Able to process high-melt polymers 	<ul style="list-style-type: none"> • More Leaking points • High investment • More power generation
Twin-Screw Extruders	<ul style="list-style-type: none"> • Easy to control • Good mixing • Good heat transfer 	<ul style="list-style-type: none"> • Cooling limited • Narrow melting/cooling range

Figure 2.26 also shows the continuous tandem extrusion system. The gas is injected and dissolved into polymer melt in the first extruder and the polymer-gas solution is cooled in second extruder.

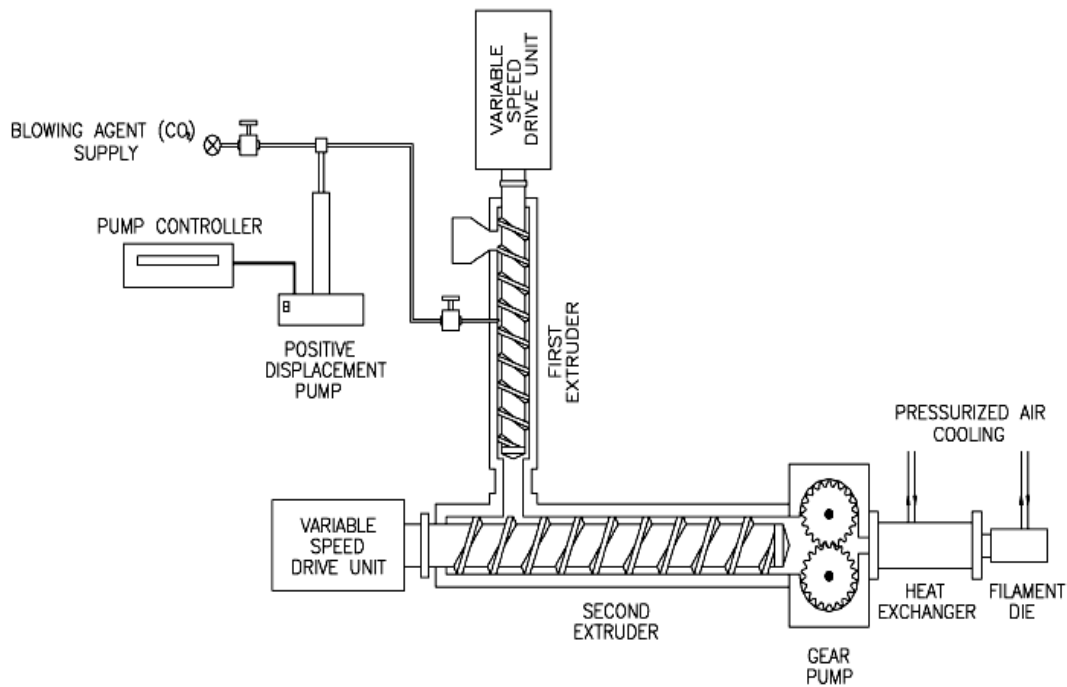


Figure 2.26 : Tandem extrusion foaming system [59].

2.3 HIPS Foaming

In 1990s, the studies about HIPS foaming are performed by using PBA (CO_2) in extrusion process. The effect of processing parameters and CBA content is investigated on HIPS. It is not faced with the study of foaming of HIPS by chemical blowing agents in literature. In foam extrusion process, the processing parameters are the most important factors in order to obtain good foam products. Barrel and die temperature profile, system and die pressure, pressure drop rate and also the content of blowing agent must be controlled very precisely. In addition, the nucleating agents also play an important role to obtain higher cell densities. The optimum content of nucleating agent must be determined and used in the foaming process.

2.3.1 Effect of gases

The effect of various gases on PP and HIPS was investigated in this study [105]. N_2 and CO_2 was injected to polymer matrices and the foaming was conducted in the extrusion process. According to solubility prediction, 10 wt% of CO_2 and 2 wt% N_2 was injected into each polymer. The cell density of CO_2 injected PP foam was 6×10^8 cells/cm³, while the N_2 injected was 3×10^7 . Moreover, the cell density of CO_2 injected HIPS foam was 8×10^9 cells/cm³, while the N_2 injected was 9×10^7 . It is

seemed that the CO₂ has higher solubility than N₂ and the main reason why CO₂ injected polymers have higher cell densities than N₂ injected.

2.3.2 Effect of the processing pressure

In addition to the effect of gases, the processing pressure effect is also investigated on cell nucleation [106]. In HIPS polymer, the amount of maximum dissolved CO₂ was injected at each processing pressure. The processing pressures were 5.4 MPa (780 psi), 10.6 MPa (1530 psi), 18.6 MPa (2700 psi), and 28.3 MPa (4100 psi). The cell densities were 7×10^5 , 2×10^7 , 2×10^8 , and 6×10^9 cells/cm³ at these processing pressure values, respectively as it is seen in Figure 2.28. The morphology analysis of foamed HIPS in each pressures is seen in Figure 2.27. According to results, the solubility of gas is proportional with the pressure and when the processing pressure increases, the cell density also increases. That means the amount of gas that dissolved in polymer is higher [62, 107]. In theoretically, the higher cell density is obtained as a consequence of higher thermodynamic instability and the increasing processing pressure ensures this. Nonetheless, the limit of increasing processing pressure depends on the extruder and gas syringe pump capacities.

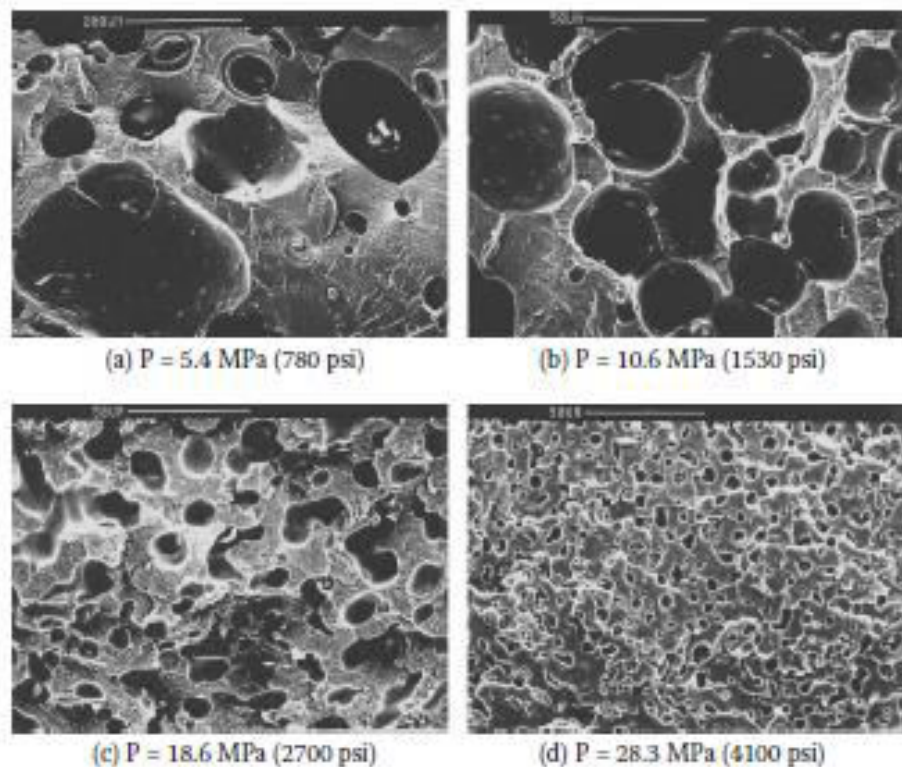


Figure 2.27 : Morphology of extruded HIPS at different processing pressures [96].

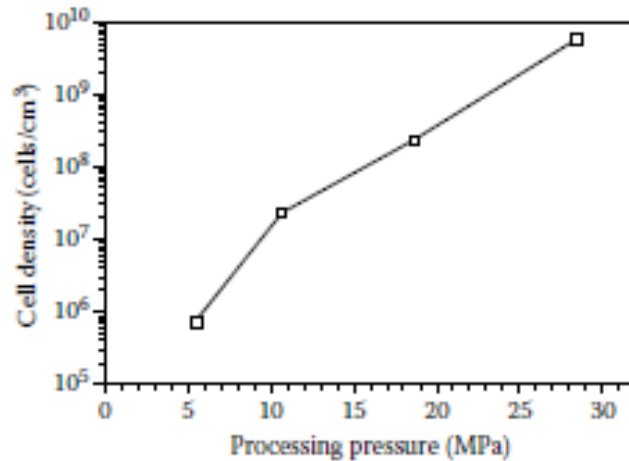


Figure 2.28 : The processing pressure effect on the cell density of extruded HIPS [96].

2.3.3 Effect of injected gas amount

Effect of PBA content on cell nucleation of HIPS was also investigated. The PBA is CO₂ and it is used in the contents of 1, 5 and 10 wt %. The pressure was 27.6 MPa (4000 psi) for all experiments. As it is plotted in Figure 2.29, the cell densities of foams were 10⁷, 4 × 10⁸, and 6 × 10⁹ cells/cm³ for 1, 5 and 10 wt % CO₂, respectively. The maximum CO₂ solubility limit of melt HIPS is 10 wt %. If the content of blowing agent is increased upper than this point, gas will not dissolve and the large gas voids were generated as noticed before. The minimum of 10⁹ cells/cm³ cell density is required in order to obtain microcellular foam as it is known. According to Figure 2.29, 7.5 wt% CO₂ content is required for microcellular nucleation at this processing pressure.

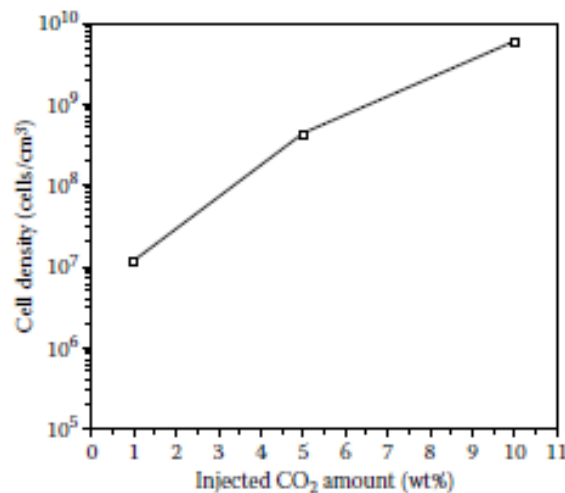


Figure 2.29 : The injected gas content effect on the cell density of extruded HIPS [96].

2.3.4 Effect of pressure drop rate

The effect of pressure drop rate on cell nucleation of HIPS was also studied. When the pressure drop rate increases, the cell density also increases as it is plotted in Figure 2.30. The cell density increased 10^8 to 10^{10} , when the pressure drop rate increased 0,2 to 10 GPa/s. This is because, the thermodynamic instability increases with the more rapidly and higher pressure drop rates [28,108,109]. The pressure drop rate amount is not effective if the solubility pressure is lower than the die pressure [108].

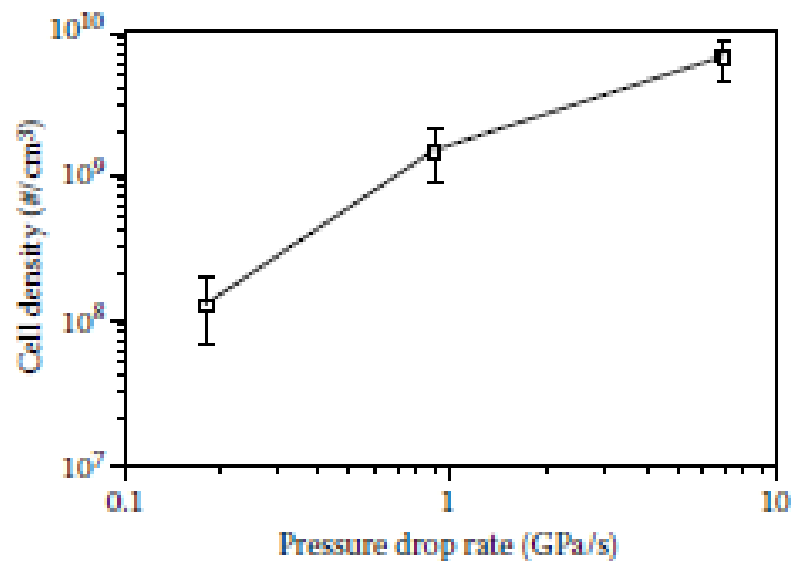


Figure 2.30 : The pressure drop rate effect on the cell density of extruded HIPS [96].

2.3.5 Effect of die temperature

The die temperature is one of the most critical parameter in order to produce high quality foam products. The temperature on the die section directly effects to pressure drop rate and thermodynamic instability. This is also related with the cell nucleation and density. In addition, when the die temperature is set at higher degrees, the gas can escape easier from the surface of polymer melt and the final foam density will be high. There are also many other problems due to the high die temperature such as cell density decrement and cell coalescence improvement [110]. In contrast, at the lower die temperatures the polymer melt strength increases and it is hard to expand of gas when it is nucleated [111]. Figure 2.31 shows the effect of various die temperature on cell morphology. It is clearly seen that, when the die temperature is decreased from 135 °C to 115 °C, the cell density increases [112].

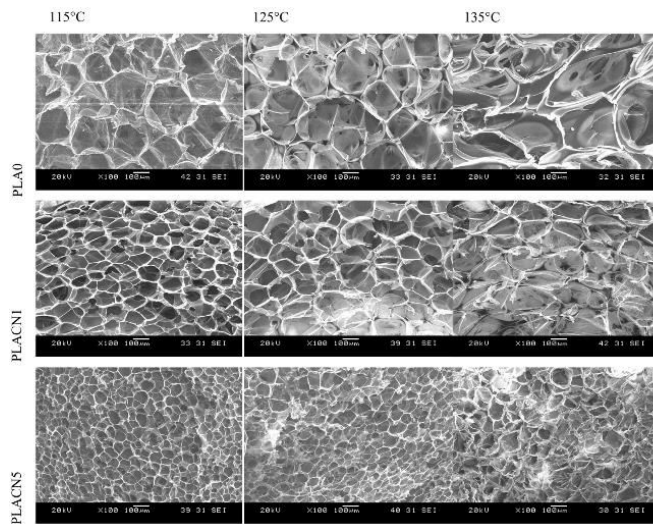


Figure 2.31 : The die temperature effect on the cell density of PLA [112].

2.3.6 Effect of nucleating agent

In order to improve the cell nucleation and to control the growth, and hence the final foams properties, inorganic fillers could be used as cell nucleating agents during foaming. The stress variations around the rigid fillers will generate pressure variation which causes heterogeneous cell nucleation around these solid particles. In the case of low melt strength polymers, the existence of these fillers could also improve the melt strength during the foaming and thereby the cell coalescence could be hindered while more expansion could be obtained. These nucleating agents included. There are various types of cell nucleating agents such as azodic calcite (calcium carbonate) [113-114], calcium stearate [113], magnesium silicate [115], rubber particles [116], stearic acid [117], silica products [114,119], talc [113, 118], and zinc stearate [113, 119]. As it is seen in micrographs in Figure 2.32, when a nucleating agent (talc particles) is added in to polymer melt during extrusion process, the cell sizes reduce and the cell density increases [17].

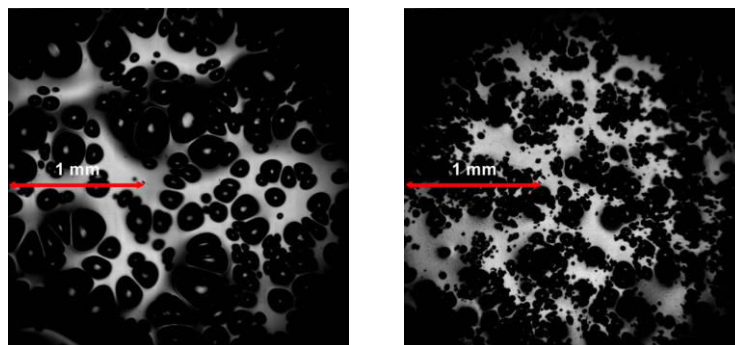


Figure 2.32 : PS foaming micrographs with CO₂ at 180°C: (a) neat PS and (b) PS + 5 wt% talc [17].

3. EXPERIMENTAL PROCEDURE

3.1 Materials

3.1.1 Polymer resin

High Impact Polystyrene (HIPS)

HIPS is made from styrene monomer (produced by free radical vinyl polymerization) and 5-12 wt. % of an elastomeric component phase including PB rubber. It is an immiscible blend of PS and PB rubber. The selected HIPS was seen in Figure 3.1. It has 1.04 g/cm^3 of density, 3.5 g/10 min MFI and $105 \text{ }^\circ\text{C}$ glass transition temperature. This HIPS shows the environmental stress cracking resistant (ESCR) behavior. Its chemical structure is illustrated in Figure 3.2. It was purchased from a company.



Figure 3.1 : HIPS as a granule form.

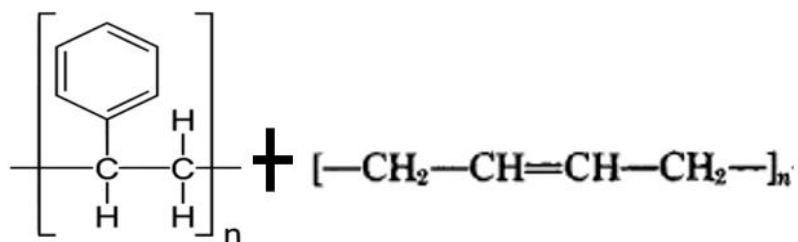


Figure 3.2 : Chemical structure of HIPS.

General Purpose Polystyrene (GPPS)

The selected GPPS was seen in Figure 3.3 which has 1.05 g/cm³ of density, 4.5 g/10 min MFI and 105 °C glass transition temperature. Its chemical structure is illustrated in Figure 3.4. It was purchased from a company.



Figure 3.3 : Granule form of GPPS.

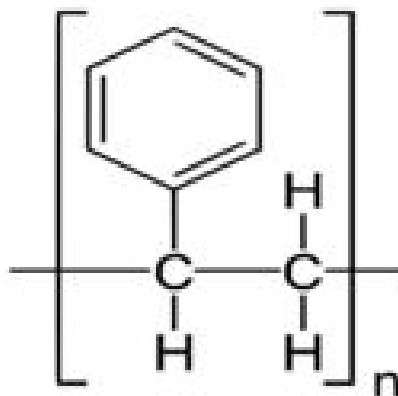


Figure 3.4 : Chemical structure of GPPS.

3.1.2 Chemical blowing agents

The CO₂ based endothermic chemical CBAs were used in these experiments. Two different grades of CBAs that have different decomposition temperatures were named as CBA 1 and 2 and purchased from a company. Both CBAs were endothermic in nature. Figure 3.5 shows the DSC and TGA curves of these CBAs, respectively. The TGA analysis shows that, CBA-1 product's decomposition temperature is around 200 °C, while CBA-2 product's is 160 °C.

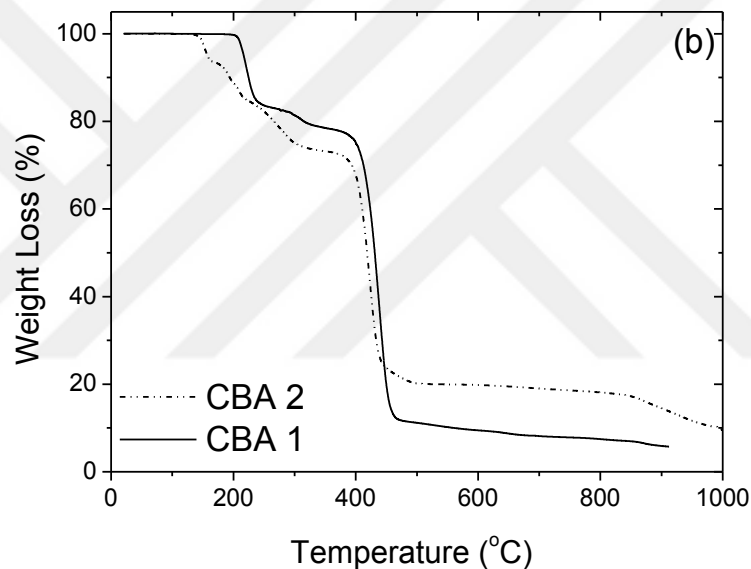
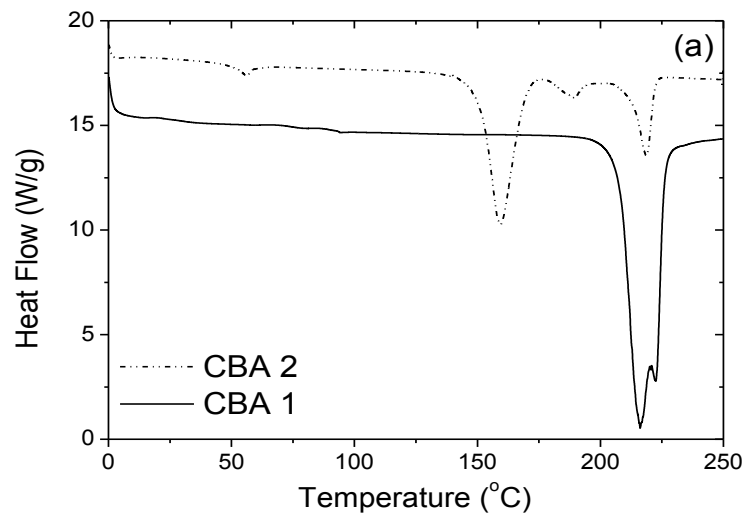


Figure 3.5 : DSC Heating thermograms (a) and TGA curves (b) of the CBAs used during the foaming.

3.1.3 Nucleating agents

Three various types of inorganic fillers (i.e. calcium carbonate, lamellar talc and micro-lamellar talc) were used as cell nucleating agent in this study. Because the individual platelets of micro-lamellar talc are smaller, the active surface area on each platelet available for nucleation is higher. They were purchased from a company.

3.2 Experimental Setup and Procedure

Due to the confidentiality of this thesis, the experimental data values are not expressed, clearly.

3.2.1 Twin screw extrusion system

Foaming was conducted in a twin screw extruder (PRISM TSE-24-HC) having an L/D ratio of 26 with filamentary die was utilized in laboratory of Arçelik. Figure 3.6 shows a schematic of this system and detailed information is provided.



Figure 3.6 : Twin screw extruder and its barrel zones.

3.2.2 Filamentary die

The filamentary die having, respectively, 2 mm diameter and 4 mm length was used in order to produce foamed filaments. Figure 3.7 shows the filamentary die which was used for all experiments.



Figure 3.7 : The filamentary die that was used in thesis studies.

3.2.3 Experimental setup and procedure

This study investigates the extrusion foaming behavior of HIPS through a twin-screw extruder using two various types of CBAs. Process based on feeding of the CBA and granule HIPS and GPPS from the two different feeders but in the same region. The die temperature profile was firstly tailored during the foaming of HIPS for two different CBAs. Then the CBA content effect on the foaming behavior of HIPS was verified for both CBAs. The effect of screw speed (RPM) on the foaming behavior of HIPS was, subsequently, illustrated for both CBAs. The HIPS extrusion

foaming behavior was further investigated via blending it with GPPS at various blending ratios, as well as, via compounding HIPS with three different inorganic fillers (i.e., microlamellar talc, talc, and calcium carbonate) at three different contents.

3.2.3.1 Processing temperatures of the extrusion system

Barrels are the inner region of the extruder where the screw is located having 7 section as seen in Figure 3.8. Each barrel's temperature is arranged by the separate resistance and measure the temperature by the thermocouple. Barrel 1, barrel 2 and barrel 3 control the temperature of the melting region of the screws, barrel 4 and barrel 5 control the temperature of the mixing region of the screws. Also, barrel 6 and barrel 7 control temperature of the homogeneous discharge region of the screws. During the execution of barrel temperature profile selection criteria, %100 HIPS were used for both CBAs.

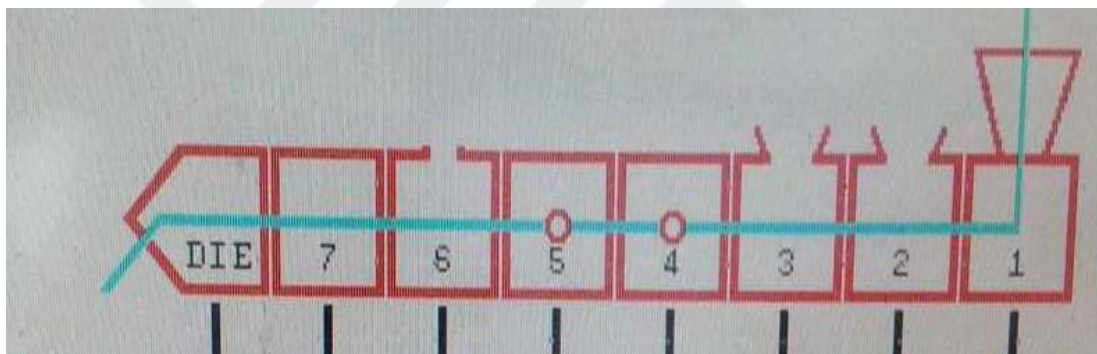


Figure 3.8 : Barrel sections of the twin screw extruder.

CBA-1

Considering the decomposition temperature of the CBA-1 blowing agent and melt strength of the mixture, 3 different temperature profiles were determined.

These profiles are expressed in the Table 3.1.

Table 3.1 : Various temperature profiles for CBA-1.

Set Profile	Barrel Temperatures
Profile 1 (°C)	Low
Profile 2 (°C)	Moderate
Profile 3 (°C)	High

CBA-2

Considering the decomposition temperature of the CBA-2 blowing agent and melt strength of the mixture, 5 different temperature profiles were determined. The set profile numbers of CBA-2 are higher than CBA-1. This is because the decomposition temperature of CBA-2 is lower than CBA-1. These profiles are expressed in the Table 3.2.

Table 3.2 : Various temperature profiles for CBA-2.

Set Profile	Barrel Temperatures
Profile 1 (°C)	Vey Low
Profile 2 (°C)	Low
Profile 3 (°C)	Moderate
Profile 4 (°C)	High
Profile 5 (°C)	Very High

3.2.3.2 Die temperature profile

In this study, five different die temperatures were set as it is expressed at Table 3.3.

Table 3.3 : Different temperature profiles for die section.

Set Profile	Barrel Temperatures
Profile 1 (°C)	Vey High
Profile 2 (°C)	High
Profile 3 (°C)	Moderate
Profile 4 (°C)	Low
Profile 5 (°C)	Very Low

During the execution of die temperature profile selection criteria, %100 HIPS were used and experiments carried out at barrel temperature profile 3 (high) for CBA-1 and profile 1 (very low) for CBA-2.

3.2.3.3 CBA type and content

CBA agent content is another parameter of the study because there is strongly relationship between blowing agent amount and cell density. Different CBA amounts (low, moderate and high) were tried for each blowing agent at constant die temperature as it is seen in Table 3.4 and 3.5.

Table 3.4 : Different CBA contents for CBA-1.

Experiments	Die Temp. (°C)	CBA Content (%)
1	Low	Low
2	Low	Moderate
3	Low	High

Table 3.5 : Different CBA contents for CBA-2.

Experiments	Die Temp. (°C)	CBA Content (%)
1	Very High	Low
2	Very High	Moderate
3	Very High	High

During the execution of die temperature profile selection criteria, %100 HIPS were used and experiments carried out at barrel temperature profile 3 (high) for CBA-1 and profile 1 (very low) for CBA-2.

3.2.3.4 Screw Speed (RPM)

The speed effect (i.e., low, moderate, high and very high) on the foaming behavior of HIPS was explored using both CBA 1 and CBA 2. During examination of the screw speed effect parameter, %100 HIPS were used and experiments carried out at barrel temperature profile 3 (high) for CBA-1 and profile 1 (very low) for CBA-2. In addition, the die temperatures are low and very high, respectively for CBA-1 and CBA-2, and also very high content of CBA was used for each screw speed value.

3.2.3.5 HIPS-GPPS blending ratios

In order to investigate the extrusion foaming behavior of PS blends via blending HIPS with GPPS, the HIPS/GPPS blends were foamed at the blending weight ratios of % 100 wt. HIPS, HIPS with low content GPPS blend and HIPS with high content GPPS blend. During the experiments, the barrel temperature profile 3 for CBA-1 and profile 1 for CBA-2 were used. Very high content of CBA was used for each experiments. The Table 3.6 and 3.7 show the other constant parameters while the effect of GPPS was investigated for both CBAs.

Table 3.6 : Different CBA contents for CBA-1.

Experiments	Die Temp.(°C)	RPM	HIPS (% wt.)	GPPS (% wt.)
1	Low	Low	100	-
2	Low	Low	High	Low
3	Low	Low	Low	High

Table 3.7 : Different CBA contents for CBA-2.

Experiments	Die Temp.(°C)	RPM	HIPS (% wt.)	GPPS (% wt.)
1	Very High	Low	100	-
2	Very High	Low	High	Low
3	Very High	Low	Low	High

3.2.3.6 Nucleating agent type and content

The HIPS foaming behavior was analyzed via compounding HIPS with three different inorganic fillers (i.e., microlamellar talc, talc, and calcium carbonate) at three different contents (low, moderate and high). Very high content of CBA 1 was fixed for all foaming experiments of blends and composites. The low die temperature and screw RPM were also fixed at for these experiments.

3.2.4 Rheological measurements

The rheological behavior of the HIPS and HIPS/GPPS blends were measured with two methods: an oscillatory rheometer (Anton Paar, Rheo Compass), and the melt flow index. Circular samples were hot pressed and prepared with a diameter of 25 mm and a gap size of 1mm for rheological measurements as it is seen in Figure 3.9.



Figure 3.9 : The samples for rheological studies.

3.2.5 Characterization techniques

3.2.5.1 Density measurement & void fraction

Density is one of the most critical physical property for this study. Density measurement progress according to archimedes principle with using Mettler A1201

density measurement device. 5 samples were cut from each filaments. Foamed samples were prepared according to ISO 845 standart. Figure 3.10 shows a Mettler density measurement device.



Figure 3.10 : Mettler density measurement device.

The pure water was used in order to measure the density of filament samples. As it is known, the density of pure wter is 1.00 g/cm³. Archimedes principle is used to calculate the density of samples which is seen in below equation:

$$d = \frac{(M_{air}) \cdot (\rho)}{(M_{air}) + (M_{water})} \quad (3.1)$$

M_{air}: Weights of each samples in atmospheric condition.

M_{water}: Weights of each samples in pure water condition.

ρ : Density of pure water.

Void fraction also calculated by using below equation in order to determine the density reduction of foamed samples.

$$\text{Void fraction} = 100 \cdot \left(1 - \frac{\rho_{foam}}{\rho_{polymer}}\right) \quad (3.2)$$

3.2.5.2 Morphological analysis and foam cell density characterization

Optical microscope (ZEISS) was used to investigate the PB size and determination in PS matrix. Scanning electron microscope (ZEISS SUPRA 55VP) was used to observe the cellular morphology and to calculate the cell density, cell distributions

and cell dimensions of each of filamentary samples as it seen in Figure 3.11. The cell density of each samples were calculated by using below equation:

$$\text{Cell Density} = \left(\frac{nM^2}{A}\right)^{3/2} \cdot \frac{\rho_{polymer}}{\rho_{foam}} \quad (3.3)$$



Figure 3.11 : Scanning electron microscope (SEM).

4. RESULTS AND DISCUSSION

4.1 Polybutylene (PB) Size Determination in PS Matrix

Figure 4.1 compares the PB orientations of neat HIPS samples before and after extrusion process. It is seen that, PB orientations are similar in both situations. The diameters of PBs are as large as 20 μm .

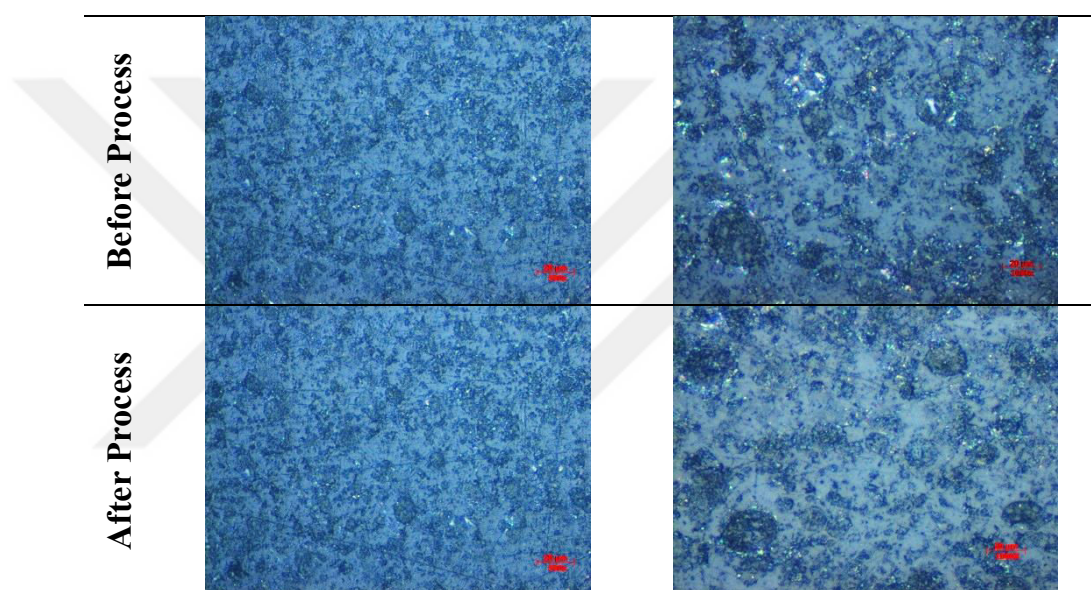


Figure 4.1 : Optical microscope images of neat HIPS reflecting the PB droplet sizes before and after process. The scale bars are 20 μm respectively.

4.2 Melt Behavior of the HIPS, GPPS and Their Blends

Figure 4.2 shows the MFI results of HIPS, GPPS and their blends at 200 $^{\circ}\text{C}$ and 5 kg. It is seen that, melt flow index values of HIPS, GPPS and their blends are very similar. This shows that; HIPS, GPPS and their blends have similar melt properties. GPPS has the highest MFI value (4,5), while HIPS has 3,5 and increasing the content of GPPS increases the MFI of blends.

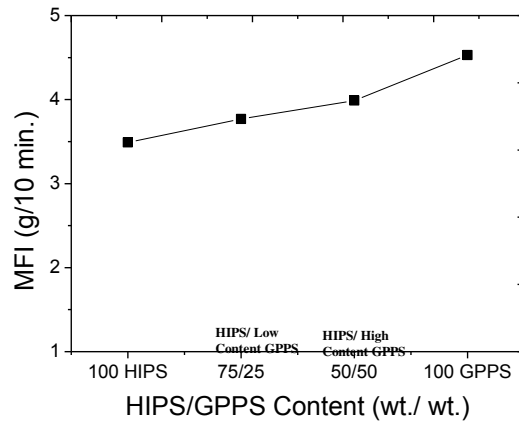


Figure 4.2 : MFI results of HIPS, GPPS and their blends.

Figure 4.3 also compares the frequency sweep short amplitude oscillation shearing (SAOS) behavior of the noted samples. As seen the complex shear viscosities and the moduli of HIPS and their blends with GPPS are pretty similar within the while frequency range. Therefore, the melt properties of HIPS, GPPS and their blends will have a similar effect on the corresponding foaming behavior of the samples. The very slight decrease of the viscosity and moduli of the HIPS blends with GPPS is due to the slightly higher MFI of GPPS compared to that of HIPS.

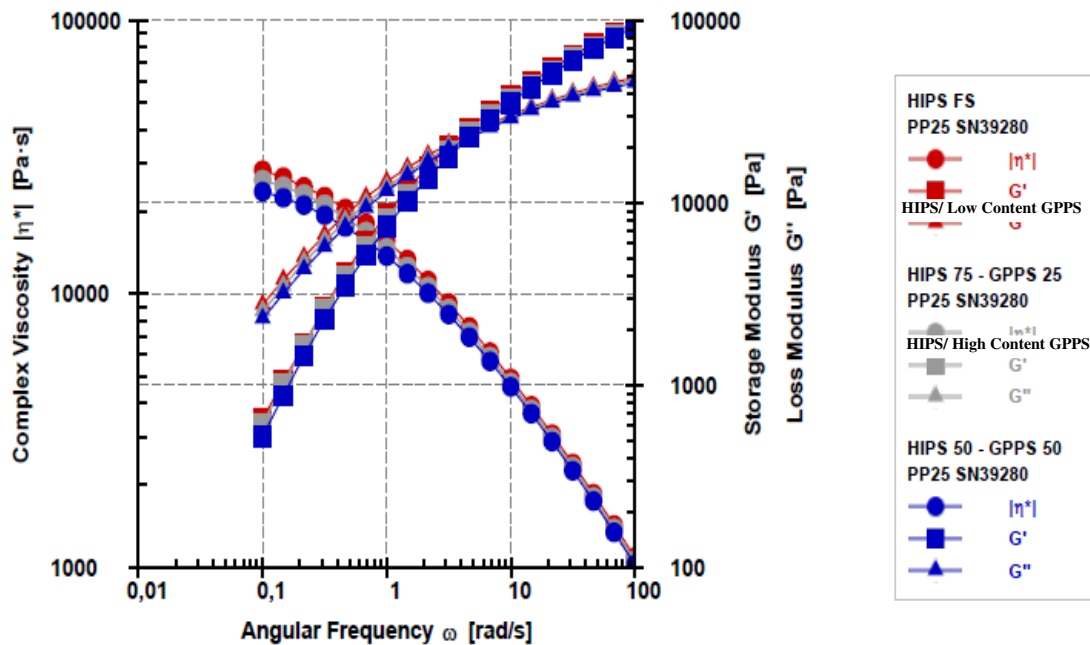


Figure 4.3 : Complex shear viscosity of HIPS and their blends with GPPS at 200°C.

4.3 Temperature Profile

4.3.1 Effect of processing temperature on cell nucleation for two different chemical blowing agents

The effect of processing temperature profile on void fraction and cell density of the foamed samples is seen in Figure 4.4 when using CBA-1. The void fraction values did not change significantly for profile 1 (low temperatures), profile 2 (moderate temperatures) and profile 3 (high temperatures). This might be because the die pressure did not show much change for all profiles as it is seen in Figure 4.6. The highest void fraction was obtained by using profile 3 (%13). In contrast, the cell density values were less than temperature profile 1 and 2, when using temperature profile 3.

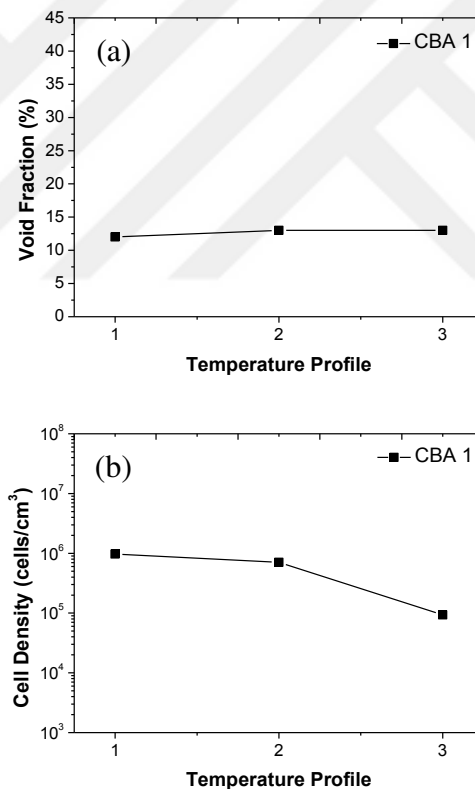


Figure 4.4 : Effect of (a) processing temperature on void fraction and (b) cell density of HIPS foams using moderate content of CBA 1 (moderate RPM).

Figure 4.5 shows the processing temperature effect when using CBA 2. It is seen that the highest void fraction (~ 19%) and the cell density (~ 10⁶ cells/cm³) is seen when using temperature profile 1 (very low temperatures). This is due to the optimum melt strength was provided for CBA-2 solubility with temperature profile 1.

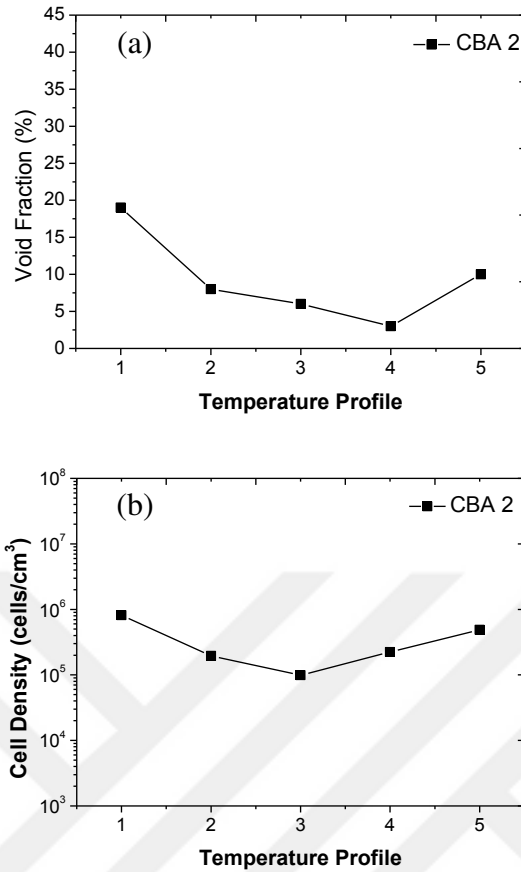


Figure 4.5 : Effect of (a) processing temperature on void fraction and (b) cell density of HIPS foams using moderate content of CBA 2 (moderate RPM).

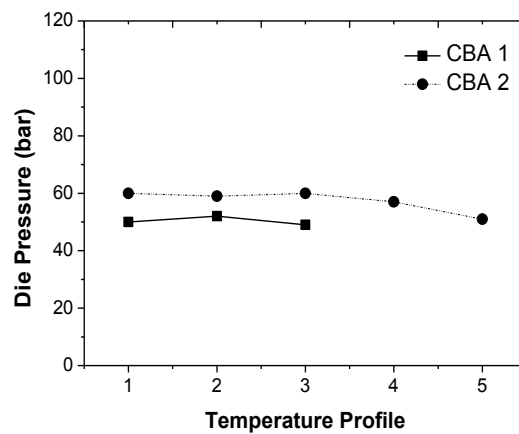


Figure 4.6 : Die pressure variations with varying temperature profiles for both CBAs.

Figure 4.7 shows the SEM images of how various barrel temperatures influenced the cell morphology of the foamed HIPS with different CBAs.

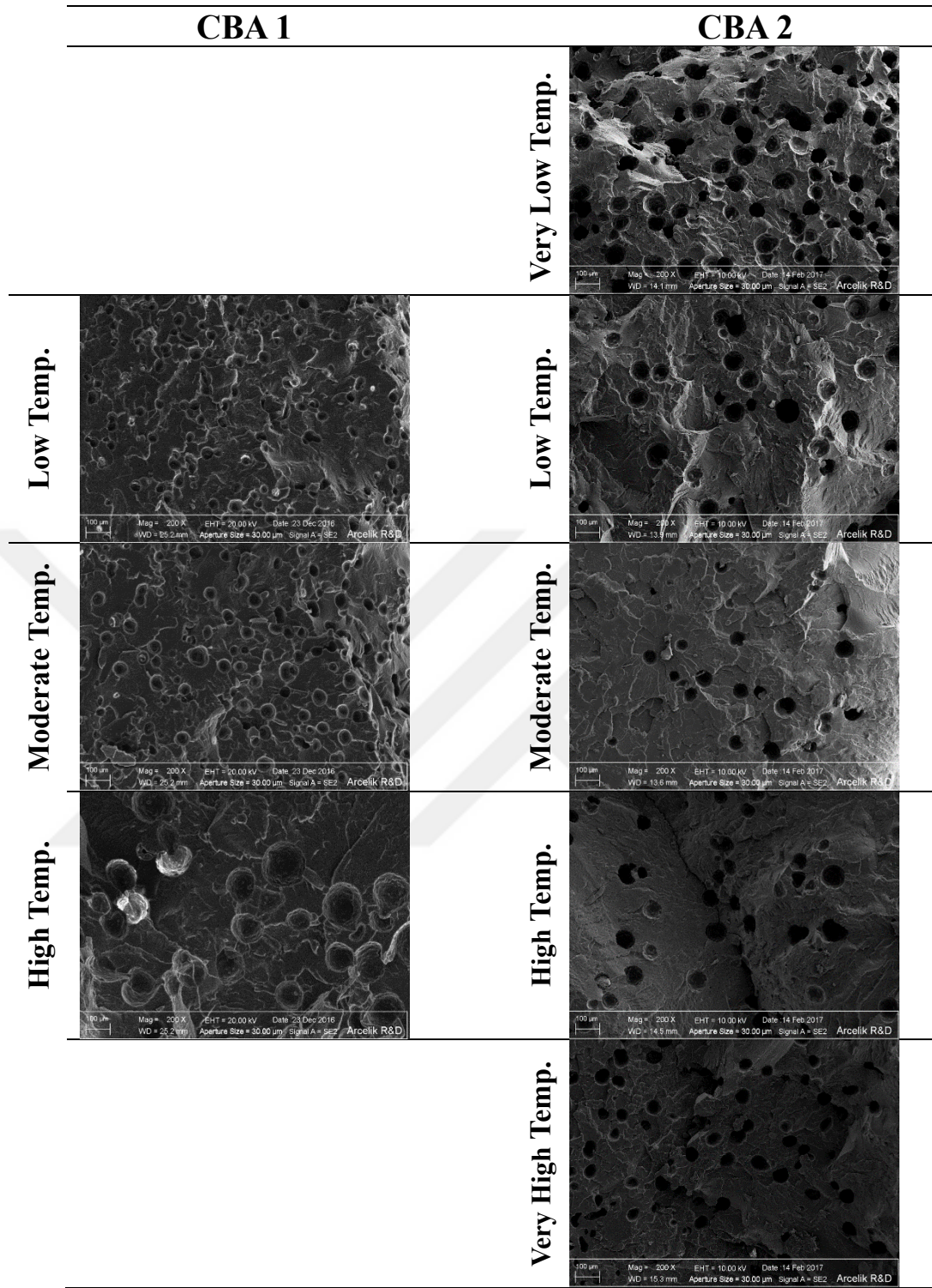


Figure 4.7 : SEM images of the HIPS foamed samples at various processing temperatures with CBA 1 and CBA 2.

4.3.2 Effect of die temperature on cell nucleation for two different chemical blowing agents

Figure 4.8 shows the effect of die temperature on void fraction and cell density values of the foamed samples as well as on the die pressure variations when using

both CBAs. In foamed samples with CBA 1, the highest void fraction (~ 22%) was obtained at the die temperature profile 2 (low temperatures) which also possessed the highest cell density (~ 6×10^5 cells/cm³). This might be because the melt strength of polymer was proper enough for better cell nucleation and expansion at low die temperature. As expected, the decrease in die temperature increased the die pressure. When using CBA 2 however, in foamed samples, despite the increased die pressure with the decrease in die temperature, the void fraction and cell density decreased with the decrease in die temperature. This could have been due to lack of solubility of CBA in melt at lower temperature as well as too high a stiff polymer melt for expansion at lower die temperatures. Figure 4.9 shows the SEM images of how various die temperatures influenced the cell morphology of the foamed HIPS with different CBAs.

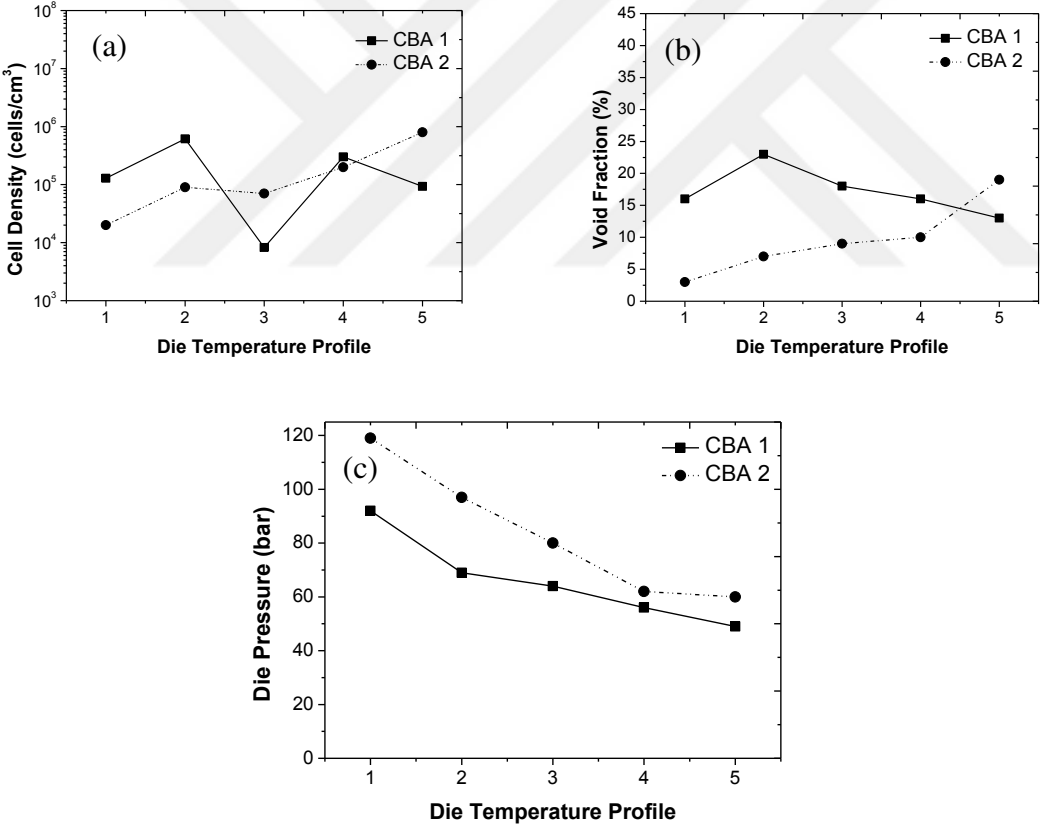


Figure 4.8 : Effect of (a) die temperature on void fraction and (b) cell density of HIPS foams using moderate content of CBA 1 (moderate RPM), and on (c) die pressure variations.

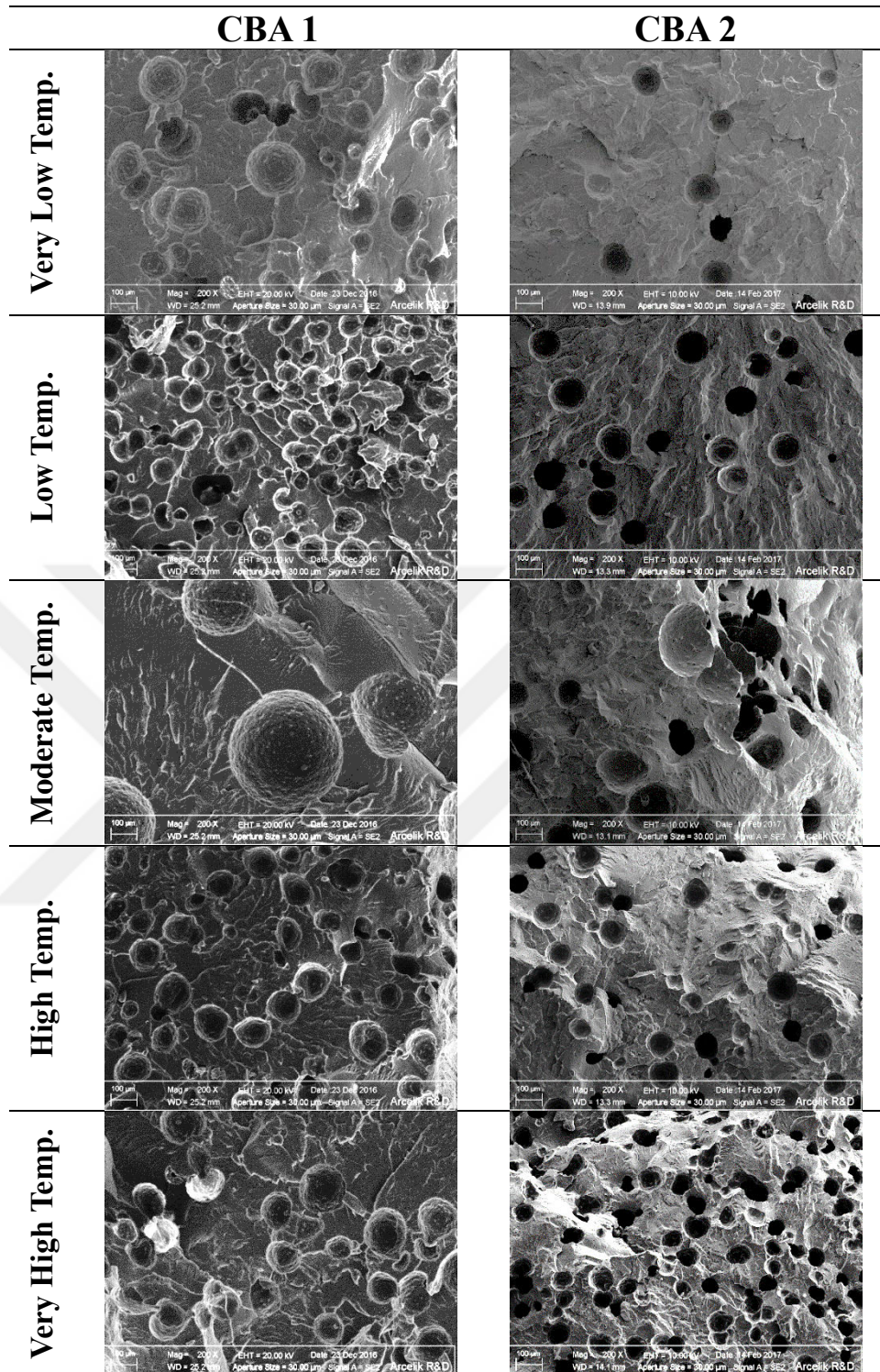


Figure 4.9 : SEM images of the HIPS foamed samples at various die temperatures with CBA 1 and CBA 2.

4.4 Chemical Blowing Agent

4.4.1 Effect of chemical blowing agent content on cell nucleation for two different chemical blowing agents

Figure 4.10 shows the effect of CBA content on the void fraction and cell density values of the foamed samples. It is shown that increasing the CBA content from low to high increased the void fraction and cell density in samples foamed with both CBA 1 and CBA 2. The highest void fraction ($\sim 32\%$) and the highest cell density ($\sim 2 \times 10^7$ cells/cm³) were obtained for samples foamed with high content of CBA 1. On the other hand, the highest void fraction ($\sim 21\%$) and the highest cell density ($\sim 8 \times 10^5$ cells/cm³) were obtained for samples foamed with high content of CBA 2. It should be noted that the cell density increased with increasing the CBA content from low to high due to the increase of the internal system pressure. Figure 4.11 shows the SEM images of how increasing CBA content influenced the cell morphology of the foamed HIPS with different CBAs.

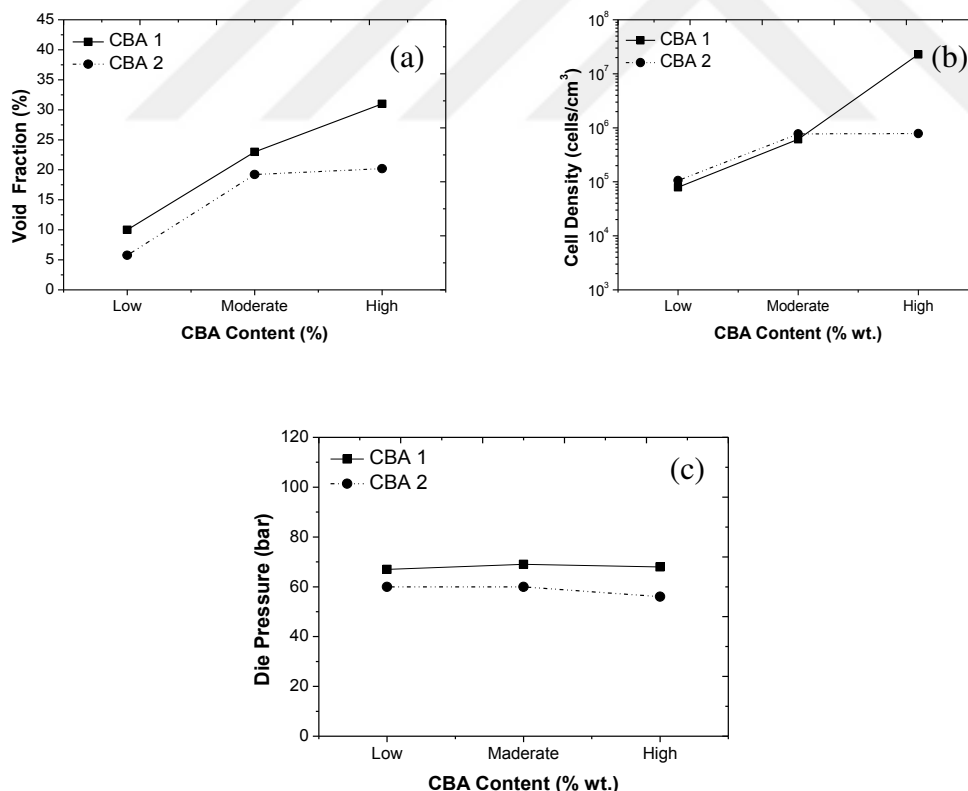


Figure 4.10 : Effect of CBA content on (a) void fraction and (b) cell density of HIPS foams at optimized at low die temperature and high die temperature, for CBA 1 and CBA 2, respectively (moderate RPM) and, on (c) die pressure variations.

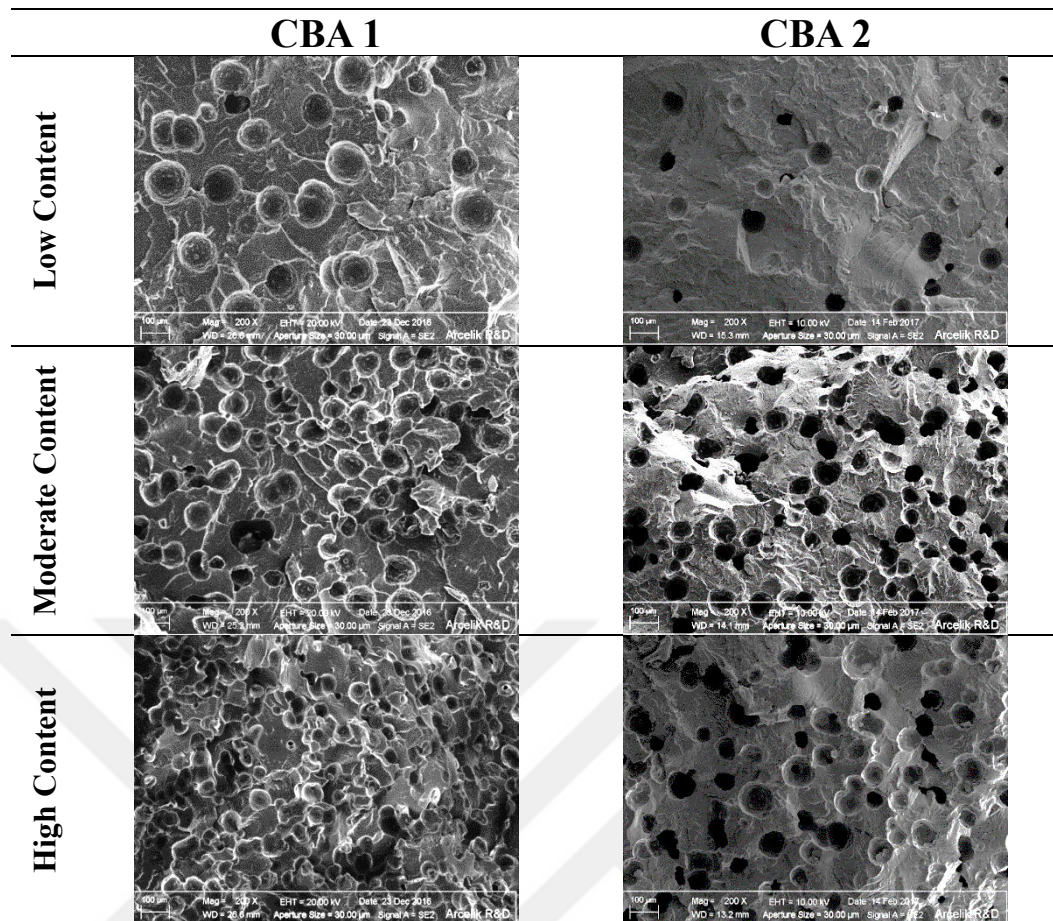


Figure 4.11 : SEM images of the HIPS foamed samples with various CBA contents for CBA 1 and CBA 2.

4.5 Screw RPM

4.5.1 Effect of screw rpm on cell nucleation for two different chemical blowing agents

Figure 4.12 shows the effect of screw RPM variations on the void fraction and cell density of the foamed samples. As the RPM decreased from around very high to low, the die pressure and consequently the void fraction of the foamed samples increased and the maximum void fraction was achieved $\sim 30\%$ for samples blown with both CBAs. On the other hand, the highest cell densities were obtained at moderate RPM and at low RPM for samples foamed with CBA 1 ($\sim 2 \times 10^7$ cells/cm³) and CBA 2 ($\sim 10^6$ cells/cm³), respectively. The cell density and void fraction increase at lower RPMs were likely due to the better mixing of polymer melt and CBA due to the increased viscosity of polymer melt at lower RPM (lower frequencies as Figure 4 shows) and higher residual time, while the die pressures showed the highest values

for both CBAs. Figure 4.13 also shows the SEM images of how various RPM values influenced the cell morphology of the samples foamed with different CBAs.

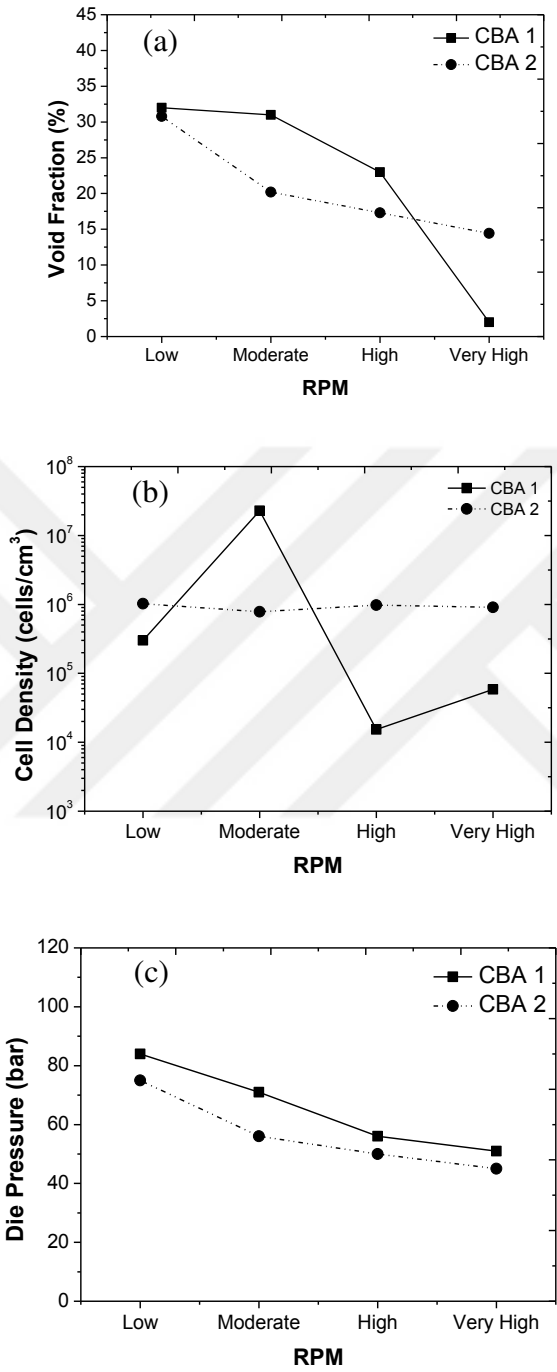


Figure 4.12 : Effect of RPM on (a) void fraction and (b) cell density of HIPS foams at low die temperature and high die temperature, for CBA 1 and CBA 2, respectively (moderate RPM) and on (c) die pressure variations.

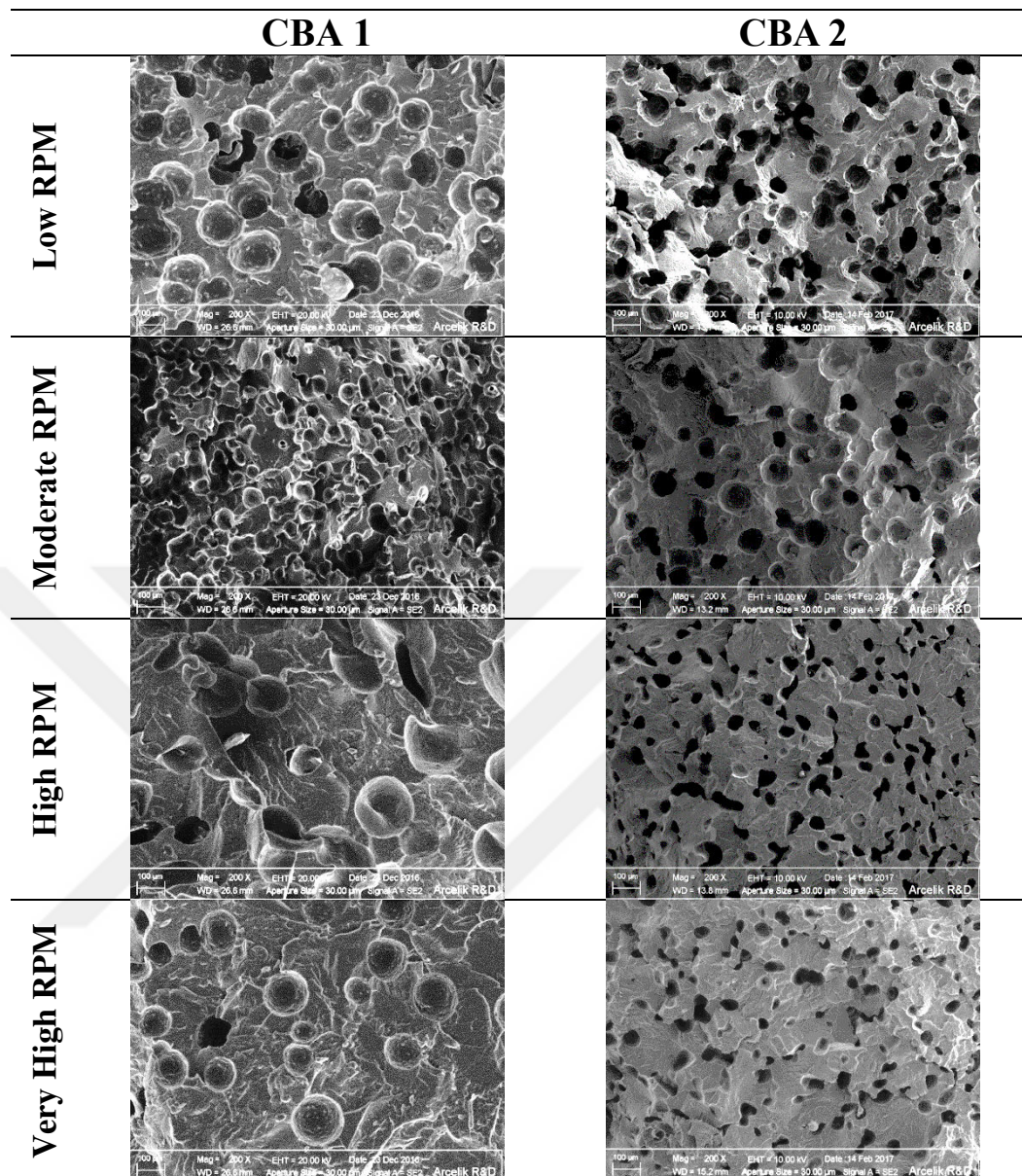


Figure 4.13 : SEM images of the HIPS foams at different screw RPMs for samples foamed with two CBAs.

4.6 Foaming Behavior of PS Blends

4.6.1 Effect of GPPS on cell nucleation for two different chemical blowing agents

Figure 4.14 shows how the blending HIPS with GPPS could affect the void fraction and cell density of the foamed samples. The increase in GPPS content increased the cell densities of HIPS/GPPS blends to around 10^6 cells/cm³ with more of open celled structure. The SEM images of the blend samples (Figure 4.15) also confirms how the

increase in GPPS increases the void fraction and cell density with more rigid but open-cell structure.

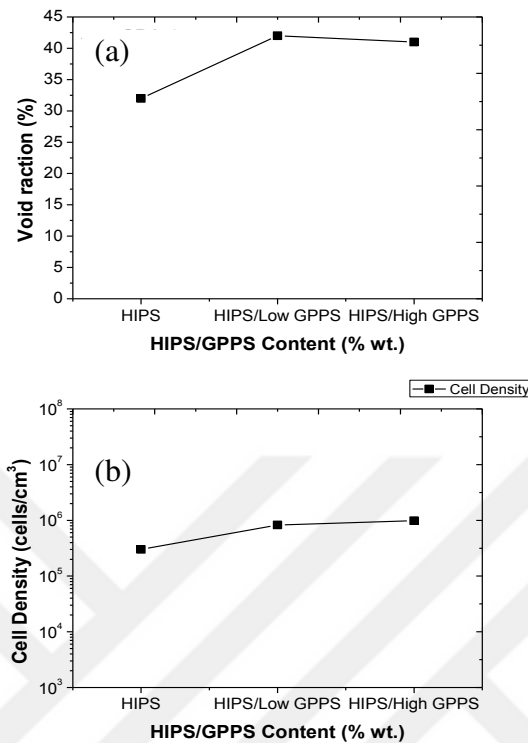


Figure 4.14 : Effect of GPPS content on (a) void fraction and (b) cell density using high content of CBA 1 at low die temperature (low RPM).

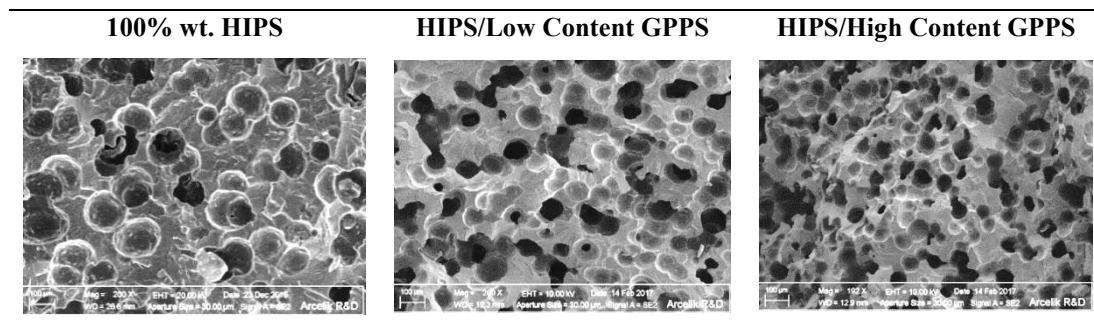


Figure 4.15 : SEM images of the HIPS blend foams using high content CBA 1 at low die temperature (low RPM).

4.7 Foaming Behavior of PS Composites

4.7.1 Effect of Inorganic filler on cell nucleation for two different chemical blowing agents

Figure 4.16 also shows the effect of various inorganic fillers as cell nucleating agents on void fraction and cell density variations of the HIPS foamed samples. Increasing the inorganic filler content from low to high, increased the cell density for all fillers.

Among these fillers, the highest cell density ($\sim 2 \times 10^6$ cells/cm³) was obtained in composites with high content of talc. Figure 4.17 also shows the SEM images of the foamed HIPS composites and how various fillers influenced the cell morphology. The void fraction decreased with increasing the inorganic filler content from low to high most probably due to the increased rigidity of the foamed samples.

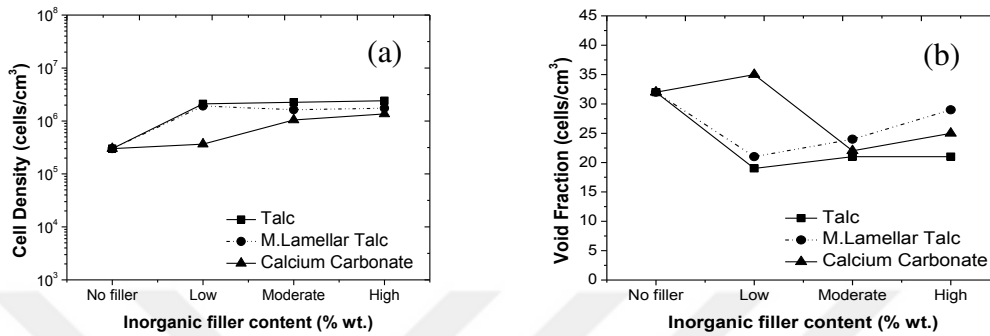


Figure 4.16 : Effect of various inorganic fillers on (a) void fraction and (b) cell density of the HIPS composite foams using high content of CBA 1 at low die temperature (low RPM).

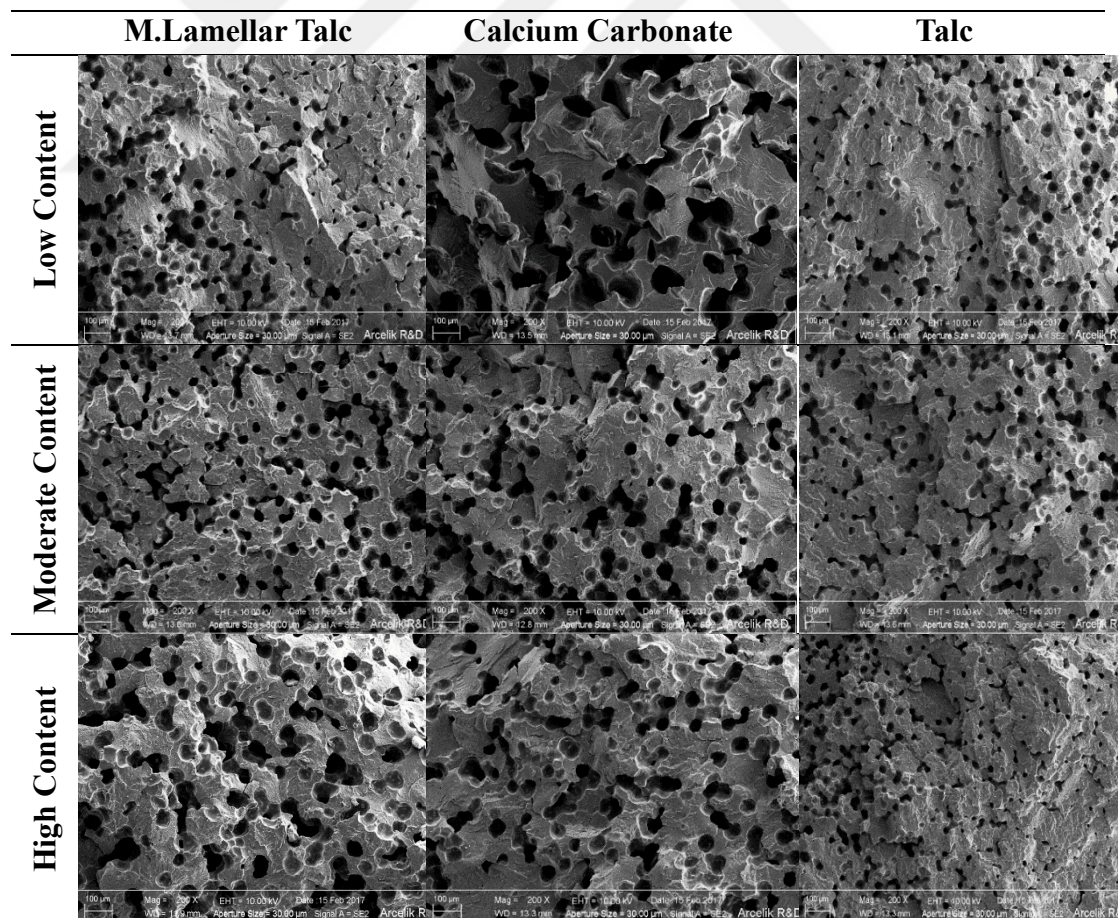


Figure 4.17 : SEM images of the HIPS composite foams using high content CBA 1 at low die temperature (low RPM).



5. CONCLUSION

In this thesis study, the extrusion foaming of HIPS through a twin-screw extruder with two different chemical blowing agents was studied by using filamentary die. The thermal characterization of both CBAs were performed and CBA 1 has lower decomposition temperature than CBA 2 according to thermal analysis.

The distribution and sizes of PB in PS matrix is investigated by using optical microscope before and after process. Results show that, PB orientations are similar in both situations. The diameters of PBs are as large as 20 μm . In addition, the melt behavior of HIPS, GPPS and their blends were investigated. Both MFI and complex shear viscosity results show that, the melt properties of HIPS, GPPS and their blends will have a similar effect on the corresponding foaming behavior of the samples.

The effects of processing temperature profile, die temperature profile and screw speed (RPM) were investigated as process parameters when using both CBAs. Moreover, CBA type and content; various inorganic fillers (i.e., microlamellar talc, talc, and calcium carbonate) at three different contents and the foaming behavior of HIPS/GPPS blends at the different blending ratios were studied. The void fraction values were calculated by using Archimedes principle. The morphological analysis were performed by using SEM and the cell density values were determined.

According to results; the void fraction values did not change significantly with three different barrel temperature profile for CBA 1. The lowest cell density is seen when using profile 3. The highest void fraction (% 19) and cell density ($\sim 10^6$ cells/cm³) was observed when using profile 1 for CBA-2. The barrel temperature profile 3 and 1 were chosen for CBA 1 and CBA 2, respectively. In foamed samples with CBA 1, the highest void fraction ($\sim 22\%$) was obtained at the die temperature profile 2 (low temperatures) which also possessed the highest cell density ($\sim 6 \times 10^5$ cells/cm³). The void fraction and cell density decreased with the decrease in die temperature when using CBA 2. The highest void fraction and cell density values were calculated at the highest die temperature. Moreover, while increasing the CBA content, the void fraction and cell density values promote for both CBAs due to the increasing internal

pressure. When the screw RPM increased from low to high, the die pressure and consequently the void fraction of the foamed samples decreased and the maximum void fraction was achieved ~ 30 % for samples blown with both CBAs. The higher cell density values were observed at lower RPMs due to the better mixing of polymer melt.

When the foaming behavior of PS blends were investigated, the increasing GPPS content increased the cell densities of HIPS/GPPS blends to around 10^6 cells/cm³ with more of open celled structure. On the other hand, the increase in inorganic filler contents increased the cell density and void fraction of HIPS foams while the type of inorganic fillers didn't reveal much differences from each other in the foaming results.



REFERENCES

- [1] Gibson, L.J., & Ashby, M.F. (1998). *Cellular Solids: Structure & Properties*, Pergamon Press.
- [2] Li, G., Wang, J., & Park, C.B. (2006). Measurement of N₂ Solubility in Polypropylene and Ethene/Octene Copolymer. *SAE Technical Paper*, 4, 3-6.
- [3] Eaves, D. (2004). *Handbook of Polymer Foams*, Rapra Technology.
- [4] Park, C.B., & Suh, N.P. (1996). Filamentary Extrusion of Microcellular Polymers Using a Rapid Decompressive Element. *Polymer Engineering and Science*, 36, 34-48.
- [5] Park, C.B., Behravesh, A.H., Venter R.D. (1998). Extrusion of Low Density Microcellular HIPS Foams Using CO₂. *Polymer Engineering and Science*, 38, 1812–1823.
- [6] Shimbo, M., Nishida, K., Nishikawa, S., Sueda, T., & Eriguiti, M. (1998). *Porous, Cellular and Microcellular Materials*, ASME.
- [7] Url-1 <<http://toxicfoam.weebly.com/history-of-polystyrene-foam.html>>
- [8] Morris, Peter J.T. (1988). *Polymer pioneers: a popular history of the science and technology of large molecules*, The Backman Center for the History of Chemistry.
- [9] URL-2 <<http://pslc.ws/macrog/radical.htm>>
- [10] URL-3 <https://www.silicycle.com/media/pdf/silicycleguide_for_chemical_synthesis_and_purification.pdf>
- [11] Wunsch, J.R. (2000). *Polystyrene – Synthesis, Production and Applications*, Rapra Technology Limited.
- [12] Yam, K. L., (2009). *The Wiley encyclopedia of packaging technology*, Wiley.
- [13] Dheeraj, S., Chaiyhal, A., & Bipin, K. (2003). *Properties and uses of Polystyrene*. Sevas Educational Society.
- [14] URL-4 <<http://www.cheresources.com/content/articles/processes/basics-of-polystyrene-production>>
- [15] NPCS Board of Consultants & Engineers. (2014). *Disposable Products Manufacturing Handbook*, 95-100
- [16] Cazenave, J., Seguela, R., Sixou, B., & Germain, Y. (2006). Short-term mechanical and structural approaches for the evaluation of polyethylene stress crack resistance. *Polymer*, 47, 3904–3914

- [17] **Leung, S.**, (2009), *Mechanisms of Cell Nucleation, Growth, and Coarsening in Plastic Foaming: Theory, Simulation, And Experiment* (Doctor of Philosophy). University of Toronto, Department of Mechanical and Industrial Engineering.
- [18] **Fox, T.G. & Flory, P.J.** (1950). Second-Order Transition Temperatures and Related Properties of Polystyrene. I. Influence of Molecular Weight. *Journal of Applied Physics*, **21**, 1950, 581-591.
- [19] **The Global Industry Analysts, Inc.** (2008). A Global Strategic Business Report (MCP.1174). San Jose, California, USA.
- [20] **Matuana, L.M., Park, C.B., & Balatinecz, J.J.** (1998). Structures and Mechanical Properties of Microcellular Foamed Polyvinyl Chloride. *Cellular Polymers*, **17**, 1-16.
- [21] **Doroudiani, S., Park, C.B., & Kortschot, M.T.** (1998). Processing and Characterization of Microcellular Foamed High Density Polyethylene/Isotactic Polypropylene Blends. *Polymer Engineering and Science*, **38**, 1205-1215.
- [22] **Collias, D.I., & Baird, D.G.** (1995). Tensile Toughness of Microcellular Foams of Polystyrene, Styrene-Acrylonitrile Copolymer, and Polycarbonate, and the Effect of Dissolved Gas on the Tensile Toughness of the Same Polymer Matrices and Microcellular Foams. *Polymer Engineering Science*, **35**, 1167-1177.
- [23] **Collias, D.I., & Baird, D.G.** (1995). Impact Behavior of Microcellular Foams of Polystyrene and Styrene-Acrylonitrile Copolymer, and Single-Edge-Notched Tensile Toughness of Microcellular Foams of Polystyrene, Styrene-Acrylonitrile Copolymer, and Polycarbonate. *Polymer Engineering Science*, **35**, 1178-1183.
- [24] **Collias, D.I., & Baird, D.G.** (1994). Impact Toughening of Polycarbonate by Microcellular Foaming. *Polymer*, **25**, 3978-3983.
- [25] **Seeler, K.A., & Kumar, V.** (1993) Tension-tension Fatigue of Microcellular Polycarbonate: Initial Results. *Journal of Reinforced Plastics and Composites*, **12**, 359-376.
- [26] **Suh, K.W., Park, C.P., Maurer, J.J., Tusim, M.H., Genova, R.D., Broos, R., & Sophiea, D.P.** (2000). Lightweight Cellular Plastics. *Advanced Materials*, **12**, 1779-2000.
- [27] **Kabumoto, A., Yoshida, N.** (1998). U.S. Patent No. 5,844,731. U.S. Patent and Trademark Office.
- [28] **Park, C.B., Baldwin, D., & Suh, N.** (1995). Effect of the pressure drop rate on cell nucleation in continuous processing of microcellular polymers. *Polymer Engineering Science*, **35**, 432-440.
- [29] **Nagy, V., & Vas, L.M.** (2005). Pore Characteristic Determination with Mercury Porosimetry in Polyester Staple Yarns. *Fibres & Textiles in Eastern Europe*, **51**, 21-26.
- [30] **Okolieocha, C., Raps, D., Subramaniam, K., & Altstädt, V.** (2015). Microcellular to nanocellular polymer foams: Progress and future directions: a review. *European Polymer Journal*, **73**, 500-519.

- [31] Klemptner, D., Sendjarević, V., & Aseeva, R. M. (2004). *Handbook of Polymeric Foams and Foam Technology*, Hanser Publishers.
- [32] Mahmoud, A.A., Nasr, E.A.A., & Maamoun, A.A.H. (2017). The Influence of Polyurethane Foam on the Insulation Characteristics of Mortar Pastes. *Journal of Minerals and Materials Characterization and Engineering*, **5**, 49-61.
- [33] Daniel, I.M., Cho, J., & Werner, B.T. (2013). Characterization and modeling of stain-rate-dependent behavior of polymeric foams. *Composites Part A: Applied Science and Manufacturing*, **45**, 70-78.
- [34] URL-5 <[http://web.deu.edu.tr/metalurjimalzeme/pdf/mme4044Polymer Applications/PolymerFoamsLecture2-2015.pptx](http://web.deu.edu.tr/metalurjimalzeme/pdf/mme4044Polymer%20Applications/PolymerFoamsLecture2-2015.pptx)>
- [35] Láinez, A., Rodríguez M.P., & Saja, J.A. (2014). Acoustic absorption coefficient of open-cell polyolefin-based foams. *Materials Letters*, **121**, 26-30.
- [36] Baldwin, D.F., Tate, D., Park, C.B., Cha, S.W. & Suh, N.P. (1994). Microcellular Plastics Processing Technology. *Journal of Japan Society of Polymer Processing*, **6**, 187-194.
- [37] Berins, L.M. (1991). *SPI Plastics Engineering Handbook of the Society of the Plastics Industry*, Springer.
- [38] Naguib, H.E., Park, C.B., Danzer, U., & Reichelt, N. (2002). Strategies for Achieving Ultra Low- Density PP Foams, *Polymer Engineering and Science*, **42**, 4181-1492.
- [39] Creazzo, J.A., & Loh, G. (2011). U.S. Patent No. 20110269980. U.S. Patent and Trademark Office.
- [40] Lee, S., Park, C.B., & Ramesh, N. (2006). *Polymeric Foams: Science and Technology*, CRC Press.
- [41] Munters, C.G., & Tandberg, J.G. (1935). U.S. Patent No. 2,023,204. U.S. Patent and Trademark Office.
- [42] Sauceau, M., Fages, J., Common, Audrey., Nikitine, C., & Rodier, E. (2011). New challenges in polymer foaming: A review of extrusion processes assisted by supercritical carbon dioxide, *Progress in Polymer Science*, **36**, 749–766.
- [43] Jacobs, W.A., & Collins, F. H. (1965). U.S. Patent No. 3,151,192. U.S. Patent and Trademark Office.
- [44] Carlson, Jr.F.A. (1957). U.S. Patent No. 2,797,443. U.S. Patent and Trademark Office.
- [45] Kolosowski, P.A. (1995). U.S. Patent No. 5,424,016. U.S. Patent and Trademark Office.
- [46] Pontiff, T.M., & Rapp, J.P. (1989). U.S. Patent No. 5,059,376. U.S. Patent and Trademark Office.
- [47] Miyamoto, A., Akiyama, H., & Usuda, Y. (1973). U.S. Patent No. 3,808,380. U.S. Patent and Trademark Office.

- [48] **Suh, K.W.** (1988). U.S. Patent No. 4,916,166. U.S. Patent and Trademark Office.
- [49] **Li, G., Wang, J., Li, G.Y., Park, C.B., & Simha, R.** (2004). Measurements of Gas Solubility for PP/Blowing-Agent Mixtures, *Foams 2004*, Wilmington, Delaware, USA, October 5-6.
- [50] **Li, Y.G., Hasan, M.M., & Park, C.B.** (2009). Determination of the Solubility of Blowing Agent in Polymer without Using any Equation of State, Society of Plastics Engineers, *Annual Technical Conference – ANTEC*, Chicago, Illinois, USA, June 22-24.
- [51] **Hasan, M.M., Li, G., Park, C.B., & Chen P.** PVT and Solubility Behaviors of CO₂/N₂ Blends in PS Melts, *Foams 2010*, Seattle, Washington, (2010).
- [52] **Sato, Y., Fujiwara, K., Takikawa, T., Sumarno, Takishima, S., & Masuoka, H.** (1999). Solubilities and diffusion coefficients of carbon dioxide and nitrogen in polypropylene, high-density polyethylene, and polystyrene under high pressures and temperatures. *Fluid Phase Equilibria*, **162**, ahmood261–276.
- [53] **Gendron, R.** (2005). Thermoplastic foam processing: principles and development, CRC press.
- [54] **Li, G., Li, H., Turng, L.S., Gong, S., & Zhang, C.** (2006). Measurement of gas solubility and diffusivity in polylactide, *Fluid Phase Equilibria*, **246**, 158-166.
- [55] **Mahmood, S.H.** (2012). *A Thermodynamic Investigation of the PVT, Solubility and Surface Tension of Polylactic Acid (PLA)/CO₂ Mixtures* (Doctor of Philosophy). University of Toronto, Department of Mechanical and Industrial Engineering.
- [56] **Hasan, M.M., Li, Y.G., Li, G., Park, C.B., & Chen, P.** (2010). Determination of Solubilities of CO₂ in Linear and Branched Polypropylene Using a Magnetic Suspension Balance and a PVT Apparatus. *Journal of Chemical Engineering Data*, **55** 4885-4895
- [57] **Pontiff, T. M.** (1998). Nucleation in Direct Gassed PS Foam Using Chemical Foaming Agents, Dubai Plast Pro '98, Maack Business Services, Dubai, UAE, May 11–13.
- [58] **Colombo, E.A.** (1979). *Controlling the Properties of Extruded Polystyrene Foam Sheet*, *Science and Technology of Polymer Processing*, The MIT Press.
- [59] **Zhang H.** (2010). Scale-Up of Extrusion Foaming Process for Manufacture of Polystyrene Foams Using Carbon Dioxid (M. Sc Thesis). University of Toronto. Department of Mechanical and Industrial Engineering.
- [60] **Crank, J., & Park, G.S.** (1968). *Diffusion in Polymers*, Academic Press Inc.
- [61] **Throne, J. L.** (1996). *Thermoplastic Foams*, Sherwood Publishers.
- [62] **Krevelen V.D.W.** (1990). *Properties of Polymers*, Elsevier Scientific Publishers Company.

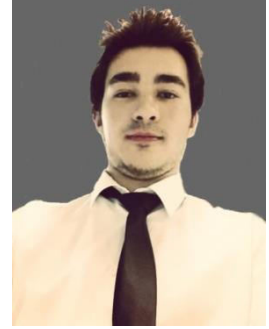
- [63] Durrill, P.L., & Griskey, R.G. (1981). Diffusion and Solution of Gases into Thermally Softened of Molten Polymers: Part II. Relation of Diffusivities and Solubilities with Temperature, Pressure and Structural Characteristics. *AIChE Journal*, **15**, 106–110.
- [64] Park, C.B., Baldwin, D.F., & Suh, N.P. (1994). Formation and Application of a Polymer/Gas Mixture in Continuous Processing of Microcellular Polymers, *ASME, Cellular and Microcellular Materials*, **53**, 109-124.
- [65] Cooper, A.I. (2000). Polymer Synthesis and Processing Using Supercritical Carbon Dioxide. *Journal of Materials Chemistry*, **10**, 207-234.
- [66] Nofar, M., Majithiya, K., Kuboki, T., & Park, C.B. (2012). The Foamability of Low Melt-strength Polypropylene with Nanoclay and Coupling Agent. *Journal of Cellular Plastic*, **48**, 271-287.
- [67] Colton, J.S., & Suh, N.P. (1987). The Nucleation of Microcellular Thermoplastic Foam with Additives: Part 1: Theoretical Consideration. *Polymer Engineering Science*, **27**, 485-492.
- [68] Colton, J.S., and Suh, N.P. (1987). The Nucleation of Microcellular Thermoplastic Foam with Additives: Part II: Experimental Results and Discussion, *Polymer Engineering Science*, **27**, 493-499.
- [69] Fisher, J. (1948). The Fracture of Liquids. *Journal of Applied Physics*, **19**, 1062-1067.
- [70] Fletcher, N.H. (1958). Size Effect in Heterogeneous Nucleation. *Journal of Chemical Physics*, **29**, 572-576.
- [71] Moore, G.R. (1959). Vaporization of Superheated Drops in Liquids. *AIChE Journal*, **5**, 458-466.
- [72] Apfel, R.E. (1971). Vapor Nucleation at a Liquid-Liquid Interface. *The Journal of Chemical Physics*, **54**, 62-63.
- [73] Jarvis, T.M., Donohue, M.D., & Katz, J.L. (1975). Bubble Nucleation Mechanisms of Liquid Droplets Superheated in Other Liquids. *Journal of Colloid and Interface Science*, (50), 359-368.
- [74] Lee, S.T. (1993). Shear Effects on Thermoplastic Foam Nucleation. *Polymer Engineering and Science*, **33**, 418-422.
- [75] Xu, D., Pop-Iliev, R., Park, C.B., & Fenton, R.G. (2005). Fundamental Study of CBA-Blown Bubble Growth and Collapse under Atmospheric Pressure. *Journal of Cellular Plastics*, **41**, 519-538.
- [76] Zhu, Z., Xu, D., Park, C.B., & Fenton, R.G. (2005). Finite Element Analysis of Cell Coarsening in Plastic Foaming. *Journal of Cellular Plastics*, **41**, 475-486.
- [77] Zhu, Z., Park, C.B., & Zong, J. (2008). Challenges to the Formation of Nano Cells in Foaming Processes. *International Polymer Processing*, **23**, 270-276.
- [78] Taki, K., Tabata, K., Kihara, S., & Ohshima, M. (2006). Bubble Coalescence in Foaming Process of Polymers. *Polymer Engineering and Science*, **46**, 680-690.

- [79] **Park C.B.** (2013). *Manufacturing of Cellular and Microcellular Polymers: Continuous Microcellular Processing* (Class notes). University of Toronto. Department of Mechanical and Industrial Engineering.
- [80] **Leung S. N., Wong A., Wang L. C., & Park C.B.** (2012). Mechanism of extensional stress-induced cell formation in polymeric foaming processes with the presence of nucleating agents. *The Journal of Supercritical Fluids*, **63**, 187–198.
- [81] **Corre, Y.M., Maazouz, A., Duchet, J., & Reignier, J.** (2011). Batch foaming of chain extended PLA with supercritical CO₂: Influence of the rheological properties and the process parameters on the cellular structure. *The Journal of Supercritical Fluids*, **58**, 177-188.
- [82] **Horvath, J.S.** (1994). Expanded Polystyrene (EPS) geofoam: An introduction to material behavior. *Geotextiles and Geomembranes*, **13**, 263-280.
- [83] **Kannan, P., Biernacki, J.J., & Visco, D.P.Jr.** (2007). A review of physical And kinetic models of thermal degradation of expanded polystyrene foam and their application to the lost foam casting process. *Journal of Analytical and Applied Pyrolysis*, **78**, 162–171.
- [84] **URL-6** <<http://clacktronics.co.uk/2015/Casting-expanded-polystyrene.html>>
- [85] **Dominick, V., Donald, V., & Matthew, R.** (2004). *Plastic Product Material and Process Selection Handbook*, Elsevier Science.
- [86] **Nofar, M., Ameli, A., & Park, C.B.** (2015). A novel technology to manufacture biodegradable polylactide bead foam products, *Materials Design*, **83**, 413-421.
- [87] **Lee K. E.** (2010). *Novel Manufacturing Processes for Polymer Bead Foams* (M.Sc Thesis). University of Toronto. Department of Materials Science and Engineering.
- [88] **Zhai, W., Kim, Y.W., & Park, C.B.** (2010). Steam-chest molding of expanded polypropylene foams. 1. DSC simulation of bead foam processing, *Industrial and Engineering Chemistry Research*, **49**, 9822–9829.
- [89] **Han, C.D., & Ma, C.Y.** (1983). Rheological Properties for Molten Polymer and Fluorocarbon Blowing Agent. I: Mixtures of low-Density Polyethylene and Fluorocarbon Blowing Agent. *Journal of Applied Polymer Science*, **28**, 831–850.
- [90] **Throne J.L.** (2004). *Thermoplastic Foam Extrusion: an introduction*, Hanser Gardner.
- [91] **Naguib H.E., Park C.B., & Lee P.C.** (2003). Effect of Talc Content on the Volume Expansion Ratio of Extruded PP Foams. *Journal of Cellular Plastics*, **39**, 499-511.
- [92] **Rabinowitsch, B.** (1929). The Viscosity and Elasticity of Sols. *Z. Physik Chemistry*, **115**, 1.
- [93] **Bagley, E.B.** (1957). End Corrections in the Capillary Flow of Polyethylene, *Journal of Applied Physics*, **28**, 624.

- [94] Han, C.D., & Ma, C.Y. (1983). Rheological Properties of Molten Polymer and Fluorocarbon Blowing Agent. II: Mixtures of Polystyrene and Fluorocarbon Blowing Agent. *Journal of Applied Polymer Science*, **28**, 851–860.
- [95] Kozicki, W., Chou, C.H., & Tiu, C. (1966). Non-Newtonian Flow in Ducts of Arbitrary Cross-Sectional Shape, *Chemical Engineering Science*, **21**, 665.
- [96] Park, C.B. (2014). *Foam Extrusion, Principles and Practice*, CRC press.
- [97] Han, C. D., & Villazimar, C.A. (1978). Studies on Structural Foam Processing. I. The Rheology of Foam Extrusion. *Polymer Engineering Science*, **18**, 687–698.
- [98] Kraynik, A.M. (1981). Rheological Aspects of Thermoplastic Foam Extrusion. *Polymer Engineering Science*, **21**, 80–85.
- [99] Han, C.D., & Ma, C.Y. (1983). Rheological Properties of Mixtures of Molten Polymer and Fluorocarbon Blowing Agent. I. Mixtures of Low-Density Polyethylene and Fluorocarbon Blowing Agent. *Journal of Applied Polymer Science*, **28**, 831–850.
- [100] Lee, M., Park C. B., & Tzoganakis C. (1999). Measurements and Modeling of PS/Supercritical CO₂ Solution Viscosities. *Polymer Engineering Science*, **39**, 99–109.
- [101] Gendron, R., L. E. Daigneault., & L. M. Caron. (1999). Rheological Behavior of Mixtures of Polystyrene with HCFC 142b and HFC 134a. *Journal of Cellular Plastics*, **35**, 221–246.
- [102] Gendron, R., & Daigneault, L. E. (1997). Rheological Behavior of Mixtures of Various Polymer Melts with CO₂. *SPE Antec Technical Papers*, **43**, 1096–1100.
- [103] Blyler, L.L.Jr., & Kwei, T. K. (1971). Flow Behavior of Polyethylene Melts Containing Dissolved Gases. *Journal of Polymer Science: Part C*, **35**, 65–176.
- [104] Gendron, R., & Correa, A. (1998). The Use of On-Line Rheometry to Characterize Polymer Melts Containing Physical Blowing Agents. *Cellular Polymers*, **17**, 93–113.
- [105] Naguib, H.E., Park, C.B., & Song, S. (2005). Effect of Supercritical Gas on Crystallization of Linear and Branched Polypropylene Resins with Foaming Additives. *Industrial Engineering Chemistry Research*, **44**, 6685–6691.
- [106] Park, C.B., & Cheung, L.K. (1997). A study of cell nucleation in the extrusion of polypropylene foams, *Polymer Engineering and Science*, **37**, 1-10.
- [107]. Shim, J.J., & Johnston, K. P. (1991). Phase Equilibria, Partial Molar Enthalpies, and Partial Molar Volumes by Supercritical Fluid Chromatography, *AIChE J.*, **37**, 607.

- [108] **Xu, X., Park, C.B., Xu, D. & Pop-Iliev, R.** (2003). Effects of Die Geometry on Cell Nucleation of PS Foams Blown with CO₂. *Polymer Engineering and Science*, **43**, 1378-1390.
- [109] **Xu, X., & Park, C.B.** (2008). Effects of the Die Geometry on Expansion of PS Foams Blown with CO₂. *Journal of Applied Polymer Science*, **109**, 3329-3336.
- [110] **Lee, J.W.S., Wang, K., & Park, C.B.** (2004). Challenge to Extrusion of Low-Density Microcellular Polycarbonate Foams Using Supercritical CO₂. *Industrial & Engineering Chemistry*, **44**, 92.
- [111] **Naguib, H.E., Park, C.B., & Reichelt, N.** (2004). Fundamental Foaming Mechanisms Governing Volume Expansion of Extruded PP Foams. *Journal of Applied Polymer Science*, **91**, 2661- 2668.
- [112] **Keshtkar, M., Nofar, M., Park, C.B., & Carreau, P.J.** (2014). Extruded PLA/clay nanocomposite foams blown with supercritical CO₂. *Polymer*, **55**, 4077.
- [113] **Yang, H.H., & Han, C.D.** (1984). The Effect of Nucleating Agents on the Foam Extrusion Characteristics," *Journal of Applied Polymer Science*, **29**, 4465-4470.
- [114] **Wilkenlog, F.N., Wilson, P.A., & Fox, S.A.** (1978). U.S. Patent No. 4,107,354. U.S. Patent and Trademark Office.
- [115] **Ehrenfreund, H.A.** (1978). U.S. Patent No. 4,110,269, U.S. Patent and Trademark Office.
- [116] **Ramesh, N.S., Kweeder, J.A., Rasmussen, D.H., & Campbell, G.A.** (1992). An Experimental Study on the Nucleation of Microcellular Foams in High Impact Polystyrene. *SPE ANTEC Technical Papers*, **38**, 1078-1081.
- [117] **Ramesh, N.S., Rasmussen, D.H., & Campbell, G.A.** (1994). The Heterogeneous Nucleation of Microcellular Foams Assisted by the survival of microvoids in polymers containing Low Glass Transition Particles. Part II: Experimental Results and Discussion. *Polymer Engineering and Science*, **34**, 1698-1706.
- [118] **Park, C.B., Cheung, L.K., & Song, S.W.** (1998). The Effect of Talc on Cell Nucleation in Extrusion Foam Processing of Polypropylene with CO₂ and Isopentane. *Cellular Polymers*, **17**, 221-251.
- [119] **Allen, R.B., & Avakian, R.W.** (1985). U.S. Patent No. 4,544,677. U.S. Patent and Trademark Office.
- [120] **Lee, S.T.** (2000). *Foam Extrusion: Principles and Practice*, Technomic Publishing Co.

CURRICULUM VITAE



Name Surname : Emre Demirtaş
Place and Date of Birth : Bursa/ 26.04.1993
E-Mail : emredmirtas@gmail.com

EDUCATION :

- **B.Sc.** : 2016, Istanbul Technical University, Faculty of Chemical & Metallurgical Engineering, Chemical Engineering Department

PROFESSIONAL EXPERIENCE AND REWARDS:

- 2016-2018 Arcelik A.S., R&D Project Engineer

PUBLICATIONS, PRESENTATIONS AND PATENTS ON THE THESIS:

- **Demirtas, E., Ozkan, H., & Nofar, M.** (2016). Plastik İç Duvar İçeren Buzdolabı, Patent Reference Number: 7.2337 (Patent Application)
- **Demirtas, E., Ozkan, H., & Nofar, M.** (2018). Extrusion Foaming of High Impact Polystyrene: Effects of Processing Parameters and Materials Composition. *International Journal of Material Science and Research*, 2018, 1(1), 9-15. (Article)
- **Demirtas, E., Ozkan, H., & Nofar, M.** (2017). Continuous foam extrusion of high impact polystyrene (HIPS): Effect of processing parameters and blowing agent type and content. *Polymer Processing Society 2017*, Europe Africa Conference, Dresden. (Conference Proceedings and Presentation)
- **Demirtas, E., Ozkan, H., Nofar, M.** (2017). Continuous Foam Extrusion of Polystyrene (PS) Blends and Composites. *Foams2013*, Bayreuth, Germany, October 11–12, 2017. (Conference Proceedings and Presentation)

